OXYFUNCTIONALIZATION OF POLYSTYRENE USING NON-HEME IRON CATALYSTS

by

Shelley McArthur

A thesis submitted to the Graduate Program in Chemistry

in conformity with the requirements for the

Degree of Master of Science

Queen's University

Kingston, Ontario, Canada

August, 2011

Abstract

The non-polar nature of polystyrene has allowed this material to be widely used in both industrial and household applications. This same property also limits its interactions with polar materials and its stability renders it slow to degrade in an environmental setting. Considering its widespread use in society, this makes polystyrene an environmental concern. The introduction of a limited number of polar groups along the backbone could increase its compatibility with polar materials as well as possibly rendering it biodegradable. The literature contains many reports of iron based catalysts that oxidize small molecule alkanes in moderate yields to introduce ketone or alcohol groups.[1-3] In principle, the chemistry applicable to small molecules should also be applicable to their macromolecular analogues. This thesis used two such iron complexes, $[(Fe(TPA)(MeCN)_2]$ $(OTf)_2$ and $Fe(BPMEN)(OTf)_2$, to catalyze the oxidation of polystyrene using hydrogen peroxide as oxidant. The polymeric product was analyzed first by IR and if oxyfunctionalization was detected in the form of a carbonyl or hydroxyl peak, the material was further analyzed by DSC, GPC and ^{1}H NMR. The results reported herein constitute a proof of principle for the use of iron based non-heme catalysts and hydrogen peroxide for the oxyfunctionalization of polystyrene.

Acknowledgements

I would like to thank Dr. Michael Baird for letting me work in his group and for his help and guidance throughout this project. I would also like to thank all the members of the Baird group for their help and for putting up with me for two years.

I wouldn't have made it this far without the continued support of my mom Allana and my friend Cindy who both helped keep me sane and kept encouraging me, even when the task seemed insurmountable. Finally I would like to thank Gina and Mrs. Berghuis for believing in me and waiting two years for me to pursue this goal.

Table of Contents

Abstract ii
Acknowledgements iii
Table of Contents iv
List of Tables vii
List of Figures viii
List of Abbreviations x
List of Symbols xiii
Chapter 1 Introduction 1
1.1 Polystyrene 1
1.2 Oxyfunctionalization of Polymers 1
1.2.1 Polymerization with Functionality 2
1.2.1.1 Copolymerization 2
1.2.1.2 Graft Copolymerization 3
1.2.2 Post Polymerization Functionalization 3
1.2.2.1 Flame/Plasma Treatment 4
1.2.2.2 Transition Metal Catalysts 4
1.3 Oxyfunctionalization of Small Molecule Alkanes with Transition Metal Catalysts 6
1.3.1 Heme-Based Systems 7
1.3.2 Non-Heme Systems 9
1.3.2.1 Fe(TPA) Complexes 10
1.3.2.2 Mechanistic considerations 11
1.3.2.3 Fe(BPMEN) 15
1.3.2.4 Ligand Effects 15
1.3.2.5 Practical Applications 17
1.4 Aims of Present Research 19
Chapter 2 Experimental 200
2.1 General Conditions 200
2.2 Preparation of Complexes 211

2.2.1 Synthesis of $Fe(MeCN)_2(OTf)$ 211
2.2.2 Synthesis of TPA 222
2.2.3 Synthesis of BPMEN 233
2.2.4 Synthesis of $Fe(TPA)(MeCN)_2(OTf)$ 244
2.2.4.1 Inert Atmosphere Procedure 24
2.2.4.2 Open to Atmosphere 25
2.2.5 Synthesis of $Fe(BPMEN)(OTf)_2$ 255
2.3 Hydrogen Peroxide Solutions 266
2.4 Catalytic Activity of Complexes – Oxyfunctionalization of Cyclohexane 277
2.4.1 Fe(TPA)/Fe(BPMEN) in MeCN 27
2.4.2 Fe(TPA)/Fe(BPMEN) in DCM 27
2.4.3 Fe(TPA)/Fe(BPMEN) in DCM/MeCN 27
2.4.4 Gas Chromatographic Analysis of the Reactions 28
2.5 Control Reactions 299
2.5.1 Fe(TPA)/Fe(BPMEN) without PS 29
2.5.2 High Molecular Weight with no Complex 29
2.5.3 Low Molecular weight PS with no Complex 30
2.6 Catalytic Reactions with PS 30
2.6.1 High Molecular Weight PS with Fe(BPMEN) in 1:1 DCM:MeCN 30
2.6.2 High Molecular Weight PS with Fe(BPMEN) in 7:3 DCM:MeCN 31
2.6.3 High Molecular Weight PS with Fe(BPMEN) in 3:7 DCM:MeCN 32
2.6.4 High Molecular Weight PS with Fe(TPA) in 1:1 DCM:MeCN 32
2.6.5 High Molecular Weight PS with Fe(TPA) - Diluted Reactions 33
2.6.6 Low Molecular Weight PS with Fe(BPMEN) in 1:1 DCM:MeCN 34
2.6.7 Low Molecular Weight PS with Fe(BPMEN) in 3:7 DCM:MeCN 35
2.6.8 Low Molecular Weight PS with Fe(TPA) in 1:1 DCM:MeCN 36
2.6.9 Low Molecular Weight PS with Fe(TPA) in 3:7 DCM:MeCN 37
2.6.10 Low Molecular Weight PS with Fe(TPA) in 3:7 DCM:MeCN - Two Additions 37

2.6.11 Low Molecular Weight PS with Fe(TPA) in 3:7 DCM:MeCN - Three Additions 39
2.7 Material Analysis 40
2.7.1 Differential Scanning Calorimetry 40
2.7.2 Gel Permeation Chromatography 41
Chapter 3 Results and Discussion 43
3.1 Synthesis of Complexes 43
3.1.1 Synthesis of $Fe(MeCN)_2(OTf)_2$ 44
3.1.2 Synthesis of Fe(BPMEN) 45
3.1.3 Synthesis of Fe(TPA) 46
3.2 Checking Activity of Complexes for Oxyfunctionalization of Cyclohexane 49
3.3 Polystyrene Oxyfunctionalization Reactions 50
3.3.1 High Molecular Weight Polystyrene 52
3.3.2 Low Molecular Weight Polystyrene 58
3.4 Control Reactions 65
3.5 Analysis of Results 66
3.6 Importance of Colours in the Catalytic Reactions 68
Chapter 4 Summary and Conclusions 70
References 72
Appendix – Crystal Structure Data for $[Fe(TPA)(MeCN)_2](OTf)_2$ 75

List of Tables

Table 1. Glass transition temperatures of both polystyrene starting materials and of select soluble products from catalytic reactions of polystyrene 41
Table 2. Number average molecular weights and polydispersity indexes of both polystyrene starting materials and of select soluble products from catalytic reactions of polystyrene. Each M_n value has an error of 9 % while each PDI value has an error of 13 % 42
Table 3. Selected bond lengths and angles for $[Fe(TPA)(MeCN)_2][OTf]_2$ 49

List of Figures

Figure 1. Functionalization of polymers via direct copolymerization (top), copolymerization with protected functional groups (middle), and copolymerization with groups with latent reactivity 3
Figure 2. Hydroxylation of polyethylethylene with $[Cp^*RhCl_2]_2$ and bispinacoldiboron 5
Figure 3. Mn(TDCPP)OAc 5
Figure 4. Oxyfunctionalization of polyethylene-*alt*-propylene using Mn(TDCPP)OAc and $KHSO_5$ 6
Figure 5. General metalloporphyrin structure 7
Figure 6. The general form of the first (left), second (centre) and third (right) generations of substituted tetraarylpophyrins, with X generally being a halide or other electron withdrawing group 8
Figure 7. Proposed generation of active species for metalloporphyrin complexes 9
Figure 8. Structure of TPA ligand 10
Figure 9. Proposed mechanistic scheme for Fe(TPA) 12
Figure 10. Decomposition pathways for the $(TPA)Fe^{III}$-OOH species 14
Figure 11. Structure of BPMEN ligand 15
Figure 12. Structure of $[Fe(S,S\text{-}PDP)][SbF_6]_2$ 17
Figure 13. Selectivity of $[Fe(S,S\text{-}PDP)][SbF_6]_2$ in presence of electron withdrawing group 18
Figure 14. Production of cyclic lactones using $[Fe(S,S\text{-}PDP)][SbF_6]_2$ 18
Figure 15. Structure of $[Fe(TPA)(MeCN)_2][OTf]_2$ (left) and $Fe(BPMEN)(OTf)_2$ (right) 44
Figure 16. Two isomers of the crystal structure of $[Fe(TPA)(MeCN)_2][OTf]_2$ with the triflates omitted 48
Figure 17. IR spectrum of PS (top) and IR spectrum of the soluble polymer resulting from the catalytic reaction of high molecular weight PS with 5 mol% Fe(BPMEN) and 10 mL of 10 % H_2O_2 in 1:1 DCM:MeCN (bottom) 53
Figure 18. General reaction conditions for polystyrene oxyfunctionalization reactions 54
Figure 19. IR spectrum of the soluble polymer resulting from the catalytic reaction of high molecular weight PS with 5 mol% Fe(TPA) and 10 mL of 10 % H_2O_2 in 1:1 DCM:MeCN 55
Figure 20. IR spectrum of the soluble polymer resulting from the catalytic reaction of high molecular weight PS with 2.5 mol% Fe(TPA) and 10 mL of 10 % H_2O_2 in 1:1 DCM:MeCN 57

Figure 21. IR spectrum of the soluble polymer resulting from the catalytic reaction of low molecular weight PS with 2 × (5 mol% Fe(TPA) and 10 mL of 10 % H_2O_2) in 3:7 DCM:MeCN 62
Figure 22. IR spectrum of the soluble polymer resulting from the catalytic reaction of low molecular weight PS with 2 × (5 mol% Fe(TPA) and 10 mL of 10 % H_2O_2) in 3:7 DCM:MeCN after having been dried over 3Å molecular sieves for 24 hours 62
Figure 23. ^1H NMR spectrum in $CDCl_3$ of the soluble product from the catalytic reaction of low molecular weight PS with 2 × (5 mol% Fe(TPA) and 10 mL of 10 % H_2O_2) in 3:7 DCM:MeCN 64
Figure 24. Locations of possible oxyfunctionalization and the adjacent protons 65
Figure 25. Structure of squalane (left) and PEP (right) 66

List of Abbreviations

^{13}C NMR	carbon nuclear magnetic resonance spectroscopy
^{1}H NMR	proton nuclear magnetic resonance spectroscopy
A/K ratio	alcohol to ketone ratio
BDTAC	benzyldimethyltetradecylammonium chloride
bp	boiling point
BPMEN	N,N'-dimethyl-N,N'-bis(2-pyridylmethyl)-ethane-1,2-diamine
$CDCl_3$	deuterated chloroform
CD_2Cl_2	deuterated methylene chloride
CD_3CN	deuterated acetonitrile
Cl	chloride
cm^{-1}	reciprocal centimeters
COSY	correlation spectroscopy
Cp*	pentamethylcyclopentadienyl ligand
Cu	copper
° C	degrees Celcius
d	doublet
DCM	dichloromethane
DSC	differential scanning calorimetry
EtOH	ethanol
Fe	iron
FG	functional group
g	gram
GC	gas chromatography
$gmol^{-1}$	grams per mole
GPC	gel permeation chromatography
H	hydrogen
H_2O	water

H_2O_2	hydrogen peroxide
HMBC	heteronuclear multiple bond coherence
HSQC	heteronuclear single quantum coherence
IR	infrared spectroscopy
$KHSO_5$	potassium peroxymonosulfate (oxone)
LG	latent reactivity group
m	multiplet
Me	methyl group
MeCN	acetonitrile
MeOH	methanol
mg	milligram
MHz	megahertz
min	minute
mL	millilitre
mM	millimolar
mmol	millimole
M_n	number average molecular weight
Mn	manganese
Mn(TDCPP)OAc	manganese *meso*-tetra-2,6-dichlorophenylporphyrin acetate
Mo	molybdenum
mol%	mole percent
NaOH	sodium hydroxide
nm	nanometer
OH	hydroxyl group
OTf	triflate
PDI	polydispersity index
PDP	2-({(S)-2-[(S)-1-(pyridin-2-ylmethyl)pyrrolidin-2-yl]pyrrolidin-1-yl}methyl)pyridine
PG	protecting group

ppm	parts per million
PS	polystyrene
Py	pyridine
Rh	rhodium
Ru	ruthenium
s	singlet
SbF_6	hexfluoroantimonate
t	triplet
T_g	glass transition temperature
THF	tetrahydrofuran
TPA	tris(2-pyridylmethyl)amine
µL	microlitre
µmol	micromole
wt%	weight percent

List of Symbols

Å	angstrom
δ	chemical shift
λ	wavelength
k_H/k_D	kinetic isotope effect
L	ligand
M	metal
R	substituent
X	halide or electron withdrawing group

Chapter 1

Introduction

1.1 Polystyrene

Polystyrene (PS) is a material that is ubiquitous in everyday life. Most people may recognize it best as recycling plastic number six. It has no taste, odour or toxicity, and exhibits low water absorption, low electrical conductivity and high refractive index.[1] It is easily processed as a hard solid for use as packaging of food and other materials and for casings of small appliances, or as extruded foam for insulation of buildings or the infamous foam packaging "peanuts" .[1] Its chemical inertness is a contributing factor to its popularity as a consumer plastic as well as to its material uses in chemistry as a cross-linked gel for separations[2] and as a resin for support of catalysts or enzymes.[3] However, the inert nature of PS poses a challenge for disposal of the consumer material. Recycling programs exist, but the material that ends up in dumps and as litter does not readily decompose. As well, its non-polar nature, which contributes to its inertness, also limits the ability to interact with polar substances, like paint for instance, limiting some applications.

1.2 Oxyfunctionalization of Polymers

While inert polymers such as polyethylene, polypropylene and polystyrene are easily processed and are used in a wide variety of applications, their lack of polarity

results in low hydrophilicity, printability, selective permeability and adhesion characteristics.[4] Thus methods have been developed to introduce polar functionality such as hydroxyl and carbonyl groups into these polymers, either during the polymerization process itself or afterward as a post polymerization modification. Low levels of functionality are desired to slightly alter the surface interactions but leave the bulk mechanical properties the same.[5]

1.2.1 Polymerization with Functionality

1.2.1.1 Copolymerization

Copolymerization is the result of the incorporation of two (or more) different monomers into the same polymer chain. In this case, one of the monomers would contain the desired functional group (Figure 1). The method opens up a vast number of possible functional groups, but if the polymerization is reliant upon a transition metal catalyst it also opens up the possibility of catalyst incompatibility with the functional groups. Catalysts have been developed to overcome this limitation[6] and can be specific to the desired polymer and functional group. Another way around this limitation is to use a monomer with either a protected functional group or a group with latent reactivity (Figure 1).[5] In both cases the group is tolerated by the catalyst and can be either deprotected or transformed into the desired functional group in a post-polymerization step. However, these methods increase the number of steps required to produce the desired polymer, possibly increasing the consumption of solvents and reagents and the complexity of the entire synthesis.

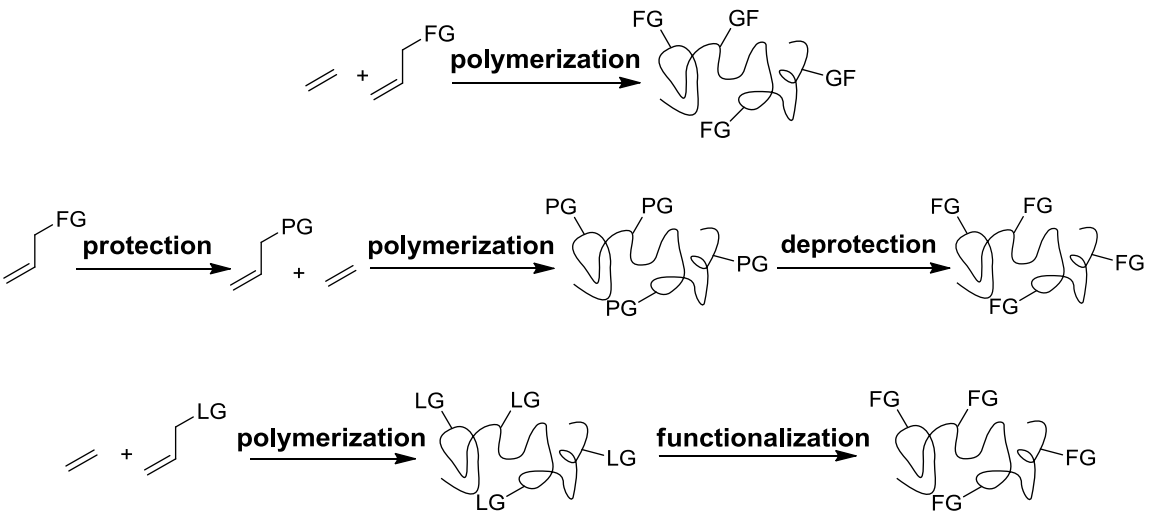

Figure 1. Functionalization of polymers via direct copolymerization (top), copolymerization with protected functional groups (middle), and copolymerization with groups with latent reactivity

1.2.1.2 Graft Copolymerization

Graft polymerization creates pendant chains at specific sites along the backbone of the polymer.[4] The functionality is included in the pendant chain. Grafting involves the creation of sites for chain attachment through various methods, generally involving the formation of either ions or radicals.[4] Unlike copolymerization, the functionality is not incorporated into the backbone of the polymer but into the branches. The branching that is a result of this method could have an impact on the bulk mechanical properties of the material.

1.2.2 Post Polymerization Functionalization

The idea of introducing functionality into an already prepared polymer has the advantage of not interfering with the standard polymerization methods. Once the

polymer is synthesized, the functionalization can then take place in either the solid state or in solution, depending on the chosen method.

1.2.2.1 Flame/Plasma Treatment

Flames[7] and plasmas[8] can be used to incorporate oxygen functionality onto the surface of a solid polymer, resulting in a surface with hydrophilic properties. The methods are generally applicable, but the use of high temperatures makes the processes destructive. There is little control as to what type of functionality results, with generation of hydroxyl, carbonyl and radical groups having been reported.[7,8] Often these groups are then used as positions for attachment of grafts for surface modification. The bulk of the material remains unfunctionalized.

1.2.2.2 Transition Metal Catalysts

The idea behind the use of transition metal catalysts for post polymerization modification is that whatever chemical reactions work with small molecule alkanes should also work on their macromolecular assemblies. However, this avenue has not been widely pursued.[5,9] In fact, the only attempts reported in the literature are those of Hillmyer, Boaen et al., who in 2002 used a $[Cp^*RhCl_2]_2$/bis-pinacoldiboron system developed by Hartwig et al. to first borylate the terminal alkane groups of polyethylethylene at 150 °C over 36 hours, then transform the borylated positions into hydroxyl groups using hydrogen peroxide under basic conditions (Figure 2) .[10] Both a

low and high molecular weight model polyethylethylenes were used – 1200 $gmol^{-1}$ and 37 000 $gmol^{-1}$ respectively. Hydroxylation of both molecular weight compounds was confirmed with detection of the α methylene position in both ^{1}H NMR (3.7 ppm) and ^{13}C NMR (60.15 ppm) as well as with a broad OH band in the IR spectrum at 3300 cm^{-1}.

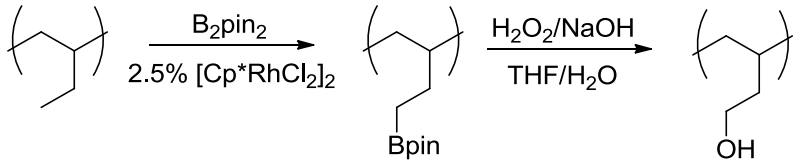

Figure 2. Hydroxylation of polyethylethylene with $[Cp^*RhCl_2]_2$ and bispinacoldiboron[10]

Hydroxylation was also suggested by an increased T_g for the materials, which could indicate significant hydrogen bonding due to hydroxyl groups. In 2003, Hillmyer and Boaen reported the use of a manganese porphyrin complex (Mn(TDCPP)OAc) (Figure 3) and $KHSO_5$ to introduce hydroxyl and ketone functionalities[11] into squalane and a model polymer, polyethylene-*alt*-propylene, with a molecular weight of 5000 $gmol^{-1}$ (Figure 4).

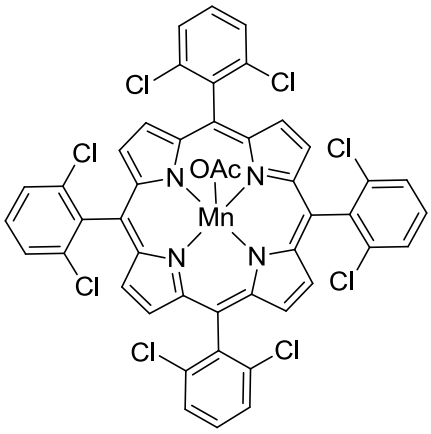

Figure 3. Mn(TDCPP)OAc

Again functionalization was observed through IR peaks for OH and ketone functionalities at 3400 and 1710 cm^{-1} respectively, as well as through the presence of signals for the α methylene position in both ^{1}H NMR (2.6 ppm) and ^{13}C NMR (42 ppm) and the quaternary carbonyl carbon (73 ppm). The T_g of the material also increased.

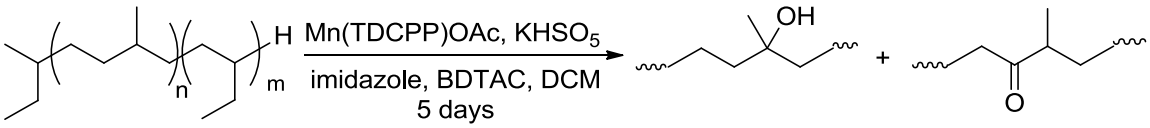

Figure 4. Oxyfunctionalization of polyethylene-*alt*-propylene using Mn(TDCPP)OAc and $KHSO_5$ [11]

1.3 Oxyfunctionalization of Small Molecule Alkanes with Transition Metal Catalysts

The real beginning of oxyfunctionalization with transition metals was when Fenton reported, in 1894, the oxyfunctionalization of tartaric acid in the presence of ferrous sulphate and hydrogen peroxide.[12] He reported various colour changes with different conditions, but did not postulate how this reaction worked. In 1934, Haber and Weiss proposed the generation of radical species[13] as the mechanism for hydrogen peroxide decomposition in the presence of iron salts, which is still the generally accepted pathway.[14] However, in 1959, Kremer and Stein proposed a non-radical decomposition pathway[15a] with supporting kinetic evidence that was the subject of further research by Kremer.[15b] The involvement of charged species rather than radicals fell in line with the type of mechanism that biochemists were looking for to explain enzymatic oxidation reactions, and indeed the proposed mechanism shows itself again in the literature decades

later for biomimetic systems[16] showing that both pathways are valid, but for different conditions. As research of enzymatic reactions progressed, so did the ability to model the active sites of the enzymes. Eventually transition metal complexes were developed as mimics for enzymes capable of alkane oxyfunctionalization such as Cytochrome P450 (heme based), methane monooxygenase (di-iron or di-copper complexes) and Rieske dioxygenase (non-heme based). Many of these model systems succeed in introducing hydroxyl or ketone functionality into alkanes as well as epoxidizing alkenes, a topic not covered in the present paper.

1.3.1 Heme-Based Systems

The distinguishing feature of the heme analogues is a metalloporphyrin motif (Figure 5). Iron-heme complexes function as oxygen transport and storage in blood yet

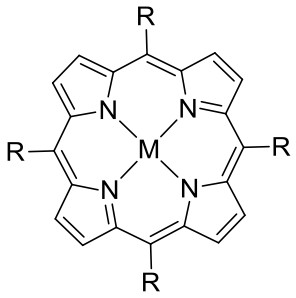

Figure 5. General metalloporphyrin structure

react catalytically with oxygen in the internal environment of Cytochrome P450 suggesting that the different environments promote different roles. Consequently, in attempts to mimic the catalytic activity variations in sterics and electronics have been accomplished by changing the nature of the R groups seen in Figure 5.

Oxyfunctionalization of alkanes with metalloporphyrins was first reported by Groves[17] in 1979. He used chloro-α,β,γ,δ-tetraphenylporphinatoiron(III) with iodosylbenzene and substrate (both alkanes and alkenes) in dichloromethane under nitrogen at room temperature. Low to moderate yields of alcohols or epoxides, depending on the substrate, were recovered proving the ability of the complex to produce oxyfunctionalized products. Since this work, three different generations of substituted tetraarylporphyrins have been developed (Figure 6), each with improved catalytic results

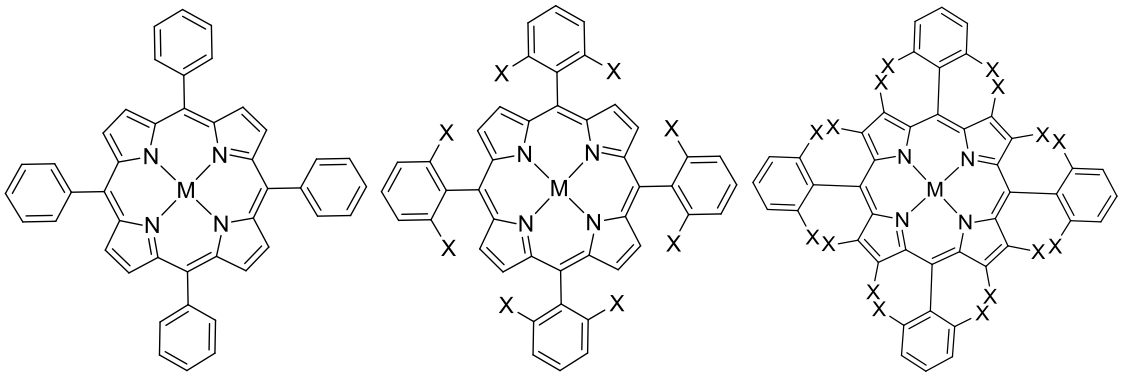

Figure 6. The general form of the first (left), second (centre) and third (right) generations of substituted tetraarylpophyrins, with X generally being a halide or other electron withdrawing group

and robustness.[18,19] For example, the complex used by Hillmyer, Boaen et al. for their oxyfunctionalization of model polymers[11] falls into the second generation. Many years later, a more highly chlorinated species, iron(III) 5-(pentafluorophenyl)-10,15,20-tris(2,6-dichlorophenyl)-2,3,7,8,12,13,17,18-octachloroporphyrin, was used to oxidize alkanes and alkenes to give alcohol, ketone and epoxide products. Both iodosylbenzene and hydrogen peroxide were used as oxidants in dichloromethane and

dichloromethane/acetonitrile solutions respectively. Overall, the third generation complex gave moderate yields with iodosylbenzene and low yields with hydrogen peroxide if the oxidant was added slowly.

In general, the more electron-withdrawing the substituted species is, the more robust and active the catalyst.[18] This statement can be explained by considering the proposed generation of the active species for the metalloporphyrins (Figure 7). The

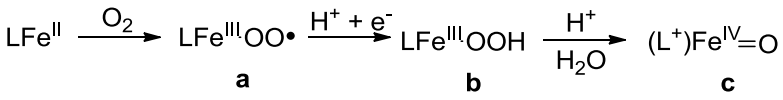

Figure 7. Proposed generation of active species for metalloporphyrin complexes[16]

binding of the oxidant results in the generation of a superoxo (Figure 7(a)) or peroxo (Figure 7(b)) Fe(III) species (depending on oxidant) that undergoes O-O bond cleavage to give a highly unstable oxoiron(V) species. However, due to the proximity of the aromatic porphyrin, there is a radical delocalization resulting in an oxidized porphyrin radical, making oxoiron(IV) (Figure 7(c)) the reactive species.[16]

Porphyrins of Fe, Mn, Cu and Ru have been successfully used for oxyfunctionalization catalysis. They show high selectivity for tertiary or activated C-H bonds, but only moderate chemo- and regio-selectivity and are limited in the variations that can be done to the structure.[20]

1.3.2 Non-Heme Systems

In comparison to heme systems, non-heme systems offer greater degrees of variability when constructing ligands and attempting to tune electronic and steric effects.

They have a broad range of substrates and, under the right conditions, can be selective. On the other hand, they are less robust[20] and the sheer number of possible ligands makes generalizing characteristics nearly impossible unless the ligands come from the same family. Consequently only a small selection relevant to the ensuing research will be discussed. Oxyfunctionalization of cyclohexane and adamantane are the standard reactions of choice throughout the literature with the oxidant generally being hydrogen peroxide or *tert*-butyl hydroperoxide and added via syringe pump over a set period of time. Many reports look at a broader substrate scope, but the use of these two substrates across studies allows for a basic comparison of the catalytic activity and selectivity of each complex.

1.3.2.1 Fe(TPA) Complexes

The TPA system seems to first appear in research conducted by Que[21] and is now a well studied and characterized non-heme system. TPA (Figure 8) is a nitrogen based tetradentate tripodal ligand and variations on the structure generally involve functionality

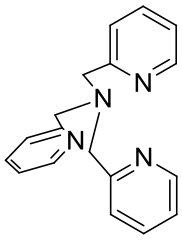

Figure 8. Structure of TPA ligand

substituted onto the pyridine rings at the 3, 5 or 6 position.[22] The iron(II) complexes have been made with various counter ions, but these become less relevant once the complex is

dissolved in acetonitrile to give $[Fe(TPA)(MeCN)_2]^{2+}$, which is the species present at the beginning of the catalytic reactions.[22] Evidence for the generation of any peroxo or oxo complexes is generally shown as a difference in solution characteristics from this species in acetonitrile.

The family of Fe(TPA) complexes, with tert-butoxide as oxidant, were shown to oxyfunctionalize cyclohexane[23] with initial yields of 16 % and an alcohol to ketone (A/K) ratio of 0.5. However, it was observed that using a syringe pump to deliver the oxidant resulted in an increased yield, and that decreasing the equivalents of oxidant from 150 to 50 resulted in a combined alcohol and ketone yield of 30 % with a significant increase in the amount of alcohol produced. In fact the A/K ratio was reported as 18.[23] These unexpected observations led to the beginning of investigation into the mechanism of these oxyfunctionalization reactions.

1.3.2.2 Mechanistic considerations

With the vast number of possible non-heme systems, it is not surprising that there are contradictions in the literature over the mechanism of alkane oxyfunctionalization reactions. Do they proceed through high-valent intermediates with assistance from the ligands like the heme system, or do they produce radicals like Fenton's reagent? Further confusion ensued when it became clear that some systems produced products with retention of stereochemistry while others did not. The answer seems to be that the mechanism depends on the system. In 1996 Que et al. published a proposed mechanistic scheme (Figure 9) for Fe(TPA) that meshed the two sides of the mechanistic argument.[23]

The proposal was based on competition between the radical pathway (a) and the metal-based pathways (b) and (c) after the generation of the iron peroxo species. In solution, the Fe(TPA)-OOH species can abstract a hydrogen from either the peroxide or the alkane. In pathway (a), the formation of the peroxo radical in solution leads to the formation of the alkyl radical, which can then be trapped by atmospheric oxygen to form both alcohol

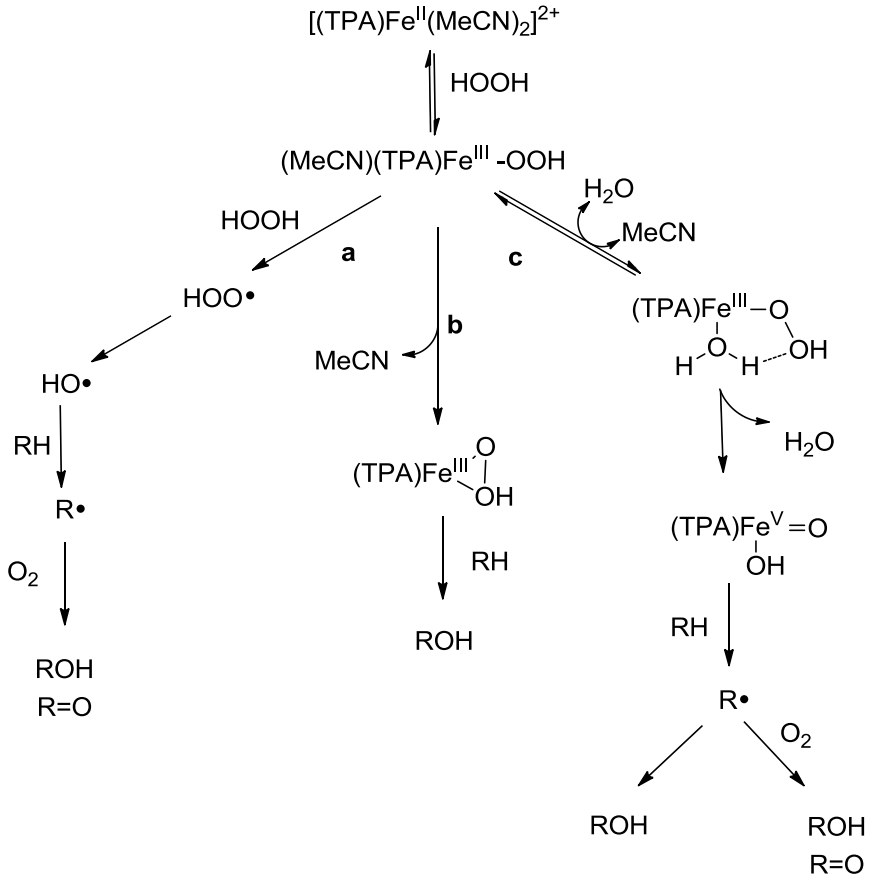

Figure 9. Proposed mechanistic scheme for Fe(TPA)

and ketone products. Alcohol to ketone (A/K) ratios of ≤ 1, lack of stereoretention and generation of oxygen by peroxide disproportionation are characteristic of this pathway. In pathway (b), the alcohol product results from the direct insertion of oxygen into the

C-H bond. This should result in product containing oxygen atoms solely derived from the hydrogen peroxide. In pathway (c), the abstraction of a hydrogen from the alkane by the peroxo species generates an alkyl radical that can also be trapped by oxygen to give alcohol and ketone products, or can react with the high-valent oxoiron species right next to it in an oxygen rebound step. The scheme was validated by satisfying the experimental observations that when large concentrations of peroxide are present in the reaction, both alcohol and ketone products are produced due to the dominance of pathway (a), but if the peroxide is maintained at a low concentration, only alcohol products result. This was further validated by kinetic isotope studies for the abstraction of hydrogen from cyclohexane. In the case of high peroxide concentration $k_H/k_D = 4$, which is characteristic of radical abstraction, while in the case of low peroxide concentration $k_H/k_D = 10$. This high value is similar to those obtained for metalloporphyrin systems known to go through a high-valent metal intermediate, supporting the metal based pathway (c). As well, increasing the bulkiness of the ligand by placing methyl groups at position 6 on the pyridines should inhibit the rebound step, and with oxygen labelling experiments it has indeed been shown that the alkyl radical is trapped by oxygen, giving rise to labelled alcohol and ketone products.[22]

None of the above evidence excludes the possibility of contributions from pathway (b). During experiments done by Que et al. with labelled water, it was noted that more ^{18}O was incorporated into products from substrates with stronger C-H bonds, indicating a competition between C-H cleavage and water exchange. It was also noted that, after a certain point, the use of more $H_2{}^{18}O$ did not change the overall incorporation

of the label into the product. This saturation level was indicative of a preequilibrium binding of water, as seen with metalloporphyrins[22] and which would not be seen if the direct insertion pathway (b) was present. The use of labelled peroxide in cyclohexane oxyfunctionalization gave 70 % labelled cyclohexanol, with the remaining alcohol unlabeled. The complementary experiment with un-labelled peroxide and labelled water returned cyclohexanol with 27 % label inclusion indicating that exchange with water contributes to the mechanism.[22] This leaves pathway (c) as the most viable option, but the generation of the high-valent species from the decomposition of the peroxo species was difficult to observe. This decomposition (Figure 10) can happen in three different ways: (a) the direct insertion into the alkane C-H bond, (b) O-O bond homolysis to give the LFe(IV)=O species and the hydroxyl radical, or (c) O-O bond heterolysis to give the LFe(V)=O species and the hydroxide ion. Direct insertion has been ruled out by the

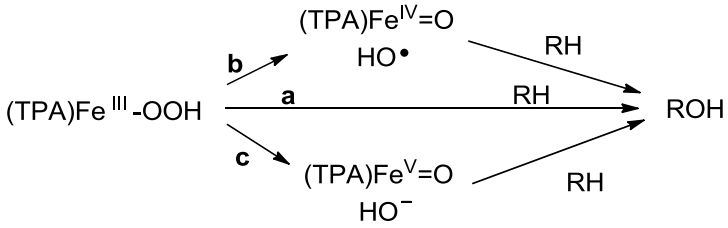

Figure 10. Decomposition pathways for the (TPA)Fe^{III}-OOH species

observations from the above water-labeling experiments. Again experiments done by Que et al. using ^{18}O labeled water and peroxide[22,24] have provided insight into the possible nature of the active iron complex. The observations that cyclohexane reacts with KIE values greater than 3 and that adamantane regioselectivity is high eliminate the possibility of hydroxyl radical involvment[22] and thus the homolysis of the O-O bond

(pathway (b)). This leaves the heterolysis of the O-O bond (pathway (c)) as the most likely candidate for the formation of the active species. All these combined results led Que et al. to propose a mechanistic pathway for Fe(TPA) complexes that includes initial equilibrium with water and the formation of an Fe(V) oxo species[22] as seen in Figure 9, pathway (c). It must be noted that this mechanistic pathway is only valid for Fe(TPA) complexes under conditions where H_2O_2 is limiting. If the ligand or metal or conditions are changed, this can change the decomposition pathway of the peroxo species, resulting in different product distributions and/or different catalyst activity.

1.3.2.3 Fe(BPMEN)

BPMEN (Figure 11) is a linear, nitrogen based tetradentate ligand whose iron complex shows characteristics and activity similar to that of Fe(TPA)[22,24] under identical conditions. It is thought to follow a similar mechanistic pathway to Fe(TPA)[24] showing retention of stereochemistry in the alcohol products when H_2O_2 is limiting.

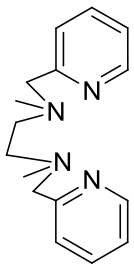

Figure 11. Structure of BPMEN ligand

1.3.2.4 Ligand Effects

The two families of ligands discussed above, TPA and BPMEN, have been used for investigations into the effects of ligands upon the iron-catalyzed oxyfunctionalization

of cyclohexane.[25-28] Throughout the literature the general catalytic conditions involve acetonitrile as solvent and peroxide as oxidant, in limiting amounts. The yields are reported as combined alcohol and ketone yields and are based on the total amount of oxidant used. The A/K ratio is also reported as an indicator of metal-based oxyfunctionalization versus radical processes. Britovsek et al. began with a comparison between the tetradentate ligands (TPA, BPMEN) and rigid tridentate ligands[27] and found that the oxyfunctionalization of cyclohexane with tetradentate iron complexes produced an approximately ten-fold greater combined yield than the tridentate ligands and with a generally two-fold better A/K ratio. It was proposed that the tridentate ligands, with the three open coordination sites, are more conducive to radical mechanisms[27] as there was generally evidence of a cyclohexyl hydroperoxide product, whereas there was none detected with the tetradentate ligands.

Britovsek et al. also investigated the effects of pyridine donors versus amine donors by taking TPA and systematically changing the pyridyl groups for amine groups.[26] BPMEN was also investigated as it is an isomer of one of the derived ligands. The results showed that the yield of oxyfunctionalized cyclohexane, along with the A/K ratio, significantly decreased for ligands with three or more amine groups. Furthermore, BPMEN had the highest yield and TPA had the second highest yield along with the highest A/K ratio, suggesting that the pyridyl groups promote the metal-based mechanism. Keeping the two pyridyl groups, Britovsek changed the other two coordinating atoms to either oxygen or sulfur[25], both elements found abundantly in nature. None of the iron complexes of these modified ligands produced any detectable

oxyfunctionalization of cyclohexane, suggesting that the coordination of a nitrogen atom is essential with these types of ligand systems.

The effect of the pyridyl groups could also be a steric one – they are larger and more rigid than the amines. To investigate the effect of rigidity in the ligands, Britovsek used a series of BPMEN ligands with biphenyl-bridged backbones.[28] The results were similar to the previous attempts to modify these ligands. The iron complexes of the modified ligands gave yields and A/K ratios three to four times smaller than the iron complexes of the unmodified ligands. Changing the metal to Mn or Co resulted in no observed oxyfunctionalization of cyclohexane. In the end, after all the variations in TPA and BPMEN, the unmodified ligands still gave the best yields and A/K ratios.

1.3.2.5 Practical Applications

The discussion so far has centered on the oxyfunctionalization of cyclohexane, but for interest in this approach to be useful a catalyst needs to be capable of functionalizing much more complex molecules in a controlled manner. White et al. did just that using the iron complex of a BPMEN derived ligand with chirality along the backbone[29,30] (Figure 12). The focus of this research was not on changes in the complex itself, but on

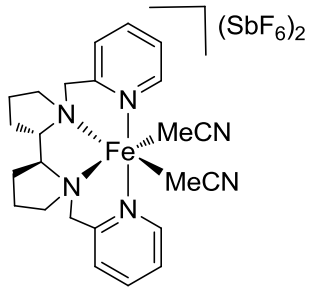

Figure 12. Structure of [Fe(S,S-PDP)][SbF_6]$_2$

how changes in the substrate affected the results from the catalytic reactions. They determined that C-H bond reactivity decreased from tertiary to secondary to primary and that, if an electron-withdrawing functional group is present, oxyfunctionalization occurs primarily at the most remote location from the group (Figure 13). The directing ability of a functional group is a stronger effect than the inherent reactivity of the C-H bond,[30] meaning that if a tertiary bond is adjacent to an electron-withdrawing group, it will be

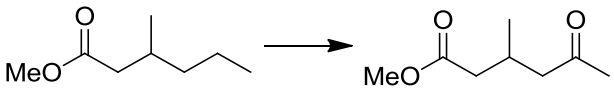

Figure 13. Selectivity of [Fe(S,S-PDP)][SbF_6]$_2$ in presence of electron withdrawing group

deactivated and other secondary C-H bonds will be functionalized first. As well, if the substrate was set up with the appropriate groups, cyclic lactones could be produced (Figure 14), increasing the synthetic utility of the approach.[29] White et al. used the

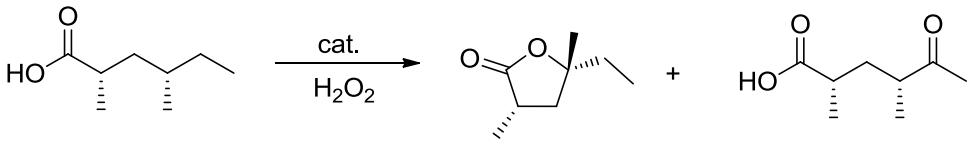

Figure 14. Production of cyclic lactones using [Fe(S,S-PDP)][SbF_6]$_2$

knowledge of how the catalyst reacts to different substrates to successfully oxyfunctionalize terpenoid derivatives in a predictable manner using H_2O_2. This type of success begins to show the possible synthetic power of the approach.

1.4 Aims of Present Research

As described above, iron complexes of nitrogen based tetradentate ligands have garnered much attention and their ability to oxyfunctionalize small molecule alkanes, as well as recently the oxyfunctionalization of more complex molecules, has been widely investigated. In principle, if functionalization is possible with these small molecules, then it should also be possible with analogous polymers but there is a significant lack of investigation into this concept. This research looks at using the Fe(TPA) and Fe(BPMEN) complexes to oxyfunctionalize polystyrene with hydrogen peroxide as oxidant. Since the general catalytic conditions for these complexes involve MeCN as the sole solvent, and PS is not soluble in MeCN, new reaction conditions must be developed and validated. The reaction could result in both hydroxyl and ketone groups and thus infrared spectroscopy (IR) will be used to initially determine the type of functionality since this analytical method has a high sensitivity for these functional groups. Finally, any polymeric products showing signs of oxyfunctionalization in the IR spectrum will be characterized by GPC for molecular weight analysis, DSC for changes in T_g and NMR spectroscopy to determine the nature and location of the oxyfunctionalization. This research will provide a proof of principle for the use of iron non-heme complexes and hydrogen peroxide to oxyfunctionalize polystyrene to a low degree. The inclusion of low levels of oxygen based functionality may increase the propensity of the material to biodegrade without significantly changing the applications of the material, but this possibility is not explored.

Chapter 2

Experimental

This chapter describes the various reactions and procedures involved in this thesis. Section 2.2 covers the synthetic reactions for ligands and catalysts while Section 2.3 describes the composition of the various hydrogen peroxide solutions. Oxyfunctionalization of cyclohexane was used to verify the catalytic activity of the synthesized complexes, as outlined in Section 2.4, and reactions done without catalyst or polystyrene, to ensure that the observed results were in fact due to catalytic oxyfunctionalization of the polymer, are described in Section 2.5. Finally, the general procedures for catalytic reactions of high molecular weight polystyrene (Sections 2.6.1 through 2.6.5), low molecular weight polystyrene (Sections 2.6.6 through 2.6.9) and low molecular weight polystyrene with iterative additions of catalyst and oxidant (Sections 2.6.10 and 2.6.11) are presented. All catalytic reactions that produced oxyfunctionalized product were repeated at least twice. The details of the analyses of the glass transition temperature (T_g) and number average molecular weight (M_n) are described in Section 2.7, along with tables of selected data.

2.1 General Conditions

All reagents were purchased from Sigma-Aldrich, with the exception of the low molecular weight polystyrene purchased through Alfa-Aesar, and were used as received unless otherwise noted. Dichloromethane (DCM), tetrahydrofuran (THF) and ether were

dried by passage through columns of activated alumina and were stored over activated 3Å molecular sieves for at least a day. Acetonitrile (MeCN) was taken directly from the bottle and dried by storage over activated 3Å molecular sieves for at least two days. All air sensitive compounds and reagents were stored under nitrogen in an MBraun Labmaster glove box and all air sensitive manipulations were done using standard Schlenk line techniques under dry, deoxygenated argon.

NMR spectra were recorded using Bruker AV 300, 400 and 600 spectrometers (600 MHz spectrometer operated by Dr. F. Sauriol) with the spectra being analyzed using either Bruker Topspin version 3.0 or ACDLabs 11.0 processing software. The chemical shifts were referenced to carbons or residual protons of the deuterated solvent. IR spectra were obtained with a Perkin-Elmer Spectrum One FT-IR spectrometer and were analyzed using Spectrum software. General IR procedure involved dissolving a small amount of the sample in a minimal amount of dichloromethane, dropping the solution onto a salt plate and allowing it to air dry before placing it in the spectrometer. X-Ray analysis was done by Dr. R. Wang using a Bruker SMART APEX II X-ray diffractometer with graphite-monochromated Mo K_α radiation (λ = 0.71073 Å).

2.2 Preparation of Complexes

2.2.1 Synthesis of $Fe(MeCN)_2(OTf)_2$[31]

Iron powder (1.13 g, 0.02 mol) and a dry stir bar were added to a dry two-neck Schlenk flask that was fitted with a condenser. The set-up was placed under vacuum and purged with argon. Dry MeCN (20 mL) was added followed by 3.81 mL (0.04 mol) of

trifluoromethanesulfonic acid, with no stirring, to give a clear green-blue effervescing solution. Once the initial effervescence had stopped, the flask was lowered into a 60 °C oil bath to ensure continued effervescence. The reaction continued overnight. Once the effervescence had stopped, the clear green-blue solution was filtered under argon to remove any remaining iron, the volume was reduced by a quarter under vacuum, and the flask sealed under argon and placed in the freezer at -30 °C. After several days, the pale green-blue crystals were collected via filtration under argon, rinsed with 2 × 5.0 mL dry ether and dried under vacuum to give a white powdery solid (5.10 g, 58 %). The recovered solution and the ether washes were re-sealed and placed back in the freezer. Several days later, a second crop of green-blue crystals was recovered in a similar manner (2.11 g, 24 %) and combined with the first crop.

2.2.2 Synthesis of TPA[26]

Sodium triacetoxyborohydride (6.24 g, 0.02 mol), dry DCM (150 mL) and 2-aminomethylpyridine (1.00 mL, 0.01 mol) were combined in a dry Schlenk flask under argon with stirring. Once the cloudy white mixture contained no clumps of sodium triacetoxyborohydride, 2-pyridine carboxaldehyde (2.00 mL, 0.02 mol) was added and stirring was continued for 18 hours resulting in a cloudy, bright yellow solution. The reaction was quenched by the addition of approximately 152 mL saturated sodium bicarbonate solution until no gas was produced, opened to the air and stirred for an additional 20 minutes. The biphasic mixture was transferred to a separatory funnel where it was extracted with ethyl acetate (166 mL). The organic layer was collected, dried with

magnesium sulfate and filtered before the solvent was removed to leave a pale yellow solid. The solid was transferred to a Soxhlet thimble and a Soxhlet apparatus was used to extract the TPA with 100 mL petroleum ether (bp. 36-69 °C) over the course of 12 hours. The solvent was removed and the light yellow solid dried under vacuum (2.39 g, 85 %). ^{1}H NMR ($CDCl_3$, 300 MHz): δ 8.54 (d, 3 H, ^{3}J = 6 Hz), 7.63 (m, 6 H), 7.15 (t, 3 H, ^{3}J = 6 Hz), 3.89 (s, 6 H). ^{13}C NMR ($CDCl_3$, 300 MHz): δ 160.5, 150.9, 137.9, 124.7, 123.0, 60.2. Literature ^{1}H NMR ($CDCl_3$)[26]: δ 8.53 (d, 3 H, 6-PyH), 7.63 (m, 6 H, 3-PyH and 4-PyH), 7.14 (t, 3 H, 5-PyH, 3.88 (s, 6 H, NCH_2). Literature ^{13}C NMR ($CDCl_3$)[26]: δ 159.3, 149.1, 136.4, 123.0, 122.0, 60.1.

2.2.3 Synthesis of BPMEN[26]

Sodium triacetoxyborohydride (7.87 g, 0.03 mol), dry DCM (170 mL) and N,N'-dimethylethylenediamine (1.42 mL, 0.013 mol) were combined in a dry Schlenk flask under argon with stirring. Once the cloudy white mixture contained no clumps of sodium triacetoxyborohydride, 2-pyridinecarboxaldehyde (2.52 mL, 0.026 mol) was added and stirring was continued for 12 hours resulting in a cloudy, bright yellow solution. The reaction was quenched by the addition of approximately 160 mL saturated sodium bicarbonate solution until no gas was produced, opened to the air and stirred for an additional 20 minutes. The biphasic mixture was transferred to a separatory funnel where it was extracted with ethyl acetate (166 mL). The organic layer was collected, dried with magnesium sulfate and filtered before the solvent was removed to leave a dark orange-brown solid. The liquid was dissolved in 40 mL dry tetrahydrofuran (THF) while 0.21 g

(8.6 mmol) sodium hydride was suspended in 40 mL dry THF and then added to the previous solution. Over the course of 90 minutes of stirring, the thick cloudy reaction mixture changed from yellow to orange, then magenta and back to orange before finally staying orange-brown. The solvent was removed under vacuum to leave a thick, dark brown liquid. Pentane (20 mL) was added to the brown liquid to extract the product. After a couple such extractions, the dark brown liquid had become a lighter orange solid that could then be transferred to a Soxhlet thimble and a Soxhlet apparatus was used to extract the BPMEN with 100 mL pentane over the course of 24 hours. The solvent was removed and the pale yellow, non-volatile liquid was dried under vacuum (1.72 g, 48 % yield). ^{1}H NMR ($CDCl_3$, 300 MHz): δ 8.49 (d, 2 H, ^{3}J = 3 Hz), 7.58 (t, 2 H, ^{3}J = 7.5 Hz), 7.38 (d, 2 H, ^{3}J = 9 Hz), 7.10 (t, 2 H, ^{3}J = 6 Hz), 3.64 (s, 4 H), 2.60 (s, 4 H), 2.23 (s, 6 H). ^{13}C NMR ($CDCl_3$, 300 MHz): δ 159.5, 149.1, 136.5, 123.2, 122.0, 64.4, 55.7, 43.0. Literature ^{1}H NMR ($CDCl_3$)[26]: δ 8.48 (d, 2 H, 6-PyH), 7.56 (t, 2 H, 4-PyH), 7.36 (d, 2 H, 3-PyH), 7.10 (t, 2 H, 5-PyH), 3.63 (s, 4 H, $PyCH_2$), 2.60 (s, 4 H, NCH_2CH_2N), 2.22 (s, 6 H, NMe). Literature ^{13}C NMR ($CDCl_3$)[26]: δ 158.9, 148.6, 136.1, 122.8, 121.6, 63.8, 55.1, 42.5.

2.2.4 Synthesis of $Fe(TPA)(MeCN)_2(OTf)_2$[32]

2.2.4.1 Inert Atmosphere Procedure

TPA (0.29 g, 1.0 mmol) was placed in a dry Schlenk flask under argon and dissolved in dry MeCN (4.0 mL) with stirring to give a clear golden solution. In a separate dry flask $Fe(OTf)_2(MeCN)_2$ (0.44 g, 1.0 mmol) was dissolved in dry MeCN (4.0

mL) to give a clear, very pale blue solution. The iron solution was added to the TPA solution and an immediate colour change to deep red occurred. The mixture was stirred for 30 minutes under argon. The slow addition of dry ether (10 mL) made the solution distinctly cloudy. The sealed flask was placed in the freezer overnight and in the morning deep red crystals were collected via filtration under argon (0.39 g, 53 % yield). ^{1}H NMR (CD_3CN, 300 MHz): δ 11.49 (broad s, 3 H), 8.76 and 8.67 (both s, combined 6 H), 7.32 (t, 3 H, ^{3}J = 7.5 Hz), 6.70 (broad s, 6 H). Literature ^{1}H NMR (CD_3CN, 360 MHz)[31]: δ 12.12 (broad s, 3 H), 9.02 (s, 3 H), 8.92 (s, 3 H), 7.33 (t, 3 H, ^{3}J = 7.3 Hz), 7.09 (s, 6 H).

2.2.4.2 Open to Atmosphere

The same general procedure was followed as above, but solvents were used as purchased and all reactions were done in open flasks. The ether was cooled in the freezer prior to addition to the reaction mixture. The crystals collected from the above procedure (yield of 83 %) were suitable for X-ray analysis. ^{1}H NMR (CD_3CN, 300 MHz): δ 13.16 (broad s, 3 H), 9.54 and 9.40 (both s, combined 6 H), 7.81 (broad s, 6 H), 7.18 (t, 3 H, ^{3}J = 7.5 Hz).

2.2.5 Synthesis of Fe(BPMEN)(OTf)$_2$[26]

BPMEN (0.33 g, 1.2 mmol) was placed in a dry Schlenk flask under argon and dissolved in dry THF (8.0 mL) with stirring to give a clear, pale yellow solution. In a separate dry flask $Fe(OTf)_2(MeCN)_2$ (0.53 g, 1.2 mmol) was dissolved in dry THF (15

mL) under argon with stirring giving a clear, colourless solution. The iron solution was added to the BPMEN solution resulting in a dark, opaque mixture that became grape-juice purple with a fine yellow solid visible in the solution. The reaction continued for 18 hours under argon with stirring, at which point the solution was concentrated to about half the volume and the fine yellow solid collected via filtration under argon. The solid was rinsed with 3 × 3.0 mL dry THF and left to dry under vacuum before collection under inert atmosphere (0.51 g, 67 % yield). ^{1}H NMR (CD_2Cl_2, 300 MHz): δ 166.01, 123.75, 93.32, 73.64, 54.54, 53.95, 27.10, 16.57, -15.44. ^{1}H NMR (CD_3CN, 300 MHz): δ 88.85, 69.92, 45.47, 31.69, 27.80, 14.78. Literature ^{1}H NMR (CD_2Cl_2)[26]: δ 169.4 (2 H), 123.5 (2 H), 94.4 (2 H), 74.7 (6 H), 54.8 (2 H), 53.6 (2 H), 28.4 (2 H), 15.9 (2 H), -15.6 (2 H). Literature ^{1}H NMR (CD_3CN)[26]: δ 81.2 (2 H), 64.1 (2 H), 41.8 (6 H), 27.2 (8 H), 13.8 (2 H), 0.6 (2 H).

2.3 Hydrogen Peroxide Solutions

Hydrogen peroxide solutions were made and added drop-wise immediately to the reactions via a buret unless otherwise noted. The 10 % solution was made by adding 3.0 mL of 30 % hydrogen peroxide in water to 7.0 mL of MeCN. The amount of hydrogen peroxide added to the reactions was controlled by either scaling the above preparation (ie. a total amount of 5.0 mL instead of 10.0 mL), or by changing the concentration of the 10.0 mL solution (ie. 1.5 mL H_2O_2 and 8.5 mL MeCN for a 5 % solution). The 70 mM solution was made using 71.5 μL of 30 wt% H_2O_2 solution and diluting it with MeCN to 10 mL.

2.4 Catalytic Activity of Complexes – Oxyfunctionalization of Cyclohexane

2.4.1 Fe(TPA)/Fe(BPMEN) in MeCN

A 1.0 μmol/mL solution of Fe(TPA) or Fe(BPMEN) was made in MeCN and 2.1 mL of this solution was placed in the reaction flask along with 0.60 mL MeCN and 0.23 mL cyclohexane. A 70 mM H_2O_2 solution in MeCN (0.30 mL) was added drop-wise from a microsyringe, at a rate of approximately 0.01 mL/min over the course of 30 minutes. The reaction was stirred for an additional 15 minutes before the entire reaction was filtered through a 3 mL plug of silica and eluted with 5.0 mL MeCN. A 1.00 mL sample of the filtered product solution was placed in a GC vial and 0.010 mL toluene was used as an internal standard for the determination of cyclohexanol and cyclohexanone yield.

2.4.2 Fe(TPA)/Fe(BPMEN) in DCM

A similar procedure to the one above was used, with the exception that Fe(TPA) and Fe(BPMEN) were dissolved in DCM to make the 1.0 μmol/mL solution and 0.60 mL DCM was used instead of MeCN. The H_2O_2 solution was still made with MeCN.

2.4.3 Fe(TPA)/Fe(BPMEN) in DCM/MeCN

A 1.0 μmol/mL solution of Fe(TPA) or Fe(BPMEN) was made in DCM and 2.1 mL of this solution was placed in the reaction flask along with 0.30 mL DCM, 0.30 mL MeCN and 0.23 mL cyclohexane. A 70 mM H_2O_2 solution in MeCN (0.30 mL) was added drop-wise from a microsyringe, at a rate of approximately 0.01 mL/min over the

course of 30 minutes. The reaction was stirred for an additional 15 minutes before the entire reaction was filtered through a 3 mL plug of silica and eluted with 5.0 mL MeCN. A 1.00 mL sample of the filtered product solution was placed in a GC vial and 0.01 mL toluene was used as an internal standard as in sections 2.4.2.

2.4.4 Gas Chromatographic Analysis of the Reactions

The instrument used for Gas Chromatography (GC) was a Varian 3900 GC equipped with a CP-8400 autosampler, a CP-1177 injector, a flame ionization detector set at 280 °C and a WCOT Fused Silica column (25 m × 0.32 mm ID). The injector was heated to 225 °C and the sample was injected using split injection (split ration of 100) onto the column at 30.0 °C. After one minute, the temperature was raised to 80.0 °C at 25.0 °C/min, then 85.0 °C at 5.0 °C, 105 °C at 10 °C/min and finally to 240 °C at 80 °C/min. The elution time of each component was determined by using the above method to separate solutions of known composition and concentration. Pure samples of cyclohexanol and cyclohexanone were used to determine the retention times of the expected products using the above method. Toluene was used as the internal standard for the analysis of cyclohexanol and cyclohexanone.

2.5 Control Reactions

2.5.1 Fe(TPA)/Fe(BPMEN) without PS

Fe(TPA) or Fe(BPMEN) (0.04 g or 0.03 g respectively) was dissolved in 3.0 mL MeCN and added to 5.0 mL DCM. The drop-wise addition of 2.0 mL of 10 % H_2O_2 solution in MeCN to the reactions (at a rate of 0.15 mL/min over the course of 15 minutes) with stirring caused both the clear red Fe(TPA) solution and the pale peach Fe(BPMEN) solution to become yellow. After stirring for a day and sitting for two, the solvent was removed under vacuum to give a dark brown, tar-like substance containing residual catalyst. An IR spectrum was taken of the product to ensure that any peaks visible in the IR spectra of the products from the catalytic reactions could not be attributed to residual catalyst.

2.5.2 High Molecular Weight PS with no Complex

PS (0.48 g) was dissolved in 50 mL DCM and 30 mL MeCN was added to make a clear, colourless solution. The drop-wise addition of 20 mL of 10 % H_2O_2 in MeCN (at 0.15 mL/min over the course of 2 hours) did not change the colour, but eventually caused a white solid to precipitate from solution. After a day, the solvent was removed and the resulting white solid was rinsed with MeCN and dried in a drying pistol at 100 °C under vacuum for a minimum of 12 hours.

2.5.3 Low Molecular Weight PS with no Complex

PS (0.50 g) was dissolved in 15 mL DCM and 25 mL MeCN was added with stirring to make the reaction mixture milky white. The drop-wise addition of 10 mL of 10 % H_2O_2 in MeCN at a rate of 0.15 mL/min over the course of one hour did not change the colour, but a white clump formed and the mixture became clearer. Stirring was stopped after a day and the reaction sat for two more days. The clump was removed, the solution was reduced to near dryness and the resulting white solid was rinsed with MeOH, dissolved in 5 mL DCM and precipitated by addition to 10 mL MeOH. Both the white clump and the recovered white solid were dried in a drying pistol at 100 °C under vacuum for a minimum of 12 hours.

2.6 Catalytic Reactions with PS

2.6.1 High Molecular Weight PS with Fe(BPMEN) in 1:1 DCM:MeCN

PS (0.50 g) was dissolved in 10 mL of DCM with heating and allowed to cool to room temperature. More DCM was added (15 mL) along with MeCN (5.0 or 10 mL depending on whether 10 mL or 5.0 mL of H_2O_2 solution was added respectively). Fe(BPMEN) (10, 5, 2.5, 0.5 mol%) was dissolved in 2.5 mL MeCN and added to the solution with stirring, turning the clear and colourless mixture pale yellow. The vial used for Fe(BPMEN) was rinsed with 3 × 2.5 mL MeCN such that the final rinse was colourless. The rinses were added to the reaction solution. Hydrogen peroxide solution (10, 5, 2.5 % or 70 mM) was added drop-wise, with stirring, at a rate of 0.15 mL/min over the course of one hour (or 30 minutes for 5 mL of 10 % H_2O_2). The oxidant

addition changed the colour of the reaction through a combination of blue, green and yellow, depending on the amount of Fe(BPMEN) and hydrogen peroxide used, and a solid material precipitated. The reaction was stirred overnight and was then allowed to sit for two days. By the end of the third day, the mixture contained a clear yellow solution and an insoluble material. The insoluble material was removed and rinsed with DCM. The solution was reduced under vacuum to ~5 mL, producing a solid product. The solid was isolated and rinsed with MeCN, dissolved in 5.0 mL DCM, warmed and precipitated by addition to 15 mL of ice cold EtOH with stirring. The solid was collected by filtration and dried in a drying pistol, along with the insoluble material, at 100 °C under vacuum for a minimum of 12 hours. All fractions soluble in DCM were analyzed by IR spectroscopy.

2.6.2 High Molecular Weight PS with Fe(BPMEN) in 7:3 DCM:MeCN

PS (0.50 g) was dissolved in 10 mL DCM with heat and allowed to cool to room temperature. More DCM was added (25 mL), along with 1.0 mL of MeCN. Fe(BPMEN) (0.15 g, 5 mol%) was dissolved in 1.0 mL of MeCN and added to the reaction resulting in a clear, pale yellow solution. The vial used for Fe(BPMEN) was rinsed with 3 × 1.0 mL MeCN such that the final rinse was colourless. The rinses were added to the reaction solution. The drop-wise addition of 10 mL of 10 % H_2O_2 solution at 0.15 mL/min over the course of one hour, changed the colour to amber, which took on shades of green and blue as the addition progressed. Stirring was continued overnight and stopped in the morning. After three days, the reaction was clear blue-green with no

solid visible at the bottom. The volume was reduced to ~5 mL giving a dark blue solid and a clear, amber solution. The solid was removed, rinsed with 2 × 5.0 mL MeCN and precipitated from DCM/EtOH (1:3) to give a cloudy blue solution with clumps at the bottom. The solid was collected and dried in a drying pistol at 100 °C under vacuum overnight before being analyzed by IR spectroscopy.

2.6.3 High Molecular Weight PS with Fe(BPMEN) in 3:7 DCM:MeCN

PS (0.04 g) was dissolved in 3.0 mL DCM with heat and allowed to cool to room temperature at which point 2.5 mL MeCN was added. Fe(BPMEN) (0.03 g, 10 mol%) was dissolved in 3.0 mL of MeCN and added to the reaction, giving a pinkish mixture where the PS was visible as white clumps. The drop-wise addition of 2.0 mL of 10 % H_2O_2 in MeCN at 0.15 mL/min over the course of 15 minutes, with stirring, resulted in colour changes to amber and then green. The solvent volume was reduced, the solid was collected, rinsed with MeCN and dried in a drying pistol at 100 °C under vacuum for at least 12 hours before being analyzed by IR spectroscopy.

2.6.4 High Molecular Weight PS with Fe(TPA) in 1:1 DCM:MCN

PS (0.50 g) was dissolved in 10 mL DCM with heat and allowed to cool to room temperature. More DCM was added (15 mL), along with MeCN (5.0 or 10 mL depending on whether 10 mL or 5.0 mL of H_2O_2 solution was added respectively). Fe(TPA) (10, 5, 2.5 or 0.5 mol%) was dissolved in 2.5 mL MeCN and added to the reaction with stirring to give a clear red solution. The vial used for Fe(TPA) was rinsed

with 3 × 2.5 mL MeCN such that the final rinse was colourless. The rinses were added to the reaction solution. Hydrogen peroxide solution (10 or 5 %) was added drop-wise, with stirring, at a rate of 0.15 mL/min over the course of one hour or 30 minutes depending on the volume. The reaction colour slowly changed from red to orange to copper then bronze with a solid material precipitating. Stirring was continued overnight and then stopped, and the reaction sat for two days. At the end of the three day period, the mixture contained a clear, bright yellow solution and a yellow/beige solid. The insoluble material was removed and rinsed with DCM. The solution was reduced in volume under vacuum to ~5 mL to precipitate an orange/yellow solid. The remaining orange solution was removed. The solid was dissolved in 5.0 mL DCM and precipitated in 15 mL cold EtOH. The reaction flask was rinsed with ~2 mL of DCM and this was added to the precipitation solution. The solution was allowed to stand until the solid settled, at which point the solid was collected via filtration with a glass frit. Both the insoluble material and the precipitated product were dried in a drying pistol at 100 °C under vacuum for a minimum of 12 hours. Afterward, upon attempts to dissolve the precipitated and dried products in DCM, only a gel resulted for certain reactions. The gel was soaked in DCM collect any soluble product. All products soluble in DCM were analyzed by IR spectroscopy. For further information see Section 3.3.1.

2.6.5 High Molecular Weight PS with Fe(TPA) – Diluted Reactions

PS (0.50 g) was dissolved in 100 mL DCM with heating and allowed to cool to room temperature. Another 400 mL DCM was added, along with 480 mL MeCN with

stirring. Fe(TPA) (10 or 5 mol%) was dissolved in 2.5 mL MeCN and added to the reaction to give a clear red solution. The vial used for Fe(TPA) was rinsed with 3 × 2.5 mL MeCN such that the final rinse was colourless. The rinses were added to the reaction solution. The addition of H_2O_2 solution (10 mL of 10 % or 20 % at a rate of 0.15 mL/min over the course of one hour) changed the colour to orange and then bright yellow. The reaction was stirred overnight and then left standing for two days. At the end of the three day period, the solvent was reduced to approximately 5.0 mL to precipitate the polymer. The solid was collected, dissolved in 20 mL DCM, precipitated with 60 mL EtOH, collected again and dried in a drying pistol at 100 °C under vacuum for a minimum of 12 hours. All fractions soluble in DCM were analyzed by IR spectroscopy.

2.6.6 Low Molecular Weight PS with Fe(BPMEN) in 1:1 DCM:MeCN

PS (0.50 g) was dissolved in 10 mL DCM with stirring. More DCM was added (15 mL) along with MeCN (5.0 or 10 mL depending on whether 10 mL or 5.0 mL of H_2O_2 solution was added respectively). Fe(BPMEN) (10, 5, 2.5, 1 or 0.5 mol%) was dissolved in 2.5 mL MeCN and added to the reaction with stirring to give a clear, light peach solution. The vial used for Fe(BPMEN) was rinsed with 3 × 2.5 mL MeCN such that the final rinse was colourless. The rinses were added to the reaction solution. Hydrogen peroxide solution (10 or 5 %) was added drop-wise, with stirring, at a rate of 0.15 mL/min over the course of one hour or 30 minutes depending on the volume. The colour slowly changed to amber then green and/or blue, depending on the amount of Fe(BPMEN) and H_2O_2 used, with a solid material precipitating. Stirring was continued

overnight and then stopped, and the reaction sat for two days. At the end of the three day period, the mixture contained a clear, bright yellow solution and a yellow/green solid. The insoluble material was removed and the solution was reduced to near dryness to give solid that was rinsed with EtOH, dissolved in 5.0 mL DCM and precipitated in 10 mL EtOH. The solid was collected and put in a drying pistol, along with the insoluble material, at 100 °C under vacuum for a minimum of 12 hours. All fractions soluble in DCM were analyzed by IR spectroscopy.

2.6.7 Low Molecular Weight PS with Fe(BPMEN) in 3:7 DCM:MeCN

PS (0.51 g) was dissolved in 10 mL DCM with stirring. More DCM was added (5.0 mL) along with MeCN (15 mL). Fe(BPMEN) (0.15 g, 5 mol%) was dissolved in 2.5 mL MeCN and added to the reaction with stirring to give a clear, light magenta solution. The vial used for Fe(BPMEN) was rinsed with 3 × 2.5 mL MeCN such that the final rinse was colourless. The rinses were added to the reaction solution. The drop-wise addition of 10 mL of 10 % H_2O_2, with stirring, at a rate of 0.15 mL/min over the course of one hour, changed the colour to amber and then green-blue and finally green-yellow with a solid material precipitating. Stirring was continued overnight and then stopped, and the reaction sat for two days. At the end of the three day period, the mixture contained a clear, bright yellow solution and a light yellow solid. The insoluble material was removed and the solution was reduced to near dryness to give a solid that was rinsed with MeOH, dissolved in 5.0 mL DCM and precipitated in 10 mL MeOH. The solid was collected and put in a drying pistol, along with the insoluble material, at 100 °C under

vacuum for a minimum of 12 hours. All fractions soluble in DCM were analyzed by IR spectroscopy.

2.6.8 Low Molecular Weight PS with FeTPA in 1:1 DCM:MCN

PS (0.50 g) was dissolved in 10 mL DCM with stirring. More DCM was added (15 mL) along with MeCN (5.0 or 10 mL depending on whether 10 mL or 5.0 mL of H_2O_2 solution was added respectively). Fe(TPA) (10, 5, or 1 mol%) was dissolved in 2.5 mL MeCN and added to the reaction with stirring to give a clear red solution. The vial used for Fe(TPA) was rinsed with 3 × 2.5 mL MeCN such that the final rinse was colourless. The rinses were added to the reaction solution. Hydrogen peroxide solution (10 or 5 %) was added drop-wise over the course of one hour or 30 minutes (depending on volume), with stirring, at a rate of 0.15 mL/min. The colour slowly changed from red to bright orange with a solid material precipitating. Stirring was continued overnight and then stopped, and the reaction sat for two days. At the end of the three day period, the mixture contained a clear, bright yellow solution and a yellow/orange solid. The insoluble material was removed and the solution was reduced to ~5 mL to precipitate a solid that was rinsed with MeOH, dissolved in 5.0 mL DCM and precipitated in 10 mL MeOH. The solid was collected and put in a drying pistol, along with the insoluble material, at 100 °C under vacuum for a minimum of 12 hours. In some cases, attempts to dissolve the precipitated and dried product in DCM resulted in the formation of gel. All fractions soluble in DCM were analyzed by IR spectroscopy.

2.6.9 Low Molecular Weight PS with Fe(TPA) in 3:7 DCM:MeCN

PS (0.50 g) was dissolved in 10 mL DCM with stirring. More DCM was added (5.0 mL) along with MeCN (15 or 20 mL depending on whether 10 mL or 5.0 mL of H_2O_2 solution was added respectively). Fe(TPA) (10, 5, or 1 mol%) was dissolved in 2.5 mL MeCN and added to the reaction with stirring to give a clear red solution. The vial used for Fe(TPA) was rinsed with 3 × 2.5 mL MeCN such that the final rinse was colourless. The rinses were added to the reaction solution. Hydrogen peroxide solution (20, 10 or 5 %) was added drop-wise, with stirring, at a rate of 0.15 mL/min over the course of one hour or 30 minutes depending on the volume. The colour slowly changed from red to bright orange with a solid material precipitating. Stirring was continued overnight then stopped and the reaction sat for two days. At the end of the three day period, the mixture contained a clear, bright yellow solution and a yellow/orange solid. The insoluble material was removed and the solution was reduced to near dryness to precipitate solid that was rinsed with MeOH, dissolved in 5.0 mL DCM and precipitated in 10 mL MeOH. The solid was collected and put in a drying pistol, along with the insoluble material, at 100 °C under vacuum for a minimum of 12 hours. All fractions soluble in DCM were analyzed by IR spectroscopy.

2.6.10 Low Molecular Weight PS with Fe(TPA) in 3:7 DCM:MeCN - Two Additions

PS (0.50 g) was dissolved in 10 mL DCM with stirring. More DCM was added (5.0 mL) along with MeCN (15 mL). Fe(TPA) (10 or 5 mol%) was divided in half with one half being dissolved in 3.0 mL MeCN and added to the reaction with stirring to give

a clear red solution. The vial used for Fe(TPA) was rinsed with 2 × 1.0 mL MeCN such that the final rinse was colourless. The rinses were added to the reaction solution. Hydrogen peroxide solution (10 mL of 10 % in MeCN or 5.0 mL of 20 % in MeCN) was added drop-wise, with stirring, at a rate of 0.15 mL/min over the course of either one hour or 30 minutes respectively. The colour slowly changed from red to brown then orange with a solid material precipitating. Stirring was continued overnight. The next day, the other half of the Fe(TPA) was used in a second addition, prepared and added in the same manner as the first. Hydrogen peroxide solution was again added in the same manner as above. Stirring was continued over night and stopped the next day, and the reaction was left for a day. At the end of the three day period, the mixture contained a clear, bright yellow solution and a light yellow solid. The insoluble material was removed and the solution was reduced to near dryness to give solid that was rinsed with MeOH, dissolved in 5.0 mL DCM and precipitated in 10 mL MeOH. The solid was collected and put in a drying pistol, along with the insoluble material, at 100 °C under vacuum for a minimum of 12 hours.

The precipitated and dried product (0.04 g) was dissolved in 5 mL dry DCM and placed over 3Å molecular sieves for 24 hours. The molecular sieves were removed and the solution reduced to dryness to recover the product, which was then dried in a drying pistol at 100 °C under vacuum for a minimum of 12 hours. All fractions soluble in DCM were analyzed by IR spectroscopy.

2.6.11 Low Molecular Weight PS with Fe(TPA) in 3:7 DCM:MeCN - Three Additions

PS (0.52 g) was dissolved in 10 mL DCM with stirring and then 5.0 mL MeCN was added. Fe(TPA) (10 or 5 mol%) was divided in thirds with one third being dissolved in 3.0 mL MeCN and added to the reaction with stirring to give a clear red solution. The vial used for Fe(TPA) was rinsed with 2 × 1.0 mL MeCN such that the final rinse was colourless. The rinses were added to the reaction solution. Hydrogen peroxide solution (5.0 mL of 13 % H_2O_2 in MeCN) was added drop-wise, with stirring, at a rate of 0.15 mL/min over the course of 30 minutes. The colour slowly changed from red to golden amber with a solid material precipitating. Stirring was continued overnight. The next day, after adding 5.0 mL DCM, the second third of Fe(TPA) and 5.0 mL of 13 % H_2O_2 in MeCN was added in the same manner as before. Stirring was again continued over night. The third day, the last third of Fe(TPA) and 5.0 mL of 13 % H_2O_2 in MeCN was added in the same manner as above, and stirring was continued over night. At the end of the three day period, the mixture contained a clear, bright yellow-orange solution and an orange solid. The insoluble material was removed and the solution was reduced to near dryness to give solid that was rinsed with MeOH, dissolved in 5.0 mL DCM and precipitated in 10 mL MeOH. The solid was collected and put in a drying pistol, along with the insoluble material, at 100 °C under vacuum for a minimum of 12 hours. All fractions soluble in DCM were analyzed by IR spectroscopy.

2.7 Material Analysis

2.7.1 Differential Scanning Calorimetry

A DSC Q2000 V24.4 (Build 116) machine was used for the collection of data. The samples were all submitted after having been dried in the drying pistol at 100°C under vacuum for at least 12 hours. Between 4.00 and 5.00 mg of sample was placed in a Terzo Aluminum pan and sealed with a Terzo Hermetic lid by a press. All manipulations of the pan were done with tweezers.

The program used for the high molecular weight PS started with the temperature equilibrating at 20.00 °C and then increasing at 5.00 °C/min to 160.00 °C where it remained isothermal for one minute. The temperature then decreased at 5.00 °C/min until the temperature reached 70.00 °C, where it remained isothermal for one minute. The cycle was repeated twice.

The program used for the low molecular weight PS started with the temperature equilibrating at 20.00 °C then increasing at 5.00 °C/min to 160.00 °C where it remained isothermal for one minute before decreasing at 5.00 °C/min to 20.00 °C and remaining isothermal for one minute before repeating the entire cycle over again twice. All data were processed in the exo-down orientation using Universal Analysis V4.5A software from TA Instruments.

Table 1. Glass transition temperatures of both polystyrene starting materials and of select soluble products from catalytic reactions of polystyrene

Sample	T_g 1 (°C)	T_g 2 (°C)	T_g 3 (°C)	T_g average (°C)
High molecular weight PS	103.7	103.7	130.4	103.6
5 mol% Fe(BPMEN), 10 mL 10 % H_2O_2	105.6	105.6	105.0	105.4
2.5 mol% Fe(TPA), 10 mL 10 % H_2O_2	108.5	108.7	108.4	108.5
Low molecular weight PS	59.4	59.2	59.5	59.4
2 × (5 mol% Fe(TPA), 10 mL 10 % H_2O_2)	99.5	98.1	99.5	99.0
2 × (2.5 mol% Fe(TPA), 5 mL 20 % H_2O_2)	82.4	81.8	82.3	82.2
3 × (1.67 mol% Fe(TPA), 5 mL 13 % H_2O_2)	87.1	86.7	86.5	86.8

2.7.2 Gel Permeation Chromatography

Gel permeation chromatography (GPC) was done on an MZ-Gel SDplus column of 300 × 8.0 mm. Chloroform with 2 % triethylamine flowing at 1.00 mL/min at 25 °C was used as the elution solvent. Changes in the index of refraction, detected by a DAWN-Heleos-II light scattering detector (Wyatt Technologies), were used to detect the elution of the polymer fractions. The samples were prepared in chloroform as 5.0 – 10.0 mg/mL solutions, filtered through 13 mm, 0.2 µm PTFE syringe filters from VWR and approximately 20 µL was injected onto the column. The results of each sample were

analyzed to determine the number average molecular weight (M_n) and the polydispersity index (PDI) using ASTRA software with a template created from PS standards.

Table 2. Number average molecular weights and polydispersity indexes of both polystyrene starting materials and of select soluble products from catalytic reactions of polystyrene. Each M_n value has an error of 9 % while each PDI value has an error of 13 %

Sample	M_n 1 ($gmol^{-1}$)	M_n 2 ($gmol^{-1}$)	M_n average ($gmol^{-1}$)	PDI 1	PDI 2	PDI average
High molecular weight PS	205 000	214 000	210 000	1.1	1.1	1.1
5 mol% Fe(BPMEN), 10 mL 10 % H_2O_2	19 000	18 000	19 000	1.9	1.9	1.9
2.5 mol% Fe(TPA), 10 mL 10 % H_2O_2	17 000	n/a	17 000	1.8	n/a	1.8
Low molecular weight PS	930	970	950	1.2	1.2	1.2
2 × (5 mol% Fe(TPA), 10 mL 10 % H_2O_2)	770	740	760	1.3	1.2	1.3
2 × (2.5 mol% Fe(TPA), 5 mL 20 % H_2O_2)	750	800	780	1.3	1.2	1.3
3 × (1.67 mol% Fe(TPA), 5 mL 13 % H_2O_2)	810	740	780	1.3	1.3	1.3
Insoluble material	48 000	60 000	54 000	1.2	1.2	1.2

Chapter 3

Results and Discussion

This chapter presents a discussion of the development of the procedures presented in Sections 2.3 through 2.6, along with a discussion of the results obtained. To begin with, a discussion of the synthesis of the complexes is presented in Section 3.1, followed by a discussion of the oxyfunctionalize cyclohexane, under reported conditions,[26] by the complexes (Section 3.2). The discussion then turns to the development of conditions for oxyfunctionalization of both high and low molecular weight polystyrene in Sections 3.3.1 and 3.3.2 respectively, with an overall analysis presented in Section 3.5. Finally, these reactions exhibited strong colour changes and possible explanations are presented in Section 3.6.

3.1 Synthesis of Complexes

The iron complexes used in this study were $[Fe(TPA)(MeCN)_2][OTf]_2$ (herein referred to as Fe(TPA)) and $Fe(BPMEN)(OTf)_2$ (herein referred to as Fe(BPMEN)) (Figure 15). These complexes were chosen based on their reported ability to oxyfunctionalize cyclohexane as well as their relative ease of synthesis. Britovsek et al[25,26,28] investigated multiple variations on the ligand structure, as well as different metals, and found that the best yields and alcohol to ketone ratios under their conditions came from the use of the above two complexes. Others have used more rigid and

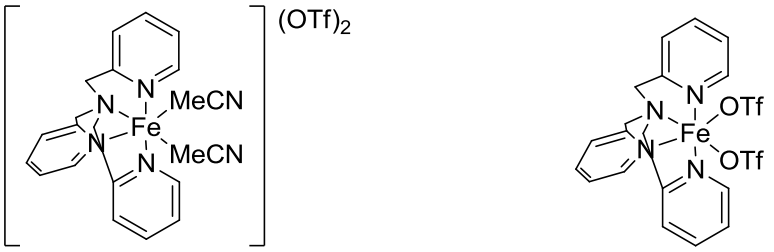

Figure 15. Structure of $[Fe(TPA)(MeCN)_2][OTf]_2$ (left) and $Fe(BPMEN)(OTf)_2$ (right)

complex ligand systems[29,30,33] that show more activity, but their synthesis is long and costly. For Fe(TPA) and Fe(BPMEN), the general procedure was to synthesize and isolate the ligand, then react the ligand with $Fe(MeCN)_2(OTf)_2$ to form the complex.

3.1.1 Synthesis of $Fe(MeCN)_2(OTf)_2$

The procedure for the synthesis of $Fe(MeCN)_2(OTf)_2$ was taken directly from Hagen[31] and scaled down since 28 g of product was not necessary. Although the reaction was performed under argon and in dry glassware, there was difficulty getting the reaction to remain blue-green (indicating an Fe^{2+} species)[31] instead of turning orange (characteristic of an Fe^{3+} species).[31] This is likely due to the use of an open bottle of iron powder instead of the recommended fresh bottle stored under nitrogen. The effect on the final product, however, should be minimal as it is reported[31] that the Fe^{3+} species resulting from any oxidized iron is significantly more soluble than the Fe^{2+} species and thus the Fe^{2+} species will crystallize preferentially leaving most of the Fe^{3+} in solution. This is further supported by the observation that the collected crystals were the desired blue-green. The presence of Fe^{3+} species also explains the low yields of this reaction in comparison to the literature as part of the product remains in solution. However, the

solid is hygroscopic, and if left out in the humid atmosphere, took on a yellow colour after a day and was liquid after three, so any exposure of the solid to moisture could result in a hydrated Fe^{3+} complex.

Hagen characterized the product using elemental analysis and crystallography. Since the product appeared as blue-green crystals that became white powder under vacuum, as expected, the complex was deemed correct and used for the formation of Fe(TPA) and Fe(BPMEN), for which a more accessible NMR characterization was performed. Any problems with the $Fe(MeCN)_2(OTf)_2$ should also appear as inconsistencies in the NMR of the subsequent complexes.

3.1.2 Synthesis of Fe(BPMEN)

The synthesis of BPMEN followed the procedure outlined by Britovsek[26] with the exception that sodium hydride was used instead of potassium hydride for removal of traces of pyridine carbinol, and the final extraction of the product was done using a Soxhlet apparatus, which simplifies the extraction procedure although the yields are no better than the literature. The ^1H NMR and the ^{13}C NMR of the pale yellow liquid in deuterated chloroform ($CDCl_3$) agree well with the literature.

The powdery yellow Fe(BPMEN) was produced in yields comparable or better than those reported in the literature. In deuterated acetonitrile (CD_3CN), the complex is paramagnetic and thus the ^1H NMR showed broad peaks that were shifted slightly from those reported in the literature. However, the ^1H NMR in deuterated methylene chloride (CD_2Cl_2) showed distinct, sharp peaks whose shifts and integration corresponded well

with literature and identified the presence of the desired complex. All of the batches of the complex showed these changes. Furthermore, as discussed later in section 3.2, the product showed the desired catalytic activity.

3.1.3 Synthesis of Fe(TPA)

TPA was synthesized following a method reported by Britovsek[26] with the exception that sodium hydride was used instead of potassium hydride for the removal of traces of pyridine carbinol. The use of a Soxhlet extraction apparatus resulted in a consistently increased yield relative to the literature. The ^{1}H NMR and ^{13}C NMR of the flakey yellow TPA in $CDCl_3$ compared exactly with the literature.

The shiny, deep red crystals of Fe(TPA) were initially made under an inert atmosphere[32] and the initial batches exhibited ^{1}H NMR spectra in CD_3CN comparable to literature, although slightly shifted in the lower field. A difficulty inherent in collection of this complex is that, under vacuum, it loses an MeCN[32] resulting in some of the complexes having only one coordinated MeCN. This is not an issue for the complex in acetonitrile solution since a solvent molecule can fill the empty site and return the desired complex, but characterization of the solid form was problematic. In general, the ^{1}H NMR spectra agreed well with the literature for peak multiplicity and integration, but the resonances of all but the γ aromatic protons were generally shifted slightly upfield. However, as discussed in section 3.2, the complex showed the desired catalytic activity towards the oxyfunctionalization of cyclohexane.

One of the preparations of Fe(TPA) resulted in a product, the ^{1}H NMR spectrum

of which exhibited an upfield shift of the triplet from 7.33 ppm to 7.25 ppm and a downfield shift of a singlet from 7.09 to 7.52 ppm as well as the broad signal at 12.12 ppm. The strongest deshielding effects were seen in the α protons of the pyridine rings and in the CH_2. With these two locations being near the iron centre, any changes may also affect the chemical shifts. To determine that the ligands were coordinated to the metal as desired, and that the MeCN were indeed the coordinating ligands (and not the triflates), a crystal structure was obtained (Figure 16 and Appendix A). The triflates were slightly disordered and thus not shown on the diagram, but the structure showed that the TPA ligand was coordinated as anticipated and that the other coordinated ligands were indeed MeCN. Another possibility that would create the different environments near the iron centre was that the iron was oxidized either during or before the reaction. The reaction was thus run without the standard precautions against air or moisture. The solvents were taken from the bottle and the reaction was open to the air. There was no difference in how the reaction progressed – still deep red – and the collected crystals were deep red as well. However, the ^1H NMR showed displacement of the triplet to 7.18 ppm from 7.32 ppm and the singlet to 7.81 ppm from 6.70 ppm, along with a general downfield shift of all other signals. This displacement is larger than for the previous spectrum but the trend is consistent, suggesting that there was the inclusion of air or moisture in the reaction. The highly hygroscopic nature of $Fe(MeCN)_2(OTf)_2$ may have led to the formation of a Fe^{+3} species, which could result in the deshielding of local protons without necessarily changing the structure. Since this result occurred further into the progress of the catalytic reactions with PS, the complex was used in a set of conditions that had produced repeatable results (0.50 g low molecular weight PS, 5 mol%

complex, 10 mL 10 % H_2O_2 and 1:1 DCM:MeCN) and no variations in the IR spectrum of the soluble product were seen. This was taken as indication of catalytic activity. Due to the ease of preparation under non-air sensitive conditions and the fact that the complex returned comparable results under similar conditions to the previous complexes, all further synthesis was done open to the air. Considering that the goal of the research was to produce functionalized PS, no further investigation into the nature of the complex was done.

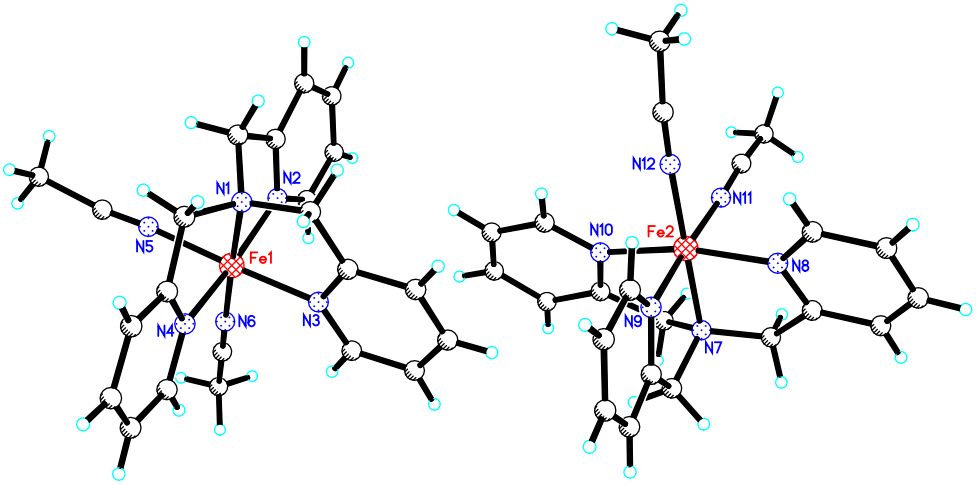

Figure 16. Two isomers of the crystal structure of $[Fe(TPA)(MeCN)_2][OTf]_2$ with the triflates omitted

Table 3. Selected bond lengths and angles for $[Fe(TPA)(MeCN)_2][OTf]_2$

Bond	Length (Å)	Bond	Angle (°)
Fe(1)-N(5)	1.936(8)	N(2)-Fe(1)-N(4)	168.4(3)
Fe(1)-N(6)	1.941(7)	N(3)-Fe(1)-N(4)	90.6(3)
Fe(1)-N(2)	1.959(6)	N(5)-Fe(1)-N(1)	91.3(3)
Fe(1)-N(3)	1.963(7)	N(6)-Fe(1)-N(1)	179.0(3)
Fe(1)-N(4)	1.972(6)	N(2)-Fe(1)-N(1)	84.7(3)
Fe(1)-N(1)	1.991(6)	N(3)-Fe(1)-N(1)	85.6(3)
Fe(2)-N(11)	1.946(7)	N(4)-Fe(1)-N(1)	83.7(3)
Fe(2)-N(12)	1.959(8)	N(11)-Fe(2)-N(12)	88.4(3)
Fe(2)-N(10)	1.966(7)	N(11)-Fe(2)-N(10)	90.2(3)
Fe(2)-N(9)	1.974(6)	N(12)-Fe(2)-N(10)	96.6(3)
Fe(2)-N(7)	1.975(7)	N(11)-Fe(2)-N(9)	176.7(3)
Fe(2)-N(8)	1.977(7)	N(12)-Fe(2)-N(9)	94.8(3)
		N(10)-Fe(2)-N(9)	90.1(3)
Bond	**Angle (°)**	N(11)-Fe(2)-N(7)	91.3(3)
N(5)-Fe(1)-N(6)	89.5(3)	N(12)-Fe(2)-N(7)	179.6(3)
N(5)-Fe(1)-N(2)	89.9(3)	N(10)-Fe(2)-N(7)	83.6(3)
N(6)-Fe(1)-N(2)	94.8(3)	N(9)-Fe(2)-N(7)	85.5(3)
N(5)-Fe(1)-N(3)	176.9(3)	N(11)-Fe(2)-N(8)	89.2(3)
N(6)-Fe(1)-N(3)	93.6(3)	N(12)-Fe(2)-N(8)	96.1(3)
N(2)-Fe(1)-N(3)	89.2(3)	N(10)-Fe(2)-N(8)	167.3(3)
N(5)-Fe(1)-N(4)	89.6(3)	N(9)-Fe(2)-N(8)	89.8(3)
N(6)-Fe(1)-N(4)	96.8(3)	N(7)-Fe(2)-N(8)	83.8(3)

3.2 Checking Activity of Complexes for Oxyfunctionalization of Cyclohexane

Since the selection of the complexes, as well as the synthetic method, was based on the work of Britovsek et al.,[26] replication of those conditions was sought to check that the synthesized complexes did indeed oxyfunctionalize cyclohexane. The only difference

in the set-up was that Britovsek used a syringe pump for the delivery of the dilute H_2O_2 while here it was added drop-wise from a microsyringe with one drop approximately every 20 seconds. It is noted in the literature that the rate of addition does affect the yield and alcohol to ketone ratio, and thus it was not expected that the exact values would be replicated but rather that cyclohexanol and cyclohexanone would be produced in identifiable quantities and confirm the ability of the complexes to induce the desired functionalization.

The literature[26] stated that H_2O_2 was added as a dilute solution, but failed to mention which solvent. Initially water was used to create the 70 mM solutions required, but no oxyfunctionalized product was detected by GC. Using MeCN instead of water produced the expected products in a roughly 56 % combined yield with an A/K ratio of 10 for Fe(BPMEN), and 20 % combined yield with an A/K ratio of 7.5 for Fe(TPA). These results compare favourably to those reported by Britovsek[26] – combined yield of 65 % and A/K of 9.5 for Fe(BPMEN); combined yield of 32 % and A/K of 12 for Fe(TPA) – confirming the ability of the synthesized complexes to oxyfunctionalize cyclohexane.

3.3 Polystyrene Oxyfunctionalization Reactions

Three possible polymers used commercially were considered for this project – polyethylene, polypropylene and polystyrene. All three are widely used in consumer applications and do not readily degrade in the environment. Of the three, PS was chosen

based on the hypothesis that its inherently weaker tertiary benzylic C-H bond would be easier to functionalize than the C-H bonds in either polyethylene or polypropylene.

To make the transition from using cyclohexane as substrate to polystyrene for the catalytic reactions, the main difficulty arose – PS is not soluble in MeCN, which is used as the solvent for the cyclohexane reaction and is apparently necessary for the dilution of the H_2O_2 solution. A good solvent for PS was needed and DCM was selected based on its ability to fully dissolve PS, as well as a report that it had previously been used in this type of reaction without becoming functionalized itself.[34] The activity of Fe(BPMEN) toward oxyfunctionalization of cyclohexane in DCM was investigated by replacing MeCN in the above catalytic reactions with DCM. Fe(BPMEN) was chosen due to its larger combined yield under the previous conditions. As expected, no oxyfunctionalization of cyclohexane was seen if only DCM was used as solvent. If H_2O_2 were diluted with MeCN to give an overall 9:1 DCM:MeCN ratio, then a weak peak was evident in the GC trace at the retention time of cyclohexanone. If the solvent ratio were altered to 4:1 DCM:MeCN, then both the alcohol and ketone products were observed, indicating that the oxyfunctionalization was possible in the presence of DCM with Fe(BPMEN), although at a very low combined yield (0.02 % with A/K ratio of 1.9). Increasing the proportion of MeCN should not adversely affect the activity of the complex since the original reactions were done in MeCN, so further solvent ratios were not investigated. The goal of the project was to develop reaction conditions for PS, so time was not taken to further optimize these conditions with cyclohexane as the substrate.

3.3.1 High Molecular Weight Polystyrene

Reaction conditions were initially kept similar to those for cyclohexane, using Fe(BPMEN) with a 4:1 DCM:MeCN ratio, PS ($M_n = 2.1 \times 10^5$ $gmol^{-1}$ as determined by GPC) dissolved in the DCM and the drop-wise addition of 70 mM H_2O_2 in MeCN. The work-up included filtering through a plug of silica and analyzing the result via IR. No oxyfunctionalization was evident in the IR spectra. Over the course of reactions, the ratio of DCM:MeCN was lowered to 1:1 in hopes of increasing the activity of the catalyst with more MeCN; the H_2O_2 solutions were changed from 70 mM to 10 % solutions, putting the oxidant in excess in hopes of increasing the chances of oxyfunctionalization; the reactions were scaled up to a final volume of 50 mL so that more PS could be reacted and have more product available for analysis; the collection of the product was facilitated by precipitation, reflecting the fact that the substrate was a polymer and not a small molecule, and finally the reaction period was lengthened. Eventually it was found that reacting PS with 5 mol% Fe(BPMEN) and 10 mL of 10 % H_2O_2 solution in a solvent ratio of 1:1 DCM:MeCN for three days resulted in the appearance of a weak carbonyl peak at 1769 cm^{-1} in the IR of the soluble fraction (Figure 17). The insoluble material was not analyzed as it was insoluble in DCM and would not powder sufficiently for a Nujol mull or KBr pellet.

The DSC analysis showed little change in the glass transition temperature (T_g) of the soluble product relative to that of the starting polymer (105 °C from 103 °C) as shown in Table 1, Section 2.7.1. The GPC analysis showed a decrease in number average molecular weight (M_n) from 2.1×10^5 $gmol^{-1}$ for starting material to 1.9×10^4

$gmol^{-1}$ as well as an increase in the polydispersity index (PDI) from 1.0 to 1.9. This suggests that the reaction was cleaving C-C bonds and breaking polymer chains, which is undesirable. Finally, the weak, broad band in the baseline between 3.5 and 4.0 ppm (the expected location for protons adjacent to a carbonyl group on PS, as predicted using

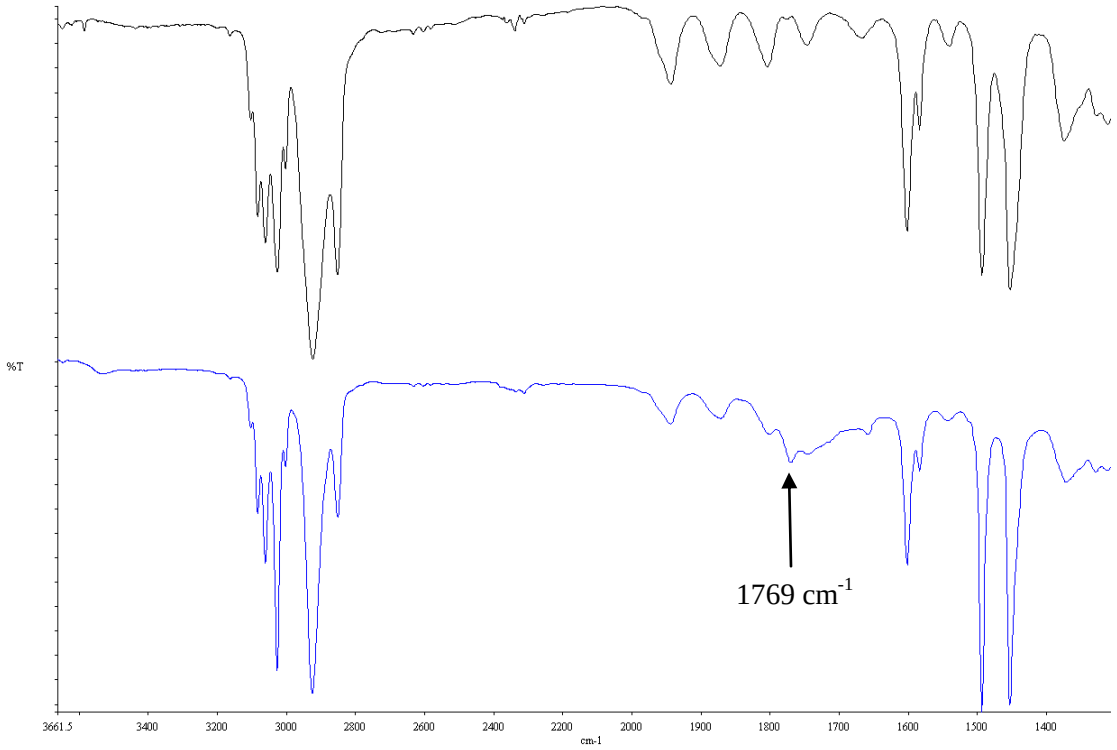

Figure 17. IR spectrum of PS (top) and IR spectrum of the soluble polymer resulting from the catalytic reaction of high molecular weight PS with 5 mol% Fe(BPMEN) and 10 mL of 10 % H_2O_2 in 1:1 DCM:MeCN (bottom)

ACDLABS NMR prediction software) evident in the ^1H NMR of the product in $CDCl_3$ showed no correlation with any other signal in COSY, HSQC or HMBC spectra, giving rise to an inconclusive result. The reactions were repeated in an attempt to increase the level of functionalization. The previous reaction was taken as a starting point and a

general reaction was devised (Figure 18) with variations in the amount and type of catalyst used, the amount and concentration of H_2O_2 solution and the solvent ratios.

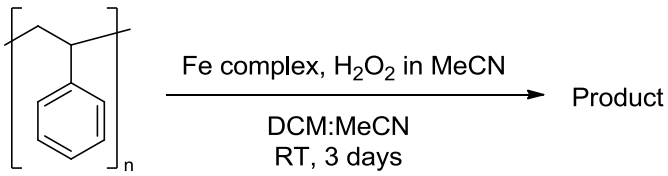

Figure 18. General reaction conditions for polystyrene oxyfunctionalization reactions

When using Fe(BPMEN), increasing the amount of catalyst (10 mol%) did not affect the intensity of the carbonyl signal in the IR, while decreasing the catalyst (2.5 or 0.5 mol%) decreased the intensity or showed no evidence of oxyfunctionalization. Similarly, changes in the amount or concentration of the H_2O_2 solution only resulted in a lesser degree of functionalization. Changing the solvent ratio to 3:7 DCM:MeCN only resulted in the precipitation of the polymer without any indication of oxyfunctionalization. Throughout these reactions, there was always an insoluble material that would come out of solution over the course of the reaction. In some cases the insoluble material showed slight solubility in DCM, and the IR spectra of these cases showed no oxyfunctionalization. The amount of insoluble material ranged from 50 to 75 % of the mass of the initial PS, while the recovered soluble material was 20 to 40 % of the initial mass. The proportion of DCM was increased to 7:3 DCM:MeCN in an attempt to keep the solid in solution, and indeed the insoluble mass was not evident, but neither was any oxyfunctionalization.

Changing the catalyst from Fe(BPMEN) to Fe(TPA) and using the initial conditions (5 mol% catalyst, 10 mL of 10 % H_2O_2 in 1:1 DCM: MeCN) more than doubled the intensity of the peak at 1769 cm^{-1} in the IR of the soluble product (Figure 19), but a different problem arose. The usual insoluble material precipitated out of

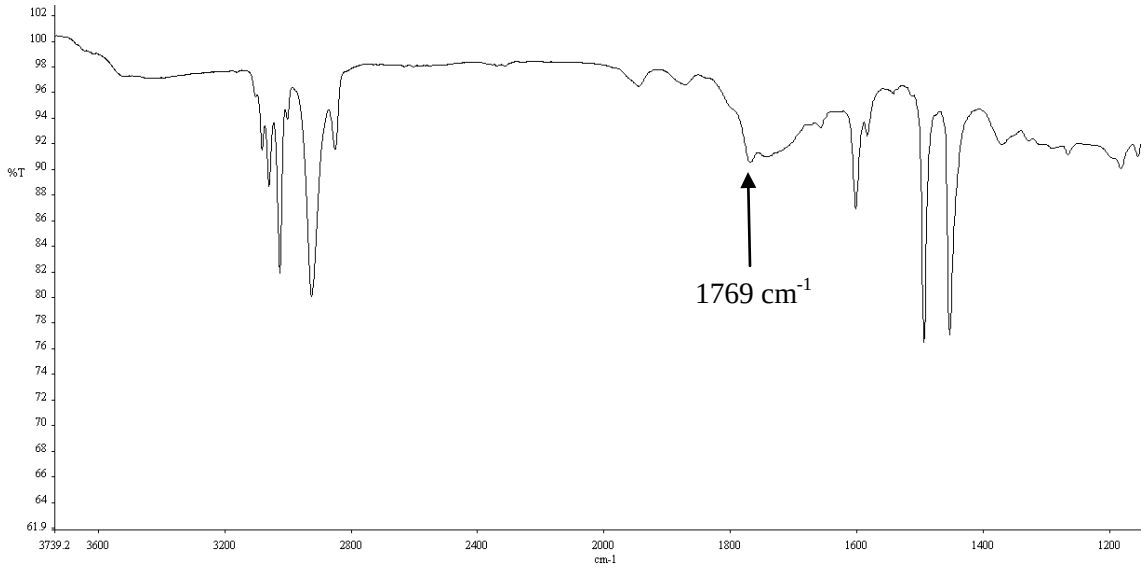

Figure 19. IR spectrum of the soluble polymer resulting from the catalytic reaction of high molecular weight PS with 5 mol% Fe(TPA) and 10 mL of 10 % H_2O_2 in 1:1 DCM:MeCN

solution during the course of the reaction, but the soluble product, once precipitated and dried, tended to form an insoluble gel (from 70 to 90 % of the initial mass) upon attempts to dissolve it in DCM. The gel was soaked in DCM to recover any soluble product and the DCM was then used to obtain a weak IR spectrum of any soluble product. The formation of gel suggested that cross-linking was predominant and thus the reaction conditions were varied as above, but now with the goal of reducing the suspected cross-

linking and increasing the solubility of the product. Decreasing the amount of catalyst to 2.5 mol% increased the recovery of soluble material (i.e. decreased the formation of gel) without significantly decreasing the intensity of the carbonyl peak in the IR spectrum of the soluble product. Reducing the complex to 0.5 mol% distinctly decreased the intensity of the carbonyl band. Reducing the amount of oxidant added by reducing the volume of H_2O_2 solution resulted in a slight increase in the intensity of the peak for the soluble product, while reducing the oxidant by decreasing the concentration had no effect on the overall strength of the peak. Neither had any significant or reproducible effects on the solubility of the product. After all the variations, using 2.5 mol% Fe(TPA) in 1:1 DCM:MeCN with 10 mL of 10 % H_2O_2 produced the most soluble material, with only a slightly weaker peak at 1769 cm^{-1} (Figure 20). DSC analysis showed an increase in T_g from 103 to 108 °C, which could suggest the presence of hydrogen bonding due to the introduction of oxygen functionality, but the NMR analysis was once again inconclusive. The broad band was more distinct, but again failed to show any correlation with other signals in the COSY, HSQC or HMBC spectra. GPC analysis of the soluble product indicated the same issue as with the previous product – the number average molecular weight (M_n) of the polymer decreased by a factor of 10 (from 2.1×10^5 to 1.7×10^4 $gmol^{-1}$) and the polydispersity increased to 1.8 from 1.0, once again indicating chain cleavage in the reaction, which is undesirable.

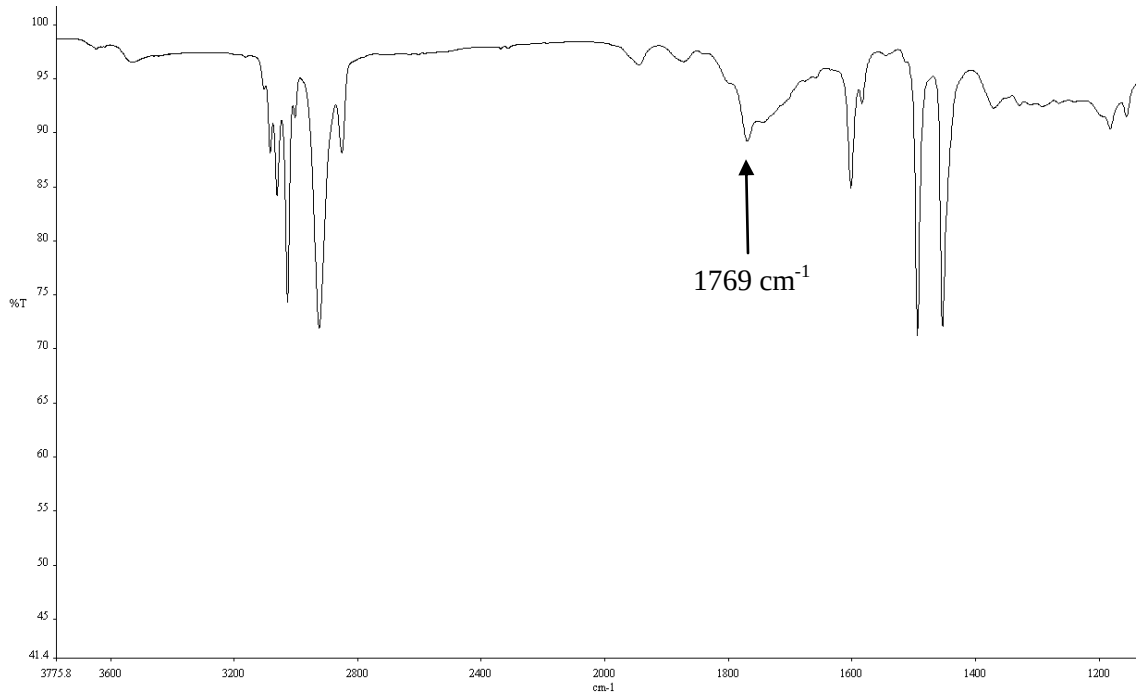

Figure 20. IR spectrum of the soluble polymer resulting from the catalytic reaction of high molecular weight PS with 2.5 mol% Fe(TPA) and 10 mL of 10 % H_2O_2 in 1:1 DCM:MeCN

The production of both the insoluble mass during the reaction as well as the insoluble gel upon precipitation and drying of the soluble fraction was hypothesized to be the result of cross-linking. In further attempts to control the cross-linking, a series of dilution experiments was run. For cross-linking to be effective, the pieces need to be in proximity to each other and thus diluting the reaction should reduce the effect. Diluting the standard 50 mL reaction to 1.0 L, retaining the 1:1 DCM:MeCN ratio, and using 5 mol% Fe(TPA) with 10 mL 10 % H_2O_2 resulted in the recovery of 86 % of the initial mass as soluble material, in comparison to only 4 % from the 50 mL reaction. However, the product from the dilution reaction showed no indication of oxyfunctionalization in the IR spectrum. Increasing the amount of complex to 10 mol% brought back the production

of insoluble material (nearly 60 % of the initial mass) while only producing a slight carbonyl signal in the IR spectrum of the soluble product. Doubling the hydrogen peroxide concentration returned fully soluble material without any oxygen functionality. Reduction of the dilution to 500 mL produced insoluble gel again and no functionalization evident in the IR spectrum of the soluble product. Thus the dilution experiments supported the hypothesis that cross-linking contributes to the formation of the insoluble products, but did not provide a viable avenue to a solution for the problem.

3.3.2 Low Molecular Weight Polystyrene

It was suggested by Dr. M. Cunningham that perhaps the propensity for cross-linking would decrease with a polymer of lower molecular weight and so the reactions were done again, but this time with polystyrene whose number average molecular weight (M_n) was 9.5×10^2 $gmol^{-1}$ as determined by GPC. The general reaction conditions remained the same and again the catalyst and amount were varied along with the amount and concentration of H_2O_2 as well as the ratio of DCM:MeCN. It was initially noted that the overall recovery of polymeric material from the reactions was significantly lower than for the high molecular weight PS – total recoveries in the 50 % range rather than in the 90 % range – likely due to the increased solubility of the smaller polymer. Making the change from ethanol to methanol in the precipitation procedure caused the overall recovery to increase to 70-80 %.

Another change that was noticed with the switch from high molecular weight PS to low molecular weight PS involved the polymeric material that precipitated over the

course of the reaction. With the high molecular weight PS, this material was insoluble in DCM, but with the low molecular weight PS it would still dissolve in DCM after collection and drying. Due to its solubility, analysis of this material was possible. GPC analysis showed that the M_n of this material increased from 950 $gmol^{-1}$ to 54 000 $gmol^{-1}$ suggesting that cross-linking was occurring and possibly responsible for the precipitation. IR spectra of this material were no different than the starting material, showing no oxyfunctionalization.

In catalytic reactions with 5 mol% Fe(BPMEN), 10 mL of 10 % H_2O_2 and 1:1 DCM:MeCN the soluble product showed a slight peak at 1769 cm^{-1} in the IR spectrum. The soluble fraction remained soluble after precipitation and drying (i.e. no gel was formed), but the degree of oxyfunctionalization was not improved. Variations in the amount of catalyst did not increase the intensity of the carbonyl peak, nor did changing the amount of oxidant. However, due to the lower molecular weight, the polymer was now more readily soluble and increasing the proportion of MeCN through 4:6 DCM:MeCN and 3:7 DCM:MeCN more than doubled the intensity of the peak at 1769 cm^{-1} in the IR of the soluble product, but increased the amount of material that precipitated over the course of the reaction. However, the carbonyl peak was still no stronger than that observed with Fe(TPA) and the high molecular weight PS, which was not sufficient for detection via NMR.

Changing from Fe(BPMEN) to Fe(TPA) under the initial conditions (5 mol% Fe(TPA), 10 mL of 10 % H_2O_2 and 1:1 DCM:MeCN) resulted in a carbonyl peak at 1769 cm^{-1} that was stronger than with Fe(BPMEN) under the same conditions and gave a better

recovery of soluble material (50 % of the mass of the starting PS). However, the peak was still no stronger than with the high molecular weight PS where the oxyfunctionalization was not detectable via NMR. The conditions were again varied in an attempt to increase the strength of the carbonyl peak. Varying the oxidant amount in 1:1 DCM:MeCN showed slight variations – mostly a slight weakening of the signal, but all peaks were stronger than for the corresponding conditions with Fe(BPMEN). A similar trend was noticed for variations in the amount of catalyst as well as variations in solvent ratios – Fe(TPA) consistently produced product with stronger carbonyl signals in the IR spectra than did Fe(BPMEN) under similar conditions. Consequently, further investigation was done only with Fe(TPA). The reactions with Fe(TPA) and low molecular weight PS produced more soluble product than the high molecular weight reactions, although higher catalyst loadings did result in the formation of some gel.

Due to the better recovery with the low molecular weight PS than the high molecular weight PS in 4:6 and 3:7 DCM:MeCN, variations of the amount of catalyst and oxidant were done within these conditions as well. The same general trends appeared, with carbonyl strength being slightly greater for the products from 3:7 DCM:MeCN. The amount of soluble material recovered was relatively consistent across the reactions at 30-40 % of the mass of the initial PS. Increasing Fe(TPA) to 10 mol% with 10 mL of 10 % H_2O_2 in 3:7 DCM:MeCN or increasing the concentration of the H_2O_2 to 20 % caused a slight increase in the carbonyl strength, but a significant decrease in the amount of soluble oxyfunctionalized product (9-15 % of the mass of initial PS).

The rest of the recovered solid remained soluble in DCM, although its IR spectrum lacked any indication of functionalization.

Although changing to a lower molecular weight PS reduced the production of insoluble gel, little headway had been made into increasing the degree of oxyfunctionalization. Returning to the literature it was found that, when attempting oxyfunctionalization of complex molecules, White and Chen[29] had better success with iterative additions of catalyst and oxidant. This procedure was developed to decrease the extent of both catalyst and oxidant decomposition during long reactions. A set of conditions was devised (see sections 2.6.10 and 2.6.11) such that after all the additions, the final solvent ratio would be 3:7 DCM:MeCN. Based on the slightly increased carbonyl peak intensity evident in the IR of the soluble product from the use of 10 mol% Fe(TPA) and 20 % H_2O_2, two additions of 5 mol% and 10 mL of 10 % H_2O_2 were initially used and an increase in carbonyl signal strength of approximately 50 % was seen at 1769 cm^{-1} in the IR spectrum of the soluble recovered product as well as the development of a broad OH stretch at 3400 cm^{-1} with a possible C-O stretch around 1224 cm^{-1} (Figure 21). Making two additions of 2.5 mol% Fe(TPA) with 5 mL of 20 % H_2O_2 caused no visible changes in the IR spectrum of the soluble recovered product, nor did dividing the overall catalyst and oxidant amounts into three additions. Placing the product in DCM solution over 3Å molecular sieves for 24 hours caused no change in the broad band at 3400 cm^{-1} (Figure 22), suggesting that the band is not due to residual water. After weeks of being open to the air, the IR spectrum of the soluble product remained unchanged. The recovery of functionalized material from the iterative addition reactions

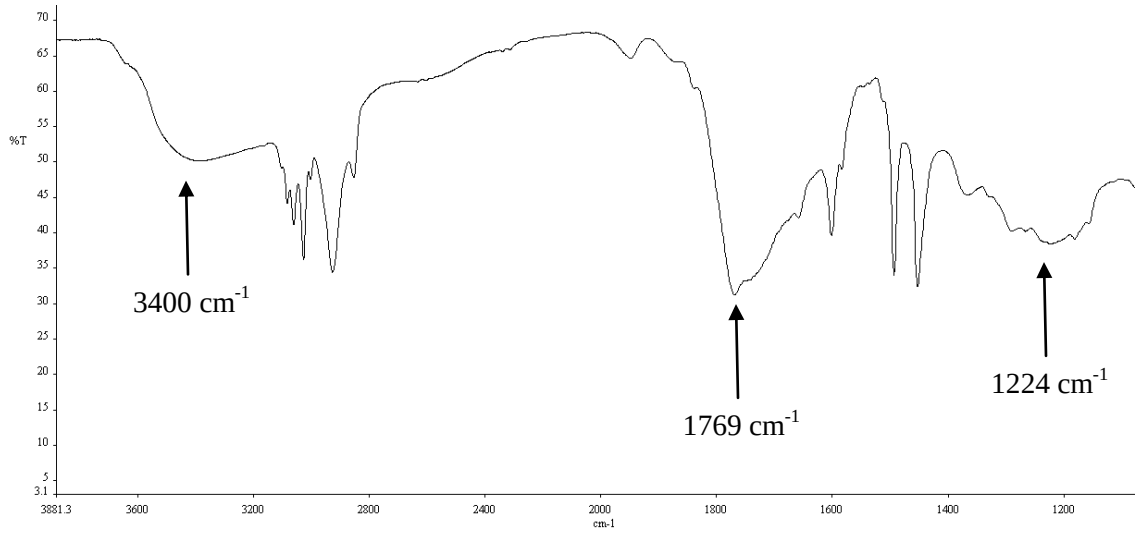

Figure 21. IR spectrum of the soluble polymer resulting from the catalytic reaction of low molecular weight PS with 2 × (5 mol% Fe(TPA) and 10 mL of 10 % H_2O_2) in 3:7 DCM:MeCN

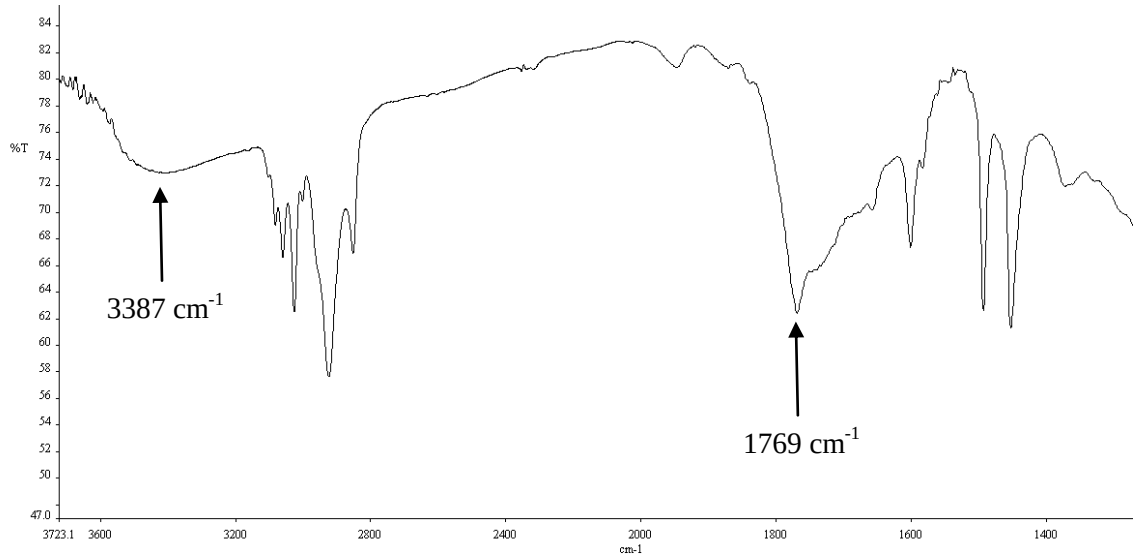

Figure 22. IR spectrum of the soluble polymer resulting from the catalytic reaction of low molecular weight PS with 2 × (5 mol% Fe(TPA) and 10 mL of 10 % H_2O_2) in 3:7 DCM:MeCN after having been dried over 3Å molecular sieves for 24 hours

was comparable with that of previous reactions (40-50 % of initial mass of PS). Furthermore, the solid that precipitated over the course of the reaction was still soluble in DCM and the IR spectrum was exactly that of polystyrene. The distinct difference between the IR spectra of this product fraction and the soluble fraction recovered from solution further supports the presence of hydroxyl and carbonyl groups in the soluble product.

GPC analysis of the products from the iterative addition reactions indicated no significant change in the molecular weight, with product M_n values ranging from 760 to 780 $gmol^{-1}$ in comparison to M_n for the starting material of 950 $gmol^{-1}$. The calibration curve for analysis was done using polystyrene standards, possibly increasing the reported 9 % error associated with all molecular weight values due to the fact that the products contain functionality not present in pure polystyrene. The polydispersity of the soluble product polymers ranged from 1.2 to 1.3, agreeing well with that of the staring material (1.2) even without taking into consideration the resulting 13 % experimental error. The data suggested that the reactions did not induce chain cleavage, unlike the reactions with the high molecular weight PS, nor did any cross-linking occur to increase the molecular weight. DSC analysis of the products showed elevated glass transition temperatures ranging from 82.2 to 99.7 °C when compared to that of the starting material (59.7 °C). This increase is much more prominent than with the high molecular weight products, where only a 5 °C increase was observed, which supports the indication of increased oxyfunctionalization seen in the IR spectra. The greatest increase in T_g corresponded to the reaction with two additions of 5 mol% Fe(TPA) with 10 mL of 10 % H_2O_2.

The ^{1}H NMR spectra of the products all showed a broad band located between 3.5 and 4 ppm (Figure 23), which was not present in the ^{1}H NMR of the starting material. This range was the location predicted by ACDLABS software for protons adjacent to any carbonyl or hydroxyl functionality along the polystyrene backbone. The sample with the most prominent broad hump, again the product from two additions of 5 mol% Fe(TPA) with 10 mL of 10 % H_2O_2, was further analyzed by NMR, but no correlation of the broad hump with any other signal was seen in the COSY, HSQC or HMBC spectra at 600 MHz. This analysis remains inconclusive since it could be that the signal is either not strong

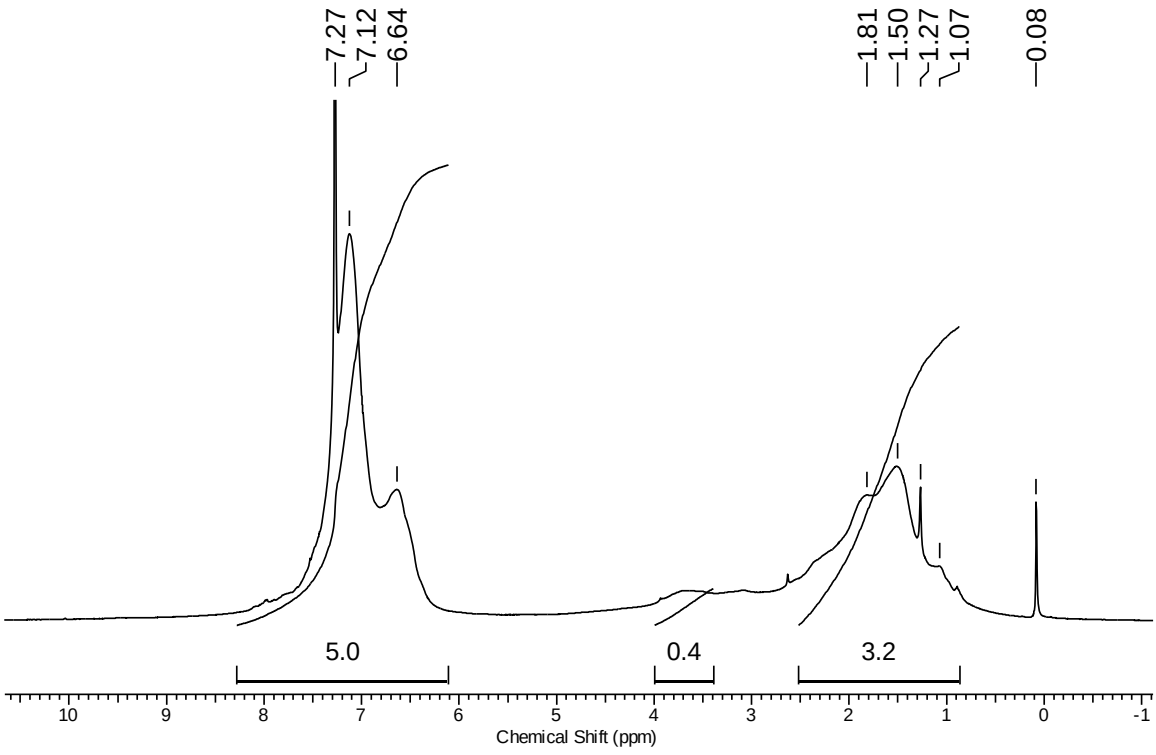

Figure 23. ^{1}H NMR spectrum in $CDCl_3$ of the soluble product from the catalytic reaction of low molecular weight PS with 2 × (5 mol% Fe(TPA) and 10 mL of 10 % H_2O_2) in 3:7 DCM:MeCN

enough or too broad to show correlation with the other signals, not necessarily that there is no oxyfunctionalization. Unfortunately, the information that could have been attained from the NMR analysis would have helped identify the type of oxyfunctionalization present. As it is, comparison of integration values suggests that for every repeat unit, there are 0.4 proton adjacent to an oxyfunctionalized site. However, depending on the location of the functionality, there could be 2, 3 or even 4 protons (Figure 24) adjacent to it, meaning that the degree of functionalization could range from 100 to 200 functional groups per 1000 repeat units.

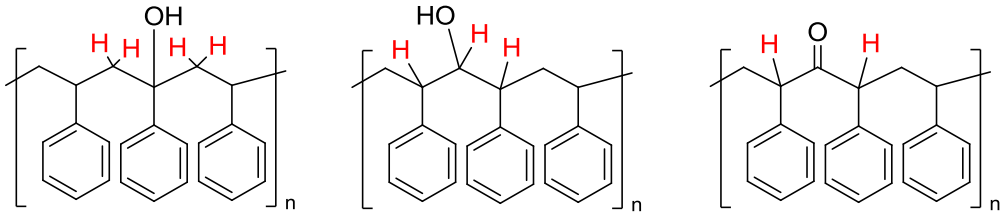

Figure 24. Locations of possible oxyfunctionalization and the adjacent protons

3.4 Control Reactions

Reactions were performed in the absence of either catalyst or polystyrene (see section 2.5) to ensure that the IR signals obtained were indeed related to the interaction of the catalyst, substrate and oxidant. The peaks in the IR spectra of the tar-like products from the reactions of Fe(TPA) and Fe(BPMEN) with H_2O_2 in the absence of PS are not present in any of the IR spectra of the polymer products from the catalytic reactions. The reaction of PS with H_2O_2 in the absence of catalyst gave product whose IR spectrum was

identical to that of the starting material. Thus any hydroxyl or carbonyl peaks present in the IR spectra of polymer products from catalytic reactions are due to the interaction of these three components.

3.5 Analysis of Results

With only one previously published report of direct polymer oxyfunctionalization,[11] comparison with literature is straightforward but not as enlightening as if there was a larger body of work with different conditions and variations. Boaen and Hillmyer[11] reported the oxyfunctionalization of squalane as well as a polymer model (PEP) (Figure 25) with a manganese porphyrin catalyst (see section 1.2.2.2). They reported a change in the T_g for their materials of only 4 °C while the changes observed here were on the order of 40 °C. Considering that the change in T_g

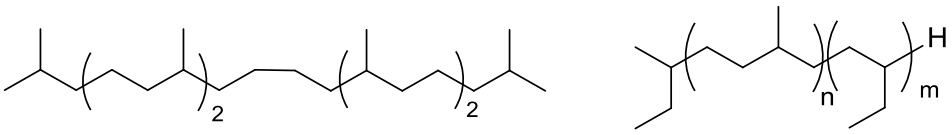

Figure 25. Structure of squalane (left) and PEP (right)

reflects the degree of functionalization, the results are consistent. The degree of oxyfunctionalization reported for squalane was up to 57 groups per 1000 repeat units, which is less than the estimated 100 to 200 groups per 1000 repeat units reported here. Thus it would be expected that the oxyfunctionalized product from this work would show a greater change in T_g value.

Boaen and Hillmyer reported peaks in the carbonyl region of the IR spectrum at 1716 and 1710 cm^{-1} for squalane and PEP respectively along with broad hydroxyl stretches around 3400 cm^{-1}. The carbonyl peaks agree well with values for similar small molecules.[35] For example, 3-pentanone has a carbonyl peak at 1716 cm^{-1} and 2-methyl-3-pentanone has one at 1713 cm^{-1}. The carbonyl stretch reported in this thesis is significantly higher than those of Boaen and Hillmyer (1769 cm^{-1}) but the related small molecules also differ by the inclusion of a phenyl group. In the case of PS, a related small molecule could be phenyl-2-propanone whose carbonyl peak[35] is located at 1742 cm^{-1}, which is still lower than that reported in this thesis. However, if one considers that the carbonyl peak for acetone[35] is located at 1715 cm^{-1}, and the addition of a phenyl group to make phenyl-2-propanone shifts the peak to 1742 cm^{-1}, then it is possible that the combined electron withdrawing effects of the multiple phenyl groups in PS could shift the location of the peak to 1769 cm^{-1}. Due to the broad nature of the hydroxyl peak, the same effect is not apparent and the values agree.

A similar comparison can be made for the ^{1}H NMR data, where Boaen and Hillmyer reported the development of a peak around 2.6 ppm. They state that this shift is consistent with the protons α to a carbonyl carbon. For the oxyfunctionalized PS product, ^{1}H NMR predicting software was used, but the same rationale for the IR spectra can be applied to the ^{1}H NMR spectra. Consider that the proton resonance for acetone is approximately 2.0 ppm,[35] and that of the CH_2 group of phenyl-2-propanone is approximately 3.0 ppm.[35] Thus the presence of the phenyl group shifts the resonance downfield by approximately one ppm. Applying this correction to the results of Boaen

and Hillmyer would predict a peak at approximately 3.6 ppm. Taking into consideration the increased deshielding effect due to the multiple phenyl groups in PS brings the value in line with that predicted by the software (3.5 – 4.0 ppm). The broad band between 3.5 and 4.0 ppm in the ^{1}H NMR of the oxyfunctionalized PS is thus consistent with predicted values

.

3.6 Importance of Colours in the Catalytic Reactions

Various colour changes, which are not without significance, were observed throughout the progress of the catalytic reactions. The goal of the project was to oxyfunctionalize polystyrene and thus although the colours were observed, no real investigation into their origin was done. However, a logical hypothesis based on observations can be set forth. The reactions with Fe(BPMEN) generally changed from initially being clear light peach before addition of H_2O_2, to amber and green, then a dark, nearly opaque blue-black before returning to a green-blue and eventually golden yellow. The reactions with Fe(TPA) generally showed the development of a blue-grey cast upon addition of H_2O_2 to the initially clear red reaction solutions, which slowly became bright orange and eventually bright yellow. The colour changes were most vivid with the high molecular weight PS and were not observed in any of the control reactions or in the reactions with cyclohexane. Thus the colour is associated with the presence of the polymer. One of the noticeable differences between the reactions with high and low molecular weight PS was the significant cross-linking that occurred with the high molecular weight PS. Similarly the colours were most vivid for these reactions. In

addition, when the high molecular weight PS reactions were diluted, little colour change was observed and little cross-linking occurred. However, the colours were not due to the polymer alone as reducing the amount of catalyst used also caused a reduction in the intensity of the observed colours. Furthermore, it has been shown that styrene radicals absorb in the 350 and 600 nm region of the visible spectrum[36,37] and that (methylethyl)benzene radicals[38] absorb at 322 nm, which could account for the observed blue and green colours. All of these observations suggest that radicals were produced from the polymer by the catalyst and H_2O_2. This rationalization is consistent with two of the proposed mechanistic pathways presented in section 1.3.2.2 and in Figure 9. Taking into account the fact that H_2O_2 is present in excess, rationalization of the observed colour changes could suggest that the reaction mechanism follows path (a) in Figure 9.

However, radicals are not generally long-lived and the colour may remain in the reaction for at least a day. Another possible explanation is the production of various transient iron complexes that are formed from the interaction of the three components – catalyst, oxidant and polymer. These complexes may have longer lifetimes than one would expect for radicals and would thus explain the persistence of the colours. This hypothesis provides no clear reason why these colours should be stronger with the high molecular weight PS, but is consistent with the observation that more catalyst produced stronger colour changes and that less catalyst produced weaker colour changes, as well as with the lack of colour changes in reactions where one of the three components was absent.

Chapter 4

Summary and Conclusions

This work provides a proof of principle for the oxyfunctionalization of polystyrene using an iron-based non-heme catalyst and hydrogen peroxide. Both $[Fe(TPA)(MeCN)_2][OTf]_2$ and $Fe(BPMEN)(OTf)_2$ were investigated with $[Fe(TPA)(MeCN)_2][OTf]_2$ consistently producing a stronger carbonyl peak at 1769 cm^{-1} than $Fe(BPMEN)(OTf)_2$ in the IR spectrum of the polymeric products. Reactions with high molecular weight polystyrene were plagued by formation of insoluble gels most likely due to cross-linking. Oxyfunctionalization was indicated by the carbonyl peak at 1769 cm^{-1} in the IR spectra, and supported by a slight increase in the glass transition temperature of the product. However, molecular weight analysis showed that significant chain cleavage was occurring, which is undesirable, and evidence of oxyfunctionalization was not seen in the ^1H NMR spectrum. Reactions with low molecular weight polystyrene produced soluble polymeric product with a carbonyl peak at 1769 cm^{-1} in the IR spectra, indicating a selective oxyfunctionalization, but at levels no greater than that of the high molecular weight polystyrene. The use of iterative additions of catalyst and oxidant resulted in increased oxyfunctionalization but with loss of specificity, since signals for both hydroxyl and carbonyl functional groups were evident (3400 and 1769 cm^{-1} respectively) in the IR spectra. The presence of oxyfunctionalization was further supported by an increase in the glass transition temperature of the polymeric product relative to the stating material, as well as evidence of a broad peak between 3.5 and 4.0 ppm in the ^1H NMR spectra, as expected for protons neighbouring a hydroxyl or carbonyl

group, but no correlation could be found with other signals through COSY, HSQC or HMBC leaving the exact nature and location of the functionality unconfirmed. Molecular weight analysis showed that the polymeric product did not undergo significant chain degradation.

The approach described in this work is but one of many possible approaches to the oxyfunctionalization of polymers using transition metal complexes. Further investigations could involve the use of other types of complexes – both porphyrins[19] and di-iron complexes[34] have shown catalytic activity towards oxyfunctionalization of alkanes. Different solvent systems could be investigated to promote or hinder the radical nature of the reaction, perhaps changing the selectivity. Finally, the initial impetus for the research was to increase the biodegradability of polystyrene without greatly altering its physical and mechanical properties so that the polymeric product could be used for similar applications. Although evidence from this research points to the successful oxyfunctionalization of the product without significant chain degradation, the physical and mechanical properties of the product would still need to be evaluated, along with its biodegradability, before it could be considered a useful material.

References

1. Brysdon, J. A. *Plastics Materials*,7th Edition.; Butterworth-Heinemann; Oxford, 1999.
2. Zhang, X.; Shen, S.; Fan, L. *J. Mater. Sci.* **2007**, 42, 7621-7629.
3. McNamara, C. A.; Dixon, M. J.; Bradley, M. *Chem. Rev.* **2002**, 102, 3275-3300.
4. Desai, S. M.; Singh, R. P. *Adv. Polym. Sci.* **2004**, 169, 231-293.
5. Boaen, N. K.; Hillmyer, M. A. *Chem. Soc. Rev.* **2005**, 34, 267-275.
6. Boffa, S.; Novak, B. M. *Chem. Rev.* **2000**, 100, 1497-1493.
7. Farris, S.; Pozzoli, S.; Biagioni, P.; Duo, L.; Manicinelli, S.; Piergiovanni, L. *Polymer*, **2010**, 51, 3591-3605.
8. Hollander, A.; Behnisch, J.; Zimmermann, H. *J. Appl. Polym. Sci.* **1993**, 49, 1857-1863.
9. Nomura, K.; Kitiyanan, B. *Curr. Org. Synth.* **2008**, 5, 217-226.
10. Kondo, Y.; Garcia-Cuadrado, D.; Hartwig, J. F.; Boaen, N. K.; Wagner, N. L.; Hillmyer, M. A. *J. Am. Chem. Soc.* **2002**, 124, 1164-1165.
11. Boaen, N.K.; Hillmyer, M.A. *Macromolecules* **2003**, 36, 7027-7034.
12. Fenton, J. H. J. *J. Chem. Soc.* **1894**, 65, 899-910.
13. Haber, F.; Weiss, J. *Proc. R. Soc. Lond. A* **1934**, 147, 332-351.
14. Walling, C. *Acc. Chem. Res.* **1975**, 8, 125-131.
15. (a) Kremer, M. L.; Stein, G. *Trans. Farr. Soc.* **1959**, 55, 959-973. (b) Kremer, M. L. *Trans. Farr. Soc.* **1962**, 58, 702-707.
16. Que, L. Jr.; Tolman, W. B. *Nature* **2008**, 455, 333-340.

17. Groves, J. T.; Nemo, T. E.; Myers, R. S. *J. Am. Chem. Soc.* **1979**, 101, 1032-1033.
18. Mansuy, D. *Coord. Chem. Rev.* **1993**, 125, 129-142.
19. Guedes, A.; Smith, J. R. L.; Nascimento, O. R.; Guedes, D. F. C.; das Dores Assis, M. *J. Braz. Chem. Soc.* **2005**, 16, 835-843.
20. Dick, A. R.; Sanford, M. S. *Tetrahedron* **2006**, 62, 2439-2463.
21. Lessing, R.A; Norman, R. E.; Que, L. Jr. *Inorg. Chem.* **1990**, 29, 2553-2555.
22. Chen, K; Que, L. Jr. *J. Am. Chem. Soc.* **2001**, 123, 6327-6337.
23. Kim, J.;Harrison, R. G.; Kim, C.; Que, L. Jr. *J. Am. Chem. Soc.* **1996**, 118, 4373-4379.
24. Chen, K.; Que, L. Jr. *Chem. Commun.* **1999**, 1375-1376.
25. England, J.; Gondhia, R.; Bigorra-Lopez, L.; Petersen, A. R.; White, A. J. P.; Britovsek, G. J. P. *Dalton Trans.* **2009**, 5319-5334.
26. Britovsek, G. J. P.; England, J.; White, A. J. P. *Inorg. Chem.* **2005**, 44, 8125-8134.
27. Britovsek, G. J. P.; England, J.; Spitzmesser, S. K.; White, A. J. P.; Williams, D. J. *Dalton Trans.* **2005**, 945-955.
28. Britovsek, G. J. P.; England, J.; White, A. J. P. *Dalton Trans.* **2006**, 1399-1408.
29. Chen, M. S.; White, M. C. *Science* **2007**, 318, 783-787.
30. Chen, M. S.; White, M. C. *Science* **2010**, 327, 566-571.
31. Hagen, K. S. *Inorg. Chem.* **2000**, 39, 5867-5869.
32. Diebold, A.; Hagen, K. S. *Inorg. Chem.* **1998**, 37, 215-223.
33. Gomez, L.; Garci-Bosch, I.; Company, A.; Benet-Buchholz, J.; Polo, A.; Sala, X.; Ribas, X.; Costas, M. *Angew. Chem. Int. Ed.* **2009**, 48, 5720-5723.

34. Visvaganesan, K.; Suresh, E.; Palaniandavar, M. *Dalton Trans.* **2009**, 3814-3823.

35. SDBSWeb: http://riodb01.ibase.aist.go.jp/sdbs/ (National Institute of Advanced Industrial Science and Technology, July 13, 2011).

36. Johnston, L.J.; Schepp, N. P. *J. Am. Chem. Soc.*, **1993**, 115, 6564-6571.

37. Nagai, T.; Miyazaki, T.; Sonoyama, Y.; Tokura, N. *J. Poly. Sci. A*, **1968**, 6, 3087-3107.

38. Ikeda, H.; Hoshi, Y.; Namai, H.; Tanaka, F.; Goodman, J. L.; Mizuno, K. *Chem. Eur. J.*, **2007**, 13, 9207-9215.

Appendix – Crystal Structure Data for $[Fe(TPA)(MeCN)_2](OTf)_2$

Table 1. Crystal data and structure refinement for $[Fe(TPA)(MeCN)_2](OTf)_2$

Identification code	mb37	
Empirical formula	C24 H24 F6 Fe N6 O6 S2	
Formula weight	726.46	
Temperature	296(2) K	
Wavelength	0.71073 Å	
Crystal system	Monoclinic	
Space group	P2(1)/c	
Unit cell dimensions	a = 18.651(10) Å	α= 90°.
	b = 18.814(12) Å	β= 90.555(10)°.
	c = 17.675(11) Å	γ = 90°.
Volume	6202(6) $Å^3$	
Z	8	
Density (calculated)	1.556 Mg/m^3	
Absorption coefficient	0.705 mm^{-1}	
F(000)	2960	
Crystal size	0.25 x 0.10 x 0.06 mm^3	
Theta range for data collection	1.92 to 26.00°.	
Index ranges	-23<=h<=16, -23<=k<=12, -21<=l<=21	
Reflections collected	24686	
Independent reflections	11969 [R(int) = 0.0718]	
Completeness to theta = 26.00°	98.2 %	
Absorption correction	Multi-scan	
Max. and min. transmission	0.9589 and 0.8434	
Refinement method	Full-matrix least-squares on F^2	
Data / restraints / parameters	11969 / 16 / 835	
Goodness-of-fit on F^2	0.967	
Final R indices [I>2sigma(I)]	R1 = 0.0955, wR2 = 0.2510	
R indices (all data)	R1 = 0.2070, wR2 = 0.3434	
Largest diff. peak and hole	1.494 and -0.553 $e.Å^{-3}$	

Table 2. Atomic coordinates (× 10^4) and equivalent isotropic displacement parameters ($Å^2$ × 10^3). U(eq) is defined as one third of the trace of the orthogonalized U^{ij} tensor.

	x	y	z	U(eq)
Fe(1)	4422(1)	7531(1)	307(1)	42(1)
Fe(2)	9357(1)	7467(1)	210(1)	48(1)
N(1)	4665(3)	8542(3)	519(3)	46(2)
N(2)	4856(3)	7710(4)	-679(3)	50(2)
N(3)	5377(3)	7315(3)	723(3)	46(2)
N(4)	4021(3)	7556(3)	1335(3)	46(2)
N(5)	3494(4)	7798(4)	-102(4)	53(2)
N(6)	4202(3)	6542(4)	97(4)	50(2)
N(7)	9533(4)	6447(4)	395(4)	59(2)
N(8)	10322(4)	7584(4)	664(4)	57(2)
N(9)	8935(3)	7474(4)	1230(4)	54(2)
N(10)	8443(4)	7125(4)	-218(3)	50(2)
N(11)	9794(4)	7407(4)	-784(4)	63(2)
N(12)	9187(3)	8480(4)	21(4)	55(2)
C(1)	4609(5)	8924(4)	-222(5)	68(3)
C(2)	4917(4)	8422(5)	-832(5)	59(2)
C(3)	5201(5)	8678(5)	-1501(5)	74(3)
C(4)	5433(6)	8178(6)	-2038(5)	88(3)
C(5)	5397(5)	7475(5)	-1888(5)	69(3)
C(6)	5112(5)	7283(5)	-1216(5)	61(2)
C(7)	5419(5)	8600(5)	823(6)	67(3)
C(8)	5765(4)	7894(4)	927(4)	49(2)
C(9)	6457(5)	7836(5)	1207(5)	67(3)
C(10)	6760(5)	7168(6)	1310(6)	73(3)
C(11)	6361(5)	6584(5)	1118(5)	72(3)
C(12)	5692(5)	6673(5)	838(5)	56(2)
C(13)	4153(4)	8812(4)	1079(4)	52(2)
C(14)	3965(4)	8225(4)	1606(4)	46(2)
C(15)	3698(4)	8356(5)	2332(4)	59(2)
C(16)	3470(5)	7785(6)	2774(5)	74(3)
C(17)	3547(5)	7117(5)	2497(5)	74(3)
C(18)	3821(4)	7016(5)	1790(5)	60(2)
C(19)	2949(6)	7904(5)	-335(5)	65(3)
C(20)	2247(5)	8126(7)	-662(6)	91(3)
C(21)	4068(4)	5966(4)	-66(5)	54(2)
C(22)	3904(6)	5252(5)	-259(6)	82(3)
C(23)	10309(5)	6325(6)	399(6)	82(3)

C(24)	10684(5)	6962(7)	727(5)	74(3)
C(25)	11351(7)	6930(8)	1020(7)	100(4)
C(26)	11681(7)	7530(9)	1280(7)	105(5)
C(27)	11323(6)	8187(8)	1227(6)	99(4)
C(28)	10630(5)	8187(6)	915(5)	69(3)
C(29)	9181(5)	6212(5)	1119(5)	70(3)
C(30)	8929(4)	6828(5)	1572(4)	53(2)
C(31)	8667(5)	6740(6)	2300(5)	67(3)
C(32)	8410(6)	7322(7)	2682(5)	92(4)
C(33)	8416(6)	7980(6)	2334(6)	87(3)
C(34)	8682(5)	8051(5)	1609(5)	68(3)
C(35)	9151(6)	6049(5)	-255(5)	75(3)
C(36)	8432(6)	6422(5)	-379(5)	69(3)
C(37)	7815(7)	6076(6)	-667(6)	92(3)
C(38)	7211(6)	6493(8)	-769(6)	89(3)
C(39)	7206(6)	7177(7)	-629(6)	78(3)
C(40)	7837(5)	7480(5)	-341(5)	61(2)
C(41)	10066(5)	7452(6)	-1365(5)	74(3)
C(42)	10402(6)	7420(8)	-2092(6)	119(5)
C(43)	9126(4)	9069(5)	-109(6)	65(2)
C(44)	9067(6)	9829(5)	-279(7)	98(4)
S(1)	5462(1)	5207(1)	-1924(2)	73(1)
O(1)	5049(5)	5523(6)	-2502(5)	136(4)
O(2)	5608(4)	5654(5)	-1286(5)	115(3)
O(3)	5254(4)	4496(4)	-1728(5)	98(2)
C(45)	6324(8)	5103(6)	-2324(8)	97(4)
F(1)	6318(5)	4715(5)	-2944(5)	157(3)
F(2)	6614(4)	5716(4)	-2529(5)	138(3)
F(3)	6789(4)	4789(5)	-1863(6)	138(3)
S(2)	7036(2)	9684(1)	-320(2)	81(1)
O(4)	7442(4)	9159(4)	96(5)	116(3)
O(5)	7342(4)	10397(4)	-289(5)	110(3)
O(6)	6276(4)	9672(4)	-253(5)	105(3)
F(4)	6966(5)	8770(5)	-1416(6)	169(4)
F(5)	7855(4)	9454(5)	-1502(5)	155(3)
F(6)	6790(5)	9808(5)	-1790(4)	141(3)
C(46)	7146(8)	9399(10)	-1259(10)	153(8)
S(3)	11928(2)	5973(2)	-892(2)	93(1)
O(7)	12644(5)	6271(6)	-810(6)	163(4)
O(8)	11428(6)	6537(5)	-1032(6)	170(5)
O(9)	11809(5)	5429(4)	-366(4)	122(3)
C(47)	11953(9)	5520(10)	-1774(8)	118(5)

F(7)	12438(9)	5009(8)	-1724(6)	272(9)
F(8)	11392(7)	5244(7)	-2001(6)	212(6)
F(9)	12154(5)	5957(6)	-2333(5)	174(4)
S(4A)	10464(3)	9990(4)	-2344(5)	80(2)
S(4B)	10511(5)	9632(8)	-1902(7)	122(5)
O(10B)	10719(17)	9165(14)	-1236(12)	162(11)
O(10A)	10575(16)	10304(13)	-3045(11)	205(12)
O(11)	10097(7)	9350(7)	-2434(8)	208(6)
O(12)	10296(5)	10422(6)	-1735(7)	157(4)
F(12A)	11372(16)	9345(16)	-1528(17)	241(9)
F(10)	11805(5)	10154(8)	-1900(10)	238(7)
F(11)	11645(6)	9184(8)	-2482(9)	242(6)
F(12B)	11416(19)	10161(18)	-2852(18)	241(9)
C(48A)	11391(12)	9688(11)	-2122(16)	140(7)
C(48B)	11420(13)	9778(10)	-2298(15)	140(7)

Table 3. Bond lengths [Å] and angles [°].

Fe(1)-N(5)	1.936(8)	N(3)-C(12)	1.356(10)
Fe(1)-N(6)	1.941(7)	N(4)-C(14)	1.351(9)
Fe(1)-N(2)	1.959(6)	N(4)-C(18)	1.352(10)
Fe(1)-N(3)	1.963(7)	N(5)-C(19)	1.111(10)
Fe(1)-N(4)	1.972(6)	N(6)-C(21)	1.148(9)
Fe(1)-N(1)	1.991(6)	N(7)-C(23)	1.466(11)
Fe(2)-N(11)	1.946(7)	N(7)-C(29)	1.511(10)
Fe(2)-N(12)	1.959(8)	N(7)-C(35)	1.539(11)
Fe(2)-N(10)	1.966(7)	N(8)-C(28)	1.345(11)
Fe(2)-N(9)	1.974(6)	N(8)-C(24)	1.355(12)
Fe(2)-N(7)	1.975(7)	N(9)-C(30)	1.358(10)
Fe(2)-N(8)	1.977(7)	N(9)-C(34)	1.361(10)
N(1)-C(13)	1.472(9)	N(10)-C(40)	1.328(11)
N(1)-C(1)	1.497(10)	N(10)-C(36)	1.354(10)
N(1)-C(7)	1.505(10)	N(11)-C(41)	1.153(10)
N(2)-C(6)	1.335(10)	N(12)-C(43)	1.138(11)
N(2)-C(2)	1.372(10)	C(1)-C(2)	1.547(11)
N(3)-C(8)	1.355(10)	C(1)-H(1A)	0.9700

C(1)-H(1B)	0.9700	C(20)-H(20B)	0.9600
C(2)-C(3)	1.387(11)	C(20)-H(20C)	0.9600
C(3)-C(4)	1.408(13)	C(21)-C(22)	1.419(11)
C(3)-H(3A)	0.9300	C(22)-H(22A)	0.9600
C(4)-C(5)	1.351(13)	C(22)-H(22B)	0.9600
C(4)-H(4A)	0.9300	C(22)-H(22C)	0.9600
C(5)-C(6)	1.355(12)	C(23)-C(24)	1.501(14)
C(5)-H(5A)	0.9300	C(23)-H(23A)	0.9700
C(6)-H(6A)	0.9300	C(23)-H(23B)	0.9700
C(7)-C(8)	1.487(11)	C(24)-C(25)	1.343(13)
C(7)-H(7A)	0.9700	C(25)-C(26)	1.364(17)
C(7)-H(7B)	0.9700	C(25)-H(25A)	0.9300
C(8)-C(9)	1.383(11)	C(26)-C(27)	1.408(16)
C(9)-C(10)	1.390(13)	C(26)-H(26A)	0.9300
C(9)-H(9A)	0.9300	C(27)-C(28)	1.399(13)
C(10)-C(11)	1.368(13)	C(27)-H(27A)	0.9300
C(10)-H(10A)	0.9300	C(28)-H(28A)	0.9300
C(11)-C(12)	1.347(11)	C(29)-C(30)	1.487(11)
C(11)-H(11A)	0.9300	C(29)-H(29A)	0.9700
C(12)-H(12A)	0.9300	C(29)-H(29B)	0.9700
C(13)-C(14)	1.489(10)	C(30)-C(31)	1.390(10)
C(13)-H(13A)	0.9700	C(31)-C(32)	1.375(14)
C(13)-H(13B)	0.9700	C(31)-H(31A)	0.9300
C(14)-C(15)	1.404(10)	C(32)-C(33)	1.382(15)
C(15)-C(16)	1.396(12)	C(32)-H(32A)	0.9300
C(15)-H(15A)	0.9300	C(33)-C(34)	1.386(12)
C(16)-C(17)	1.357(13)	C(33)-H(33A)	0.9300
C(16)-H(16A)	0.9300	C(34)-H(34A)	0.9300
C(17)-C(18)	1.367(12)	C(35)-C(36)	1.527(13)
C(17)-H(17A)	0.9300	C(35)-H(35A)	0.9700
C(18)-H(18A)	0.9300	C(35)-H(35B)	0.9700
C(19)-C(20)	1.485(13)	C(36)-C(37)	1.413(13)
C(20)-H(20A)	0.9600	C(37)-C(38)	1.381(15)

C(37)-H(37A)	0.9300	C(47)-F(7)	1.323(17)
C(38)-C(39)	1.311(15)	C(47)-F(9)	1.342(14)
C(38)-H(38A)	0.9300	S(4A)-S(4B)	1.035(13)
C(39)-C(40)	1.399(13)	S(4A)-O(12)	1.386(12)
C(39)-H(39A)	0.9300	S(4A)-O(10A)	1.390(19)
C(40)-H(40A)	0.9300	S(4A)-O(11)	1.395(13)
C(41)-C(42)	1.437(12)	S(4A)-C(48B)	1.83(3)
C(42)-H(42A)	0.9600	S(4A)-C(48A)	1.86(2)
C(42)-H(42B)	0.9600	S(4A)-F(12B)	2.02(3)
C(42)-H(42C)	0.9600	S(4B)-O(11)	1.323(12)
C(43)-C(44)	1.464(13)	S(4B)-O(10B)	1.52(3)
C(44)-H(44A)	0.9600	S(4B)-O(12)	1.568(17)
C(44)-H(44B)	0.9600	S(4B)-C(48A)	1.69(2)
C(44)-H(44C)	0.9600	S(4B)-F(12A)	1.81(3)
S(1)-O(1)	1.406(7)	S(4B)-C(48B)	1.86(2)
S(1)-O(2)	1.431(8)	O(10B)-F(12A)	1.37(3)
S(1)-O(3)	1.436(7)	O(10A)-F(12B)	1.62(3)
S(1)-C(45)	1.775(13)	F(12A)-C(48A)	1.233(17)
C(45)-F(1)	1.317(13)	F(12A)-C(48B)	1.59(4)
C(45)-F(3)	1.323(14)	F(10)-C(48B)	1.224(15)
C(45)-F(2)	1.326(12)	F(10)-C(48A)	1.230(14)
S(2)-O(6)	1.423(7)	F(11)-C(48A)	1.238(14)
S(2)-O(4)	1.441(7)	F(11)-C(48B)	1.239(15)
S(2)-O(5)	1.458(7)	F(12B)-C(48B)	1.216(17)
S(2)-C(46)	1.758(16)	F(12B)-C(48A)	1.57(4)
F(4)-C(46)	1.260(17)		
F(5)-C(46)	1.398(18)	N(5)-Fe(1)-N(6)	89.5(3)
F(6)-C(46)	1.380(17)	N(5)-Fe(1)-N(2)	89.9(3)
S(3)-O(9)	1.402(7)	N(6)-Fe(1)-N(2)	94.8(3)
S(3)-O(8)	1.433(9)	N(5)-Fe(1)-N(3)	176.9(3)
S(3)-O(7)	1.455(9)	N(6)-Fe(1)-N(3)	93.6(3)
S(3)-C(47)	1.777(16)	N(2)-Fe(1)-N(3)	89.2(3)
C(47)-F(8)	1.232(15)	N(5)-Fe(1)-N(4)	89.6(3)

N(6)-Fe(1)-N(4)	96.8(3)	C(8)-N(3)-Fe(1)	114.4(5)
N(2)-Fe(1)-N(4)	168.4(3)	C(12)-N(3)-Fe(1)	129.1(6)
N(3)-Fe(1)-N(4)	90.6(3)	C(14)-N(4)-C(18)	117.9(7)
N(5)-Fe(1)-N(1)	91.3(3)	C(14)-N(4)-Fe(1)	112.4(5)
N(6)-Fe(1)-N(1)	179.0(3)	C(18)-N(4)-Fe(1)	129.8(5)
N(2)-Fe(1)-N(1)	84.7(3)	C(19)-N(5)-Fe(1)	175.3(8)
N(3)-Fe(1)-N(1)	85.6(3)	C(21)-N(6)-Fe(1)	176.5(7)
N(4)-Fe(1)-N(1)	83.7(3)	C(23)-N(7)-C(29)	112.8(7)
N(11)-Fe(2)-N(12)	88.4(3)	C(23)-N(7)-C(35)	112.3(7)
N(11)-Fe(2)-N(10)	90.2(3)	C(29)-N(7)-C(35)	106.8(7)
N(12)-Fe(2)-N(10)	96.6(3)	C(23)-N(7)-Fe(2)	108.4(6)
N(11)-Fe(2)-N(9)	176.7(3)	C(29)-N(7)-Fe(2)	110.6(5)
N(12)-Fe(2)-N(9)	94.8(3)	C(35)-N(7)-Fe(2)	105.9(5)
N(10)-Fe(2)-N(9)	90.1(3)	C(28)-N(8)-C(24)	119.3(9)
N(11)-Fe(2)-N(7)	91.3(3)	C(28)-N(8)-Fe(2)	127.8(7)
N(12)-Fe(2)-N(7)	179.6(3)	C(24)-N(8)-Fe(2)	112.9(7)
N(10)-Fe(2)-N(7)	83.6(3)	C(30)-N(9)-C(34)	119.3(7)
N(9)-Fe(2)-N(7)	85.5(3)	C(30)-N(9)-Fe(2)	114.0(5)
N(11)-Fe(2)-N(8)	89.2(3)	C(34)-N(9)-Fe(2)	126.7(6)
N(12)-Fe(2)-N(8)	96.1(3)	C(40)-N(10)-C(36)	116.5(8)
N(10)-Fe(2)-N(8)	167.3(3)	C(40)-N(10)-Fe(2)	129.1(6)
N(9)-Fe(2)-N(8)	89.8(3)	C(36)-N(10)-Fe(2)	114.3(6)
N(7)-Fe(2)-N(8)	83.8(3)	C(41)-N(11)-Fe(2)	172.3(8)
C(13)-N(1)-C(1)	112.5(6)	C(43)-N(12)-Fe(2)	176.0(7)
C(13)-N(1)-C(7)	110.2(6)	N(1)-C(1)-C(2)	107.1(6)
C(1)-N(1)-C(7)	109.5(6)	N(1)-C(1)-H(1A)	110.3
C(13)-N(1)-Fe(1)	108.0(5)	C(2)-C(1)-H(1A)	110.3
C(1)-N(1)-Fe(1)	106.3(5)	N(1)-C(1)-H(1B)	110.3
C(7)-N(1)-Fe(1)	110.3(5)	C(2)-C(1)-H(1B)	110.3
C(6)-N(2)-C(2)	114.6(7)	H(1A)-C(1)-H(1B)	108.6
C(6)-N(2)-Fe(1)	133.1(6)	N(2)-C(2)-C(3)	122.6(8)
C(2)-N(2)-Fe(1)	112.2(5)	N(2)-C(2)-C(1)	115.3(7)
C(8)-N(3)-C(12)	116.5(7)	C(3)-C(2)-C(1)	122.0(8)

C(2)-C(3)-C(4)	117.8(9)	N(1)-C(13)-C(14)	108.8(6)
C(2)-C(3)-H(3A)	121.1	N(1)-C(13)-H(13A)	109.9
C(4)-C(3)-H(3A)	121.1	C(14)-C(13)-H(13A)	109.9
C(5)-C(4)-C(3)	120.4(9)	N(1)-C(13)-H(13B)	109.9
C(5)-C(4)-H(4A)	119.8	C(14)-C(13)-H(13B)	109.9
C(3)-C(4)-H(4A)	119.8	H(13A)-C(13)-H(13B)	108.3
C(4)-C(5)-C(6)	117.0(9)	N(4)-C(14)-C(15)	121.1(7)
C(4)-C(5)-H(5A)	121.5	N(4)-C(14)-C(13)	116.8(6)
C(6)-C(5)-H(5A)	121.5	C(15)-C(14)-C(13)	122.0(7)
N(2)-C(6)-C(5)	127.6(9)	C(16)-C(15)-C(14)	119.3(8)
N(2)-C(6)-H(6A)	116.2	C(16)-C(15)-H(15A)	120.4
C(5)-C(6)-H(6A)	116.2	C(14)-C(15)-H(15A)	120.4
C(8)-C(7)-N(1)	112.5(7)	C(17)-C(16)-C(15)	118.5(8)
C(8)-C(7)-H(7A)	109.1	C(17)-C(16)-H(16A)	120.8
N(1)-C(7)-H(7A)	109.1	C(15)-C(16)-H(16A)	120.7
C(8)-C(7)-H(7B)	109.1	C(16)-C(17)-C(18)	120.0(8)
N(1)-C(7)-H(7B)	109.1	C(16)-C(17)-H(17A)	120.0
H(7A)-C(7)-H(7B)	107.8	C(18)-C(17)-H(17A)	120.0
N(3)-C(8)-C(9)	121.7(8)	N(4)-C(18)-C(17)	123.1(8)
N(3)-C(8)-C(7)	117.1(7)	N(4)-C(18)-H(18A)	118.4
C(9)-C(8)-C(7)	121.1(8)	C(17)-C(18)-H(18A)	118.4
C(8)-C(9)-C(10)	119.7(8)	N(5)-C(19)-C(20)	173.9(11)
C(8)-C(9)-H(9A)	120.2	C(19)-C(20)-H(20A)	109.5
C(10)-C(9)-H(9A)	120.2	C(19)-C(20)-H(20B)	109.5
C(11)-C(10)-C(9)	118.3(9)	H(20A)-C(20)-H(20B)	109.5
C(11)-C(10)-H(10A)	120.8	C(19)-C(20)-H(20C)	109.5
C(9)-C(10)-H(10A)	120.8	H(20A)-C(20)-H(20C)	109.5
C(12)-C(11)-C(10)	119.4(9)	H(20B)-C(20)-H(20C)	109.5
C(12)-C(11)-H(11A)	120.3	N(6)-C(21)-C(22)	179.4(10)
C(10)-C(11)-H(11A)	120.3	C(21)-C(22)-H(22A)	109.5
C(11)-C(12)-N(3)	124.3(9)	C(21)-C(22)-H(22B)	109.5
C(11)-C(12)-H(12A)	117.8	H(22A)-C(22)-H(22B)	109.5
N(3)-C(12)-H(12A)	117.8	C(21)-C(22)-H(22C)	109.5

H(22A)-C(22)-H(22C)	109.5	C(32)-C(31)-H(31A)	120.4
H(22B)-C(22)-H(22C)	109.5	C(30)-C(31)-H(31A)	120.4
N(7)-C(23)-C(24)	109.5(8)	C(31)-C(32)-C(33)	119.4(9)
N(7)-C(23)-H(23A)	109.8	C(31)-C(32)-H(32A)	120.3
C(24)-C(23)-H(23A)	109.8	C(33)-C(32)-H(32A)	120.3
N(7)-C(23)-H(23B)	109.8	C(32)-C(33)-C(34)	120.1(9)
C(24)-C(23)-H(23B)	109.8	C(32)-C(33)-H(33A)	120.0
H(23A)-C(23)-H(23B)	108.2	C(34)-C(33)-H(33A)	120.0
C(25)-C(24)-N(8)	122.0(12)	N(9)-C(34)-C(33)	120.5(9)
C(25)-C(24)-C(23)	122.6(12)	N(9)-C(34)-H(34A)	119.7
N(8)-C(24)-C(23)	115.3(9)	C(33)-C(34)-H(34A)	119.7
C(24)-C(25)-C(26)	120.4(13)	C(36)-C(35)-N(7)	106.5(7)
C(24)-C(25)-H(25A)	119.8	C(36)-C(35)-H(35A)	110.4
C(26)-C(25)-H(25A)	119.8	N(7)-C(35)-H(35A)	110.4
C(25)-C(26)-C(27)	119.4(12)	C(36)-C(35)-H(35B)	110.4
C(25)-C(26)-H(26A)	120.3	N(7)-C(35)-H(35B)	110.4
C(27)-C(26)-H(26A)	120.3	H(35A)-C(35)-H(35B)	108.6
C(28)-C(27)-C(26)	117.6(12)	N(10)-C(36)-C(37)	122.4(10)
C(28)-C(27)-H(27A)	121.2	N(10)-C(36)-C(35)	114.0(9)
C(26)-C(27)-H(27A)	121.2	C(37)-C(36)-C(35)	123.5(9)
N(8)-C(28)-C(27)	121.3(11)	C(38)-C(37)-C(36)	116.5(11)
N(8)-C(28)-H(28A)	119.4	C(38)-C(37)-H(37A)	121.8
C(27)-C(28)-H(28A)	119.4	C(36)-C(37)-H(37A)	121.8
C(30)-C(29)-N(7)	111.8(7)	C(39)-C(38)-C(37)	122.7(11)
C(30)-C(29)-H(29A)	109.3	C(39)-C(38)-H(38A)	118.7
N(7)-C(29)-H(29A)	109.3	C(37)-C(38)-H(38A)	118.7
C(30)-C(29)-H(29B)	109.3	C(38)-C(39)-C(40)	117.4(11)
N(7)-C(29)-H(29B)	109.3	C(38)-C(39)-H(39A)	121.3
H(29A)-C(29)-H(29B)	107.9	C(40)-C(39)-H(39A)	121.3
N(9)-C(30)-C(31)	121.6(8)	N(10)-C(40)-C(39)	124.5(9)
N(9)-C(30)-C(29)	117.0(7)	N(10)-C(40)-H(40A)	117.8
C(31)-C(30)-C(29)	121.4(8)	C(39)-C(40)-H(40A)	117.8
C(32)-C(31)-C(30)	119.2(9)	N(11)-C(41)-C(42)	173.4(12)

C(41)-C(42)-H(42A)	109.5	F(6)-C(46)-F(5)	101.5(17)
C(41)-C(42)-H(42B)	109.5	F(4)-C(46)-S(2)	117.5(18)
H(42A)-C(42)-H(42B)	109.5	F(6)-C(46)-S(2)	114.3(8)
C(41)-C(42)-H(42C)	109.5	F(5)-C(46)-S(2)	112.8(9)
H(42A)-C(42)-H(42C)	109.5	O(9)-S(3)-O(8)	123.3(6)
H(42B)-C(42)-H(42C)	109.5	O(9)-S(3)-O(7)	111.5(6)
N(12)-C(43)-C(44)	178.6(10)	O(8)-S(3)-O(7)	109.0(7)
C(43)-C(44)-H(44A)	109.5	O(9)-S(3)-C(47)	103.8(6)
C(43)-C(44)-H(44B)	109.5	O(8)-S(3)-C(47)	103.1(7)
H(44A)-C(44)-H(44B)	109.5	O(7)-S(3)-C(47)	103.9(7)
C(43)-C(44)-H(44C)	109.5	F(8)-C(47)-F(7)	107.0(18)
H(44A)-C(44)-H(44C)	109.5	F(8)-C(47)-F(9)	105.1(13)
H(44B)-C(44)-H(44C)	109.5	F(7)-C(47)-F(9)	107.3(13)
O(1)-S(1)-O(2)	115.0(6)	F(8)-C(47)-S(3)	117.3(12)
O(1)-S(1)-O(3)	115.0(6)	F(7)-C(47)-S(3)	108.3(11)
O(2)-S(1)-O(3)	114.1(5)	F(9)-C(47)-S(3)	111.3(12)
O(1)-S(1)-C(45)	104.4(6)	S(4B)-S(4A)-O(12)	79.3(10)
O(2)-S(1)-C(45)	102.2(6)	S(4B)-S(4A)-O(10A)	159.7(15)
O(3)-S(1)-C(45)	104.0(5)	O(12)-S(4A)-O(10A)	118.7(14)
F(1)-C(45)-F(3)	105.4(11)	S(4B)-S(4A)-O(11)	64.0(8)
F(1)-C(45)-F(2)	104.8(11)	O(12)-S(4A)-O(11)	118.7(10)
F(3)-C(45)-F(2)	106.9(12)	O(10A)-S(4A)-O(11)	110.0(14)
F(1)-C(45)-S(1)	113.1(10)	S(4B)-S(4A)-C(48B)	75.5(10)
F(3)-C(45)-S(1)	113.2(9)	O(12)-S(4A)-C(48B)	108.7(8)
F(2)-C(45)-S(1)	112.8(9)	O(10A)-S(4A)-C(48B)	88.8(15)
O(6)-S(2)-O(4)	117.7(5)	O(11)-S(4A)-C(48B)	107.1(9)
O(6)-S(2)-O(5)	113.7(5)	S(4B)-S(4A)-C(48A)	64.5(11)
O(4)-S(2)-O(5)	114.1(5)	O(12)-S(4A)-C(48A)	103.4(9)
O(6)-S(2)-C(46)	101.4(6)	O(10A)-S(4A)-C(48A)	99.9(16)
O(4)-S(2)-C(46)	101.9(6)	O(11)-S(4A)-C(48A)	102.4(9)
O(5)-S(2)-C(46)	105.5(8)	C(48B)-S(4A)-C(48A)	11.1(15)
F(4)-C(46)-F(6)	104.4(11)	S(4B)-S(4A)-F(12B)	111.7(10)
F(4)-C(46)-F(5)	104.6(10)	O(12)-S(4A)-F(12B)	117.2(13)

O(10A)-S(4A)-F(12B)	53.0(13)	O(10B)-F(12A)-S(4B)	54.8(15)
O(11)-S(4A)-F(12B)	121.2(13)	C(48B)-F(12A)-S(4B)	66.0(13)
C(48B)-S(4A)-F(12B)	36.4(7)	C(48B)-F(10)-C(48A)	17(2)
C(48A)-S(4A)-F(12B)	47.4(13)	C(48A)-F(11)-C(48B)	17(2)
S(4A)-S(4B)-O(11)	71.4(10)	C(48B)-F(12B)-C(48A)	2.7(10)
S(4A)-S(4B)-O(10B)	169.3(14)	C(48B)-F(12B)-O(10A)	105(3)
O(11)-S(4B)-O(10B)	117.5(16)	C(48A)-F(12B)-O(10A)	103(2)
S(4A)-S(4B)-O(12)	60.3(11)	C(48B)-F(12B)-S(4A)	63.1(19)
O(11)-S(4B)-O(12)	111.5(13)	C(48A)-F(12B)-S(4A)	60.8(14)
O(10B)-S(4B)-O(12)	117.9(13)	O(10A)-F(12B)-S(4A)	43.1(10)
S(4A)-S(4B)-C(48A)	82.0(12)	F(10)-C(48A)-F(12A)	97(3)
O(11)-S(4B)-C(48A)	114.9(12)	F(10)-C(48A)-F(11)	118(2)
O(10B)-S(4B)-C(48A)	88.4(15)	F(12A)-C(48A)-F(11)	93(2)
O(12)-S(4B)-C(48A)	103.6(10)	F(10)-C(48A)-F(12B)	81(2)
S(4A)-S(4B)-F(12A)	122.5(13)	F(12A)-C(48A)-F(12B)	177(2)
O(11)-S(4B)-F(12A)	130.4(15)	F(11)-C(48A)-F(12B)	90(2)
O(10B)-S(4B)-F(12A)	47.5(12)	F(10)-C(48A)-S(4B)	125.3(14)
O(12)-S(4B)-F(12A)	116.2(12)	F(12A)-C(48A)-S(4B)	74.7(19)
C(48A)-S(4B)-F(12A)	41.0(8)	F(11)-C(48A)-S(4B)	116.6(14)
S(4A)-S(4B)-C(48B)	72.0(10)	F(12B)-C(48A)-S(4B)	105(2)
O(11)-S(4B)-C(48B)	108.7(11)	F(10)-C(48A)-S(4A)	115.4(15)
O(10B)-S(4B)-C(48B)	98.6(17)	F(12A)-C(48A)-S(4A)	107.7(19)
O(12)-S(4B)-C(48B)	99.6(10)	F(11)-C(48A)-S(4A)	119.1(16)
C(48A)-S(4B)-C(48B)	10.2(15)	F(12B)-C(48A)-S(4A)	71.8(17)
F(12A)-S(4B)-C(48B)	51.2(15)	S(4B)-C(48A)-S(4A)	33.4(6)
F(12A)-O(10B)-S(4B)	77.6(15)	F(12B)-C(48B)-F(10)	97(2)
S(4A)-O(10A)-F(12B)	83.9(15)	F(12B)-C(48B)-F(11)	109(2)
S(4B)-O(11)-S(4A)	44.7(7)	F(10)-C(48B)-F(11)	118(2)
S(4A)-O(12)-S(4B)	40.4(5)	F(12B)-C(48B)-F(12A)	174(2)
C(48A)-F(12A)-O(10B)	119(3)	F(10)-C(48B)-F(12A)	81.0(19)
C(48A)-F(12A)-C(48B)	1.7(9)	F(11)-C(48B)-F(12A)	77.6(17)
O(10B)-F(12A)-C(48B)	121(2)	F(12B)-C(48B)-S(4A)	81(2)
C(48A)-F(12A)-S(4B)	64.4(17)	F(10)-C(48B)-S(4A)	117.8(14)

F(11)-C(48B)-S(4A)	121.2(15)	F(11)-C(48B)-S(4B)	106.2(15)
F(12A)-C(48B)-S(4A)	95.0(17)	F(12A)-C(48B)-S(4B)	62.8(15)
F(12B)-C(48B)-S(4B)	113(2)	S(4A)-C(48B)-S(4B)	32.6(6)
F(10)-C(48B)-S(4B)	113.6(16)		

Symmetry transformations used to generate equivalent atoms

Table 4. Anisotropic displacement parameters ($Å^2 x\ 10^3$) for mb37. The anisotropic displacement factor exponent takes the form: $-2\pi^2[\ h^2\ a^{*2}U^{11} + ... + 2\ h\ k\ a^*\ b^*\ U^{12}\ ]$

	U^{11}	U^{22}	U^{33}	U^{23}	U^{13}	U^{12}
Fe(1)	50(1)	37(1)	38(1)	-3(1)	4(1)	3(1)
Fe(2)	53(1)	53(1)	37(1)	4(1)	8(1)	1(1)
N(1)	53(4)	40(4)	44(4)	-8(3)	-2(3)	5(3)
N(2)	58(4)	56(4)	36(3)	0(3)	3(3)	6(3)
N(3)	51(4)	46(4)	41(3)	-6(3)	11(3)	2(3)
N(4)	53(4)	42(4)	43(3)	-2(3)	3(3)	3(3)
N(5)	60(5)	53(4)	46(4)	-7(3)	0(4)	5(4)
N(6)	48(4)	52(4)	49(4)	4(3)	-3(3)	10(3)
N(7)	68(5)	64(5)	45(4)	7(3)	12(3)	11(4)
N(8)	54(4)	80(6)	39(4)	11(4)	6(3)	-3(4)
N(9)	51(4)	64(4)	47(4)	-4(4)	12(3)	0(3)
N(10)	57(5)	52(4)	41(4)	8(3)	10(3)	3(4)
N(11)	52(4)	90(6)	47(4)	3(4)	5(3)	5(4)
N(12)	49(4)	63(5)	52(4)	5(4)	-4(3)	-7(4)
C(1)	110(8)	40(5)	54(5)	6(4)	-1(5)	-1(5)
C(2)	72(6)	52(5)	52(5)	6(4)	1(4)	5(4)
C(3)	102(8)	72(7)	49(5)	13(5)	2(5)	-3(6)
C(4)	110(9)	105(9)	51(6)	-8(6)	25(6)	-2(7)
C(5)	82(7)	66(6)	59(6)	-18(5)	5(5)	-3(5)
C(6)	73(6)	65(6)	47(5)	-23(4)	-1(4)	9(5)
C(7)	61(6)	56(6)	84(7)	-11(5)	4(5)	-3(5)
C(8)	52(5)	48(5)	46(5)	-12(4)	6(4)	6(4)
C(9)	57(6)	77(7)	66(6)	-24(5)	6(5)	-18(5)
C(10)	62(6)	75(7)	80(7)	-5(6)	-8(5)	7(6)
C(11)	67(7)	67(7)	81(7)	0(5)	-14(5)	15(5)
C(12)	59(6)	55(5)	54(5)	1(4)	5(4)	8(4)
C(13)	60(5)	44(5)	53(5)	-7(4)	12(4)	4(4)
C(14)	42(4)	57(5)	41(4)	-6(4)	-1(3)	11(4)

C(15)	65(6)	65(6)	47(5)	-15(4)	8(4)	7(5)
C(16)	84(7)	86(7)	52(5)	18(5)	25(5)	24(6)
C(17)	89(7)	60(6)	74(7)	26(5)	24(6)	12(5)
C(18)	65(6)	53(5)	64(6)	9(4)	11(5)	15(4)
C(19)	77(7)	74(7)	44(5)	-4(4)	-1(5)	10(6)
C(20)	62(7)	131(10)	80(7)	-5(7)	-5(5)	10(7)
C(21)	62(6)	41(5)	59(5)	1(4)	-5(4)	-1(4)
C(22)	94(8)	54(6)	98(8)	-6(5)	-15(6)	-10(5)
C(23)	70(7)	80(7)	96(8)	17(6)	15(6)	25(6)
C(24)	52(6)	119(10)	52(6)	13(6)	1(5)	19(6)
C(25)	77(9)	146(13)	77(8)	22(8)	-3(6)	18(8)
C(26)	71(8)	171(15)	72(8)	11(9)	-2(6)	25(10)
C(27)	81(8)	155(13)	60(7)	-9(7)	-9(6)	-30(8)
C(28)	59(6)	106(8)	42(5)	-10(5)	-6(4)	-7(6)
C(29)	98(7)	63(6)	50(5)	13(4)	17(5)	6(5)
C(30)	60(5)	56(5)	42(5)	5(4)	1(4)	-4(4)
C(31)	73(6)	93(7)	36(4)	2(5)	14(4)	-16(5)
C(32)	104(9)	127(11)	45(5)	-11(6)	29(5)	-30(8)
C(33)	85(7)	106(9)	72(7)	-44(7)	31(6)	-20(7)
C(34)	67(6)	66(6)	71(6)	-16(5)	17(5)	-6(5)
C(35)	115(9)	54(6)	57(6)	-9(5)	11(5)	0(6)
C(36)	102(8)	51(6)	55(5)	0(4)	14(5)	-4(6)
C(37)	134(11)	68(7)	74(7)	-21(6)	-5(7)	-33(7)
C(38)	75(8)	121(11)	72(7)	-2(7)	0(6)	-10(8)
C(39)	69(7)	93(8)	72(7)	4(6)	0(5)	-2(6)
C(40)	68(6)	61(6)	54(5)	4(4)	4(4)	-15(5)
C(41)	68(6)	104(8)	49(5)	14(5)	6(5)	16(6)
C(42)	83(8)	224(16)	51(6)	19(8)	27(5)	30(8)
C(43)	43(5)	66(7)	85(7)	7(5)	-3(4)	-8(5)
C(44)	90(8)	61(7)	143(11)	30(7)	-27(7)	-7(6)
S(1)	81(2)	65(2)	73(2)	12(1)	-9(1)	6(1)
O(1)	113(6)	177(9)	116(7)	67(6)	-26(5)	40(6)
O(2)	122(7)	102(6)	122(7)	-27(5)	-11(5)	6(5)
O(3)	105(6)	64(4)	124(6)	22(4)	20(5)	-10(4)
C(45)	129(12)	63(7)	100(9)	-7(7)	22(8)	-3(7)
F(1)	155(7)	167(8)	150(8)	-43(7)	55(6)	-12(6)
F(2)	138(6)	105(6)	172(8)	25(5)	40(5)	-30(5)
F(3)	89(5)	135(7)	190(9)	32(6)	10(5)	28(5)
S(2)	83(2)	61(2)	100(2)	11(2)	20(2)	16(1)
O(4)	141(7)	88(6)	119(7)	12(5)	-5(5)	45(5)
O(5)	110(6)	57(4)	163(8)	2(5)	-12(5)	-11(4)
O(6)	68(5)	94(6)	153(7)	20(5)	43(4)	13(4)

F(4)	170(8)	123(7)	212(10)	-69(7)	-50(7)	34(6)
F(5)	85(5)	241(10)	141(7)	-38(6)	31(4)	19(6)
F(6)	160(8)	156(8)	107(6)	28(5)	24(5)	55(6)
C(46)	99(11)	161(15)	198(16)	-123(13)	-80(11)	87(11)
S(3)	91(2)	100(2)	88(2)	2(2)	6(2)	9(2)
O(7)	104(7)	166(10)	219(12)	18(8)	-53(7)	-42(7)
O(8)	180(10)	147(9)	185(10)	40(8)	32(8)	96(8)
O(9)	224(10)	78(5)	65(5)	18(4)	35(5)	-38(6)
C(47)	109(11)	152(14)	92(10)	31(10)	15(8)	-13(11)
F(7)	385(19)	293(16)	137(9)	-14(9)	16(10)	226(16)
F(8)	229(11)	243(13)	161(9)	29(8)	-70(8)	-129(10)
F(9)	194(9)	214(10)	115(7)	29(7)	21(6)	-46(7)
S(4A)	90(4)	83(4)	67(4)	-6(3)	-11(3)	-4(3)
S(4B)	92(6)	179(11)	95(8)	-45(8)	5(5)	-42(6)
O(10B)	220(30)	170(20)	95(15)	50(15)	27(16)	-25(18)
O(10A)	260(30)	240(30)	114(15)	110(17)	14(16)	0(20)
O(11)	163(10)	195(13)	263(15)	-65(11)	-98(10)	-41(9)
O(12)	123(8)	148(9)	201(11)	-68(8)	17(7)	-8(6)
F(12A)	230(20)	260(20)	230(20)	70(18)	11(17)	74(18)
F(10)	97(7)	231(13)	390(20)	-104(15)	-7(9)	-29(7)
F(11)	183(10)	253(14)	291(16)	-130(13)	39(10)	27(9)
F(12B)	230(20)	260(20)	230(20)	70(18)	11(17)	74(18)

Table 5. Hydrogen coordinates ($\times 10^4$) and isotropic displacement parameters ($Å^2 \times 10^3$).

	x	y	z	U(eq)
H(1A)	4881	9363	-203	82
H(1B)	4112	9037	-338	82
H(3A)	5238	9163	-1592	89
H(4A)	5613	8332	-2499	106
H(5A)	5559	7137	-2231	83
H(6A)	5094	6798	-1117	74
H(7A)	5702	8881	477	81
H(7B)	5411	8846	1306	81
H(9A)	6719	8242	1325	80
H(10A)	7222	7119	1505	87
H(11A)	6549	6130	1180	86
H(12A)	5429	6268	716	67
H(13A)	3724	8985	824	63

H(13B)	4366	9204	1359	63
H(15A)	3672	8818	2517	71
H(16A)	3271	7861	3247	88
H(17A)	3412	6728	2787	89
H(18A)	3873	6553	1615	73
H(20A)	1871	8006	-318	136
H(20B)	2169	7884	-1135	136
H(20C)	2249	8630	-747	136
H(22A)	3397	5206	-346	123
H(22B)	4048	4943	148	123
H(22C)	4156	5122	-710	123
H(23A)	10472	6243	-113	98
H(23B)	10422	5908	700	98
H(25A)	11588	6496	1045	120
H(26A)	12139	7505	1491	126
H(27A)	11538	8605	1393	118
H(28A)	10379	8613	880	83
H(29A)	8776	5907	998	85
H(29B)	9521	5938	1418	85
H(31A)	8667	6294	2525	81
H(32A)	8233	7273	3169	110
H(33A)	8240	8376	2587	105
H(34A)	8689	8495	1379	82
H(35A)	9435	6069	-711	90
H(35B)	9077	5555	-121	90
H(37A)	7814	5594	-782	110
H(38A)	6792	6279	-945	107
H(39A)	6798	7450	-717	94
H(40A)	7832	7962	-228	73
H(42A)	10186	7765	-2423	179
H(42B)	10339	6954	-2303	179
H(42C)	10904	7520	-2037	179
H(44A)	9187	9910	-799	147
H(44B)	9390	10090	42	147
H(44C)	8585	9984	-192	147

Table 6. Torsion angles [°].

N(5)-Fe(1)-N(1)-C(13)	63.2(5)	N(2)-Fe(1)-N(1)-C(13)	153.0(5)
N(6)-Fe(1)-N(1)-C(13)	-150(15)	N(3)-Fe(1)-N(1)-C(13)	-117.4(5)

N(4)-Fe(1)-N(1)-C(13)	-26.3(5)	N(2)-Fe(1)-N(4)-C(14)	8.9(16)
N(5)-Fe(1)-N(1)-C(1)	-57.7(5)	N(3)-Fe(1)-N(4)-C(14)	98.0(5)
N(6)-Fe(1)-N(1)-C(1)	89(15)	N(1)-Fe(1)-N(4)-C(14)	12.5(5)
N(2)-Fe(1)-N(1)-C(1)	32.1(5)	N(5)-Fe(1)-N(4)-C(18)	102.9(7)
N(3)-Fe(1)-N(1)-C(1)	121.7(5)	N(6)-Fe(1)-N(4)-C(18)	13.4(7)
N(4)-Fe(1)-N(1)-C(1)	-147.2(5)	N(2)-Fe(1)-N(4)-C(18)	-169.4(11)
N(5)-Fe(1)-N(1)-C(7)	-176.4(5)	N(3)-Fe(1)-N(4)-C(18)	-80.2(7)
N(6)-Fe(1)-N(1)-C(7)	-29(15)	N(1)-Fe(1)-N(4)-C(18)	-165.7(7)
N(2)-Fe(1)-N(1)-C(7)	-86.6(5)	N(6)-Fe(1)-N(5)-C(19)	14(9)
N(3)-Fe(1)-N(1)-C(7)	3.1(5)	N(2)-Fe(1)-N(5)-C(19)	108(9)
N(4)-Fe(1)-N(1)-C(7)	94.2(5)	N(3)-Fe(1)-N(5)-C(19)	-177(7)
N(5)-Fe(1)-N(2)-C(6)	-107.2(8)	N(4)-Fe(1)-N(5)-C(19)	-83(9)
N(6)-Fe(1)-N(2)-C(6)	-17.7(8)	N(1)-Fe(1)-N(5)-C(19)	-167(9)
N(3)-Fe(1)-N(2)-C(6)	75.8(8)	N(5)-Fe(1)-N(6)-C(21)	60(11)
N(4)-Fe(1)-N(2)-C(6)	165.1(11)	N(2)-Fe(1)-N(6)-C(21)	-30(11)
N(1)-Fe(1)-N(2)-C(6)	161.5(8)	N(3)-Fe(1)-N(6)-C(21)	-120(11)
N(5)-Fe(1)-N(2)-C(2)	74.2(6)	N(4)-Fe(1)-N(6)-C(21)	149(11)
N(6)-Fe(1)-N(2)-C(2)	163.7(6)	N(1)-Fe(1)-N(6)-C(21)	-87(19)
N(3)-Fe(1)-N(2)-C(2)	-102.8(6)	N(11)-Fe(2)-N(7)-C(23)	62.8(6)
N(4)-Fe(1)-N(2)-C(2)	-13.5(16)	N(12)-Fe(2)-N(7)-C(23)	36(53)
N(1)-Fe(1)-N(2)-C(2)	-17.1(6)	N(10)-Fe(2)-N(7)-C(23)	152.9(6)
N(5)-Fe(1)-N(3)-C(8)	8(5)	N(9)-Fe(2)-N(7)-C(23)	-116.5(6)
N(6)-Fe(1)-N(3)-C(8)	177.2(5)	N(8)-Fe(2)-N(7)-C(23)	-26.2(6)
N(2)-Fe(1)-N(3)-C(8)	82.4(5)	N(11)-Fe(2)-N(7)-C(29)	-173.1(6)
N(4)-Fe(1)-N(3)-C(8)	-86.0(5)	N(12)-Fe(2)-N(7)-C(29)	160(92)
N(1)-Fe(1)-N(3)-C(8)	-2.3(5)	N(10)-Fe(2)-N(7)-C(29)	-83.0(6)
N(5)-Fe(1)-N(3)-C(12)	-173(4)	N(9)-Fe(2)-N(7)-C(29)	7.6(6)
N(6)-Fe(1)-N(3)-C(12)	-3.7(7)	N(8)-Fe(2)-N(7)-C(29)	97.9(6)
N(2)-Fe(1)-N(3)-C(12)	-98.4(7)	N(11)-Fe(2)-N(7)-C(35)	-57.8(5)
N(4)-Fe(1)-N(3)-C(12)	93.2(6)	N(12)-Fe(2)-N(7)-C(35)	-85(53)
N(1)-Fe(1)-N(3)-C(12)	176.9(7)	N(10)-Fe(2)-N(7)-C(35)	32.2(5)
N(5)-Fe(1)-N(4)-C(14)	-78.9(5)	N(9)-Fe(2)-N(7)-C(35)	122.8(5)
N(6)-Fe(1)-N(4)-C(14)	-168.3(5)	N(8)-Fe(2)-N(7)-C(35)	-146.9(5)

N(11)-Fe(2)-N(8)-C(28)	102.6(7)	N(7)-Fe(2)-N(11)-C(41)	-156(6)
N(12)-Fe(2)-N(8)-C(28)	14.4(7)	N(8)-Fe(2)-N(11)-C(41)	-73(6)
N(10)-Fe(2)-N(8)-C(28)	-170.1(9)	N(11)-Fe(2)-N(12)-C(43)	-37(11)
N(9)-Fe(2)-N(8)-C(28)	-80.5(7)	N(10)-Fe(2)-N(12)-C(43)	-127(11)
N(7)-Fe(2)-N(8)-C(28)	-166.0(7)	N(9)-Fe(2)-N(12)-C(43)	143(11)
N(11)-Fe(2)-N(8)-C(24)	-78.4(6)	N(7)-Fe(2)-N(12)-C(43)	-10(59)
N(12)-Fe(2)-N(8)-C(24)	-166.7(6)	N(8)-Fe(2)-N(12)-C(43)	52(11)
N(10)-Fe(2)-N(8)-C(24)	8.9(14)	C(13)-N(1)-C(1)-C(2)	-157.1(7)
N(9)-Fe(2)-N(8)-C(24)	98.5(6)	C(7)-N(1)-C(1)-C(2)	80.0(8)
N(7)-Fe(2)-N(8)-C(24)	13.0(6)	Fe(1)-N(1)-C(1)-C(2)	-39.2(8)
N(11)-Fe(2)-N(9)-C(30)	-13(6)	C(6)-N(2)-C(2)-C(3)	1.8(12)
N(12)-Fe(2)-N(9)-C(30)	178.2(6)	Fe(1)-N(2)-C(2)-C(3)	-179.3(7)
N(10)-Fe(2)-N(9)-C(30)	81.6(6)	C(6)-N(2)-C(2)-C(1)	178.9(7)
N(7)-Fe(2)-N(9)-C(30)	-1.9(6)	Fe(1)-N(2)-C(2)-C(1)	-2.3(9)
N(8)-Fe(2)-N(9)-C(30)	-85.7(6)	N(1)-C(1)-C(2)-N(2)	28.2(10)
N(11)-Fe(2)-N(9)-C(34)	164(5)	N(1)-C(1)-C(2)-C(3)	-154.7(8)
N(12)-Fe(2)-N(9)-C(34)	-3.8(7)	N(2)-C(2)-C(3)-C(4)	0.1(14)
N(10)-Fe(2)-N(9)-C(34)	-100.5(7)	C(1)-C(2)-C(3)-C(4)	-176.7(9)
N(7)-Fe(2)-N(9)-C(34)	176.0(7)	C(2)-C(3)-C(4)-C(5)	-2.0(15)
N(8)-Fe(2)-N(9)-C(34)	92.2(7)	C(3)-C(4)-C(5)-C(6)	1.7(15)
N(11)-Fe(2)-N(10)-C(40)	-108.2(7)	C(2)-N(2)-C(6)-C(5)	-2.3(13)
N(12)-Fe(2)-N(10)-C(40)	-19.8(7)	Fe(1)-N(2)-C(6)-C(5)	179.2(7)
N(9)-Fe(2)-N(10)-C(40)	75.0(7)	C(4)-C(5)-C(6)-N(2)	0.5(15)
N(7)-Fe(2)-N(10)-C(40)	160.5(7)	C(13)-N(1)-C(7)-C(8)	115.8(7)
N(8)-Fe(2)-N(10)-C(40)	164.6(10)	C(1)-N(1)-C(7)-C(8)	-120.0(7)
N(11)-Fe(2)-N(10)-C(36)	74.6(6)	Fe(1)-N(1)-C(7)-C(8)	-3.3(8)
N(12)-Fe(2)-N(10)-C(36)	162.9(6)	C(12)-N(3)-C(8)-C(9)	2.9(11)
N(9)-Fe(2)-N(10)-C(36)	-102.2(6)	Fe(1)-N(3)-C(8)-C(9)	-177.9(6)
N(7)-Fe(2)-N(10)-C(36)	-16.7(6)	C(12)-N(3)-C(8)-C(7)	-178.4(7)
N(8)-Fe(2)-N(10)-C(36)	-12.6(14)	Fe(1)-N(3)-C(8)-C(7)	0.9(9)
N(12)-Fe(2)-N(11)-C(41)	23(6)	N(1)-C(7)-C(8)-N(3)	1.7(10)
N(10)-Fe(2)-N(11)-C(41)	120(6)	N(1)-C(7)-C(8)-C(9)	-179.6(7)
N(9)-Fe(2)-N(11)-C(41)	-145(6)	N(3)-C(8)-C(9)-C(10)	-2.5(12)

C(7)-C(8)-C(9)-C(10)	178.8(8)	N(8)-C(24)-C(25)-C(26)	1.2(16)
C(8)-C(9)-C(10)-C(11)	1.0(13)	C(23)-C(24)-C(25)-C(26)	177.1(11)
C(9)-C(10)-C(11)-C(12)	-0.1(14)	C(24)-C(25)-C(26)-C(27)	-1.1(18)
C(10)-C(11)-C(12)-N(3)	0.6(14)	C(25)-C(26)-C(27)-C(28)	1.0(17)
C(8)-N(3)-C(12)-C(11)	-2.0(11)	C(24)-N(8)-C(28)-C(27)	1.0(12)
Fe(1)-N(3)-C(12)-C(11)	178.9(6)	Fe(2)-N(8)-C(28)-C(27)	179.9(6)
C(1)-N(1)-C(13)-C(14)	151.1(7)	C(26)-C(27)-C(28)-N(8)	-0.9(14)
C(7)-N(1)-C(13)-C(14)	-86.4(8)	C(23)-N(7)-C(29)-C(30)	110.0(9)
Fe(1)-N(1)-C(13)-C(14)	34.1(7)	C(35)-N(7)-C(29)-C(30)	-126.3(8)
C(18)-N(4)-C(14)-C(15)	-1.0(11)	Fe(2)-N(7)-C(29)-C(30)	-11.6(9)
Fe(1)-N(4)-C(14)-C(15)	-179.5(6)	C(34)-N(9)-C(30)-C(31)	0.3(12)
C(18)-N(4)-C(14)-C(13)	-176.9(7)	Fe(2)-N(9)-C(30)-C(31)	178.4(6)
Fe(1)-N(4)-C(14)-C(13)	4.6(8)	C(34)-N(9)-C(30)-C(29)	177.4(8)
N(1)-C(13)-C(14)-N(4)	-26.3(10)	Fe(2)-N(9)-C(30)-C(29)	-4.5(10)
N(1)-C(13)-C(14)-C(15)	157.8(7)	N(7)-C(29)-C(30)-N(9)	10.8(11)
N(4)-C(14)-C(15)-C(16)	-1.5(12)	N(7)-C(29)-C(30)-C(31)	-172.1(8)
C(13)-C(14)-C(15)-C(16)	174.2(8)	N(9)-C(30)-C(31)-C(32)	0.0(13)
C(14)-C(15)-C(16)-C(17)	2.9(13)	C(29)-C(30)-C(31)-C(32)	-177.0(9)
C(15)-C(16)-C(17)-C(18)	-1.9(15)	C(30)-C(31)-C(32)-C(33)	0.1(15)
C(14)-N(4)-C(18)-C(17)	2.1(13)	C(31)-C(32)-C(33)-C(34)	-0.3(16)
Fe(1)-N(4)-C(18)-C(17)	-179.7(7)	C(30)-N(9)-C(34)-C(33)	-0.5(13)
C(16)-C(17)-C(18)-N(4)	-0.6(15)	Fe(2)-N(9)-C(34)-C(33)	-178.4(7)
Fe(1)-N(5)-C(19)-C(20)	-171(5)	C(32)-C(33)-C(34)-N(9)	0.6(15)
Fe(1)-N(6)-C(21)-C(22)	177(100)	C(23)-N(7)-C(35)-C(36)	-159.4(7)
C(29)-N(7)-C(23)-C(24)	-88.8(9)	C(29)-N(7)-C(35)-C(36)	76.5(8)
C(35)-N(7)-C(23)-C(24)	150.5(8)	Fe(2)-N(7)-C(35)-C(36)	-41.4(7)
Fe(2)-N(7)-C(23)-C(24)	34.0(9)	C(40)-N(10)-C(36)-C(37)	0.4(12)
C(28)-N(8)-C(24)-C(25)	-1.2(13)	Fe(2)-N(10)-C(36)-C(37)	178.0(7)
Fe(2)-N(8)-C(24)-C(25)	179.8(7)	C(40)-N(10)-C(36)-C(35)	177.8(7)
C(28)-N(8)-C(24)-C(23)	-177.3(8)	Fe(2)-N(10)-C(36)-C(35)	-4.6(9)
Fe(2)-N(8)-C(24)-C(23)	3.7(10)	N(7)-C(35)-C(36)-N(10)	30.7(10)
N(7)-C(23)-C(24)-C(25)	158.6(9)	N(7)-C(35)-C(36)-C(37)	-151.9(8)
N(7)-C(23)-C(24)-N(8)	-25.3(11)	N(10)-C(36)-C(37)-C(38)	-0.8(14)

C(35)-C(36)-C(37)-C(38)	-178.0(9)	O(8)-S(3)-C(47)-F(9)	58.3(13)
C(36)-C(37)-C(38)-C(39)	1.7(16)	O(7)-S(3)-C(47)-F(9)	-55.4(13)
C(37)-C(38)-C(39)-C(40)	-2.1(16)	O(12)-S(4A)-S(4B)-O(11)	129.6(9)
C(36)-N(10)-C(40)-C(39)	-0.8(12)	O(10A)-S(4A)-S(4B)-O(11)	-77(4)
Fe(2)-N(10)-C(40)-C(39)	-177.9(6)	C(48B)-S(4A)-S(4B)-O(11)	-117.7(9)
C(38)-C(39)-C(40)-N(10)	1.7(14)	C(48A)-S(4A)-S(4B)-O(11)	-119.8(10)
Fe(2)-N(11)-C(41)-C(42)	173(6)	F(12B)-S(4A)-S(4B)-O(11)	-115.2(14)
Fe(2)-N(12)-C(43)-C(44)	-22(54)	O(12)-S(4A)-S(4B)-O(10B)	-83(8)
O(1)-S(1)-C(45)-F(1)	-58.3(11)	O(10A)-S(4A)-S(4B)-O(10B)	70(9)
O(2)-S(1)-C(45)-F(1)	-178.4(10)	O(11)-S(4A)-S(4B)-O(10B)	147(8)
O(3)-S(1)-C(45)-F(1)	62.6(11)	C(48B)-S(4A)-S(4B)-O(10B)	29(8)
O(1)-S(1)-C(45)-F(3)	-178.1(9)	C(48A)-S(4A)-S(4B)-O(10B)	27(8)
O(2)-S(1)-C(45)-F(3)	61.8(10)	F(12B)-S(4A)-S(4B)-O(10B)	32(8)
O(3)-S(1)-C(45)-F(3)	-57.2(10)	O(10A)-S(4A)-S(4B)-O(12)	153(4)
O(1)-S(1)-C(45)-F(2)	60.4(12)	O(11)-S(4A)-S(4B)-O(12)	-129.6(9)
O(2)-S(1)-C(45)-F(2)	-59.8(12)	C(48B)-S(4A)-S(4B)-O(12)	112.7(7)
O(3)-S(1)-C(45)-F(2)	-178.8(10)	C(48A)-S(4A)-S(4B)-O(12)	110.6(8)
O(6)-S(2)-C(46)-F(4)	-66.1(10)	F(12B)-S(4A)-S(4B)-O(12)	115.2(14)
O(4)-S(2)-C(46)-F(4)	55.7(11)	O(12)-S(4A)-S(4B)-C(48A)	-110.6(8)
O(5)-S(2)-C(46)-F(4)	175.1(9)	O(10A)-S(4A)-S(4B)-C(48A)	43(4)
O(6)-S(2)-C(46)-F(6)	56.8(15)	O(11)-S(4A)-S(4B)-C(48A)	119.8(10)
O(4)-S(2)-C(46)-F(6)	178.6(13)	C(48B)-S(4A)-S(4B)-C(48A)	2.1(7)
O(5)-S(2)-C(46)-F(6)	-62.0(14)	F(12B)-S(4A)-S(4B)-C(48A)	4.6(15)
O(6)-S(2)-C(46)-F(5)	172.1(12)	O(12)-S(4A)-S(4B)-F(12A)	-103.8(15)
O(4)-S(2)-C(46)-F(5)	-66.1(15)	O(10A)-S(4A)-S(4B)-F(12A)	49(4)
O(5)-S(2)-C(46)-F(5)	53.3(14)	O(11)-S(4A)-S(4B)-F(12A)	126.6(16)
O(9)-S(3)-C(47)-F(8)	66.8(15)	C(48B)-S(4A)-S(4B)-F(12A)	8.9(15)
O(8)-S(3)-C(47)-F(8)	-62.8(15)	C(48A)-S(4A)-S(4B)-F(12A)	6.8(14)
O(7)-S(3)-C(47)-F(8)	-176.5(13)	F(12B)-S(4A)-S(4B)-F(12A)	11(2)
O(9)-S(3)-C(47)-F(7)	-54.4(14)	O(12)-S(4A)-S(4B)-C(48B)	-112.7(7)
O(8)-S(3)-C(47)-F(7)	176.0(13)	O(10A)-S(4A)-S(4B)-C(48B)	41(4)
O(7)-S(3)-C(47)-F(7)	62.3(14)	O(11)-S(4A)-S(4B)-C(48B)	117.7(9)
O(9)-S(3)-C(47)-F(9)	-172.1(11)	C(48A)-S(4A)-S(4B)-C(48B)	-2.1(7)

F(12B)-S(4A)-S(4B)-C(48B)	2.5(14)	S(4A)-S(4B)-F(12A)-C(48A)	-10(2)
S(4A)-S(4B)-O(10B)-F(12A)	-23(9)	O(11)-S(4B)-F(12A)-C(48A)	82(2)
O(11)-S(4B)-O(10B)-F(12A)	120.9(19)	O(10B)-S(4B)-F(12A)-C(48A)	175(3)
O(12)-S(4B)-O(10B)-F(12A)	-101.1(19)	O(12)-S(4B)-F(12A)-C(48A)	-80.4(18)
C(48A)-S(4B)-O(10B)-F(12A)	3.4(18)	C(48B)-S(4B)-F(12A)-C(48A)	0.6(9)
C(48B)-S(4B)-O(10B)-F(12A)	4.6(19)	S(4A)-S(4B)-F(12A)-O(10B)	175.0(18)
S(4B)-S(4A)-O(10A)-F(12B)	-46(5)	O(11)-S(4B)-F(12A)-O(10B)	-92(2)
O(12)-S(4A)-O(10A)-F(12B)	104.0(18)	O(12)-S(4B)-F(12A)-O(10B)	104.9(19)
O(11)-S(4A)-O(10A)-F(12B)	-114.6(17)	C(48A)-S(4B)-F(12A)-O(10B)	-175(3)
C(48B)-S(4A)-O(10A)-F(12B)	-6.8(17)	C(48B)-S(4B)-F(12A)-O(10B)	-174(2)
C(48A)-S(4A)-O(10A)-F(12B)	-7.4(18)	S(4A)-S(4B)-F(12A)-C(48B)	-10.9(18)
O(10B)-S(4B)-O(11)-S(4A)	-173.4(17)	O(11)-S(4B)-F(12A)-C(48B)	82(2)
O(12)-S(4B)-O(11)-S(4A)	46.0(11)	O(10B)-S(4B)-F(12A)-C(48B)	174(2)
C(48A)-S(4B)-O(11)-S(4A)	-71.4(14)	O(12)-S(4B)-F(12A)-C(48B)	-80.9(15)
F(12A)-S(4B)-O(11)-S(4A)	-117.2(18)	C(48A)-S(4B)-F(12A)-C(48B)	-0.6(9)
C(48B)-S(4B)-O(11)-S(4A)	-62.7(11)	S(4A)-O(10A)-F(12B)-C(48B)	11(3)
O(12)-S(4A)-O(11)-S(4B)	-59.7(12)	S(4A)-O(10A)-F(12B)-C(48A)	9(2)
O(10A)-S(4A)-O(11)-S(4B)	158.9(16)	S(4B)-S(4A)-F(12B)-C(48B)	-4(2)
C(48B)-S(4A)-O(11)-S(4B)	63.7(11)	O(12)-S(4A)-F(12B)-C(48B)	84.8(19)
C(48A)-S(4A)-O(11)-S(4B)	53.3(12)	O(10A)-S(4A)-F(12B)-C(48B)	-169(3)
F(12B)-S(4A)-O(11)-S(4B)	100.7(13)	O(11)-S(4A)-F(12B)-C(48B)	-76(2)
O(10A)-S(4A)-O(12)-S(4B)	-169.7(17)	C(48A)-S(4A)-F(12B)-C(48B)	1.5(10)
O(11)-S(4A)-O(12)-S(4B)	52.2(10)	S(4B)-S(4A)-F(12B)-C(48A)	-5.6(18)
C(48B)-S(4A)-O(12)-S(4B)	-70.5(10)	O(12)-S(4A)-F(12B)-C(48A)	83.2(15)
C(48A)-S(4A)-O(12)-S(4B)	-60.3(10)	O(10A)-S(4A)-F(12B)-C(48A)	-170(2)
F(12B)-S(4A)-O(12)-S(4B)	-109.1(11)	O(11)-S(4A)-F(12B)-C(48A)	-77.5(18)
O(11)-S(4B)-O(12)-S(4A)	-51.7(12)	C(48B)-S(4A)-F(12B)-C(48A)	-1.5(10)
O(10B)-S(4B)-O(12)-S(4A)	167.9(16)	S(4B)-S(4A)-F(12B)-O(10A)	164.5(17)
C(48A)-S(4B)-O(12)-S(4A)	72.4(13)	O(12)-S(4A)-F(12B)-O(10A)	-106.7(19)
F(12A)-S(4B)-O(12)-S(4A)	114.1(14)	O(11)-S(4A)-F(12B)-O(10A)	92.6(18)
C(48B)-S(4B)-O(12)-S(4A)	62.8(10)	C(48B)-S(4A)-F(12B)-O(10A)	169(3)
S(4B)-O(10B)-F(12A)-C(48A)	-5(3)	C(48A)-S(4A)-F(12B)-O(10A)	170(2)
S(4B)-O(10B)-F(12A)-C(48B)	-6(3)	C(48B)-F(10)-C(48A)-F(12A)	173(4)

C(48B)-F(10)-C(48A)-F(11)	76(4)	O(10A)-F(12B)-C(48A)-S(4B)	-4(3)
C(48B)-F(10)-C(48A)-F(12B)	-9(3)	S(4A)-F(12B)-C(48A)-S(4B)	3.3(10)
C(48B)-F(10)-C(48A)-S(4B)	-111(4)	C(48B)-F(12B)-C(48A)-S(4A)	-149(20)
C(48B)-F(10)-C(48A)-S(4A)	-74(4)	O(10A)-F(12B)-C(48A)-S(4A)	-7.0(17)
O(10B)-F(12A)-C(48A)-F(10)	130(3)	S(4A)-S(4B)-C(48A)-F(10)	83(3)
C(48B)-F(12A)-C(48A)-F(10)	-73(28)	O(11)-S(4B)-C(48A)-F(10)	148(3)
S(4B)-F(12A)-C(48A)-F(10)	124.7(15)	O(10B)-S(4B)-C(48A)-F(10)	-92(3)
O(10B)-F(12A)-C(48A)-F(11)	-112(3)	O(12)-S(4B)-C(48A)-F(10)	27(3)
C(48B)-F(12A)-C(48A)-F(11)	46(28)	F(12A)-S(4B)-C(48A)-F(10)	-88(3)
S(4B)-F(12A)-C(48A)-F(11)	-116.8(14)	C(48B)-S(4B)-C(48A)-F(10)	94(4)
O(10B)-F(12A)-C(48A)-F(12B)	90(52)	S(4A)-S(4B)-C(48A)-F(12A)	171.2(18)
C(48B)-F(12A)-C(48A)-F(12B)	-113(66)	O(11)-S(4B)-C(48A)-F(12A)	-124(2)
S(4B)-F(12A)-C(48A)-F(12B)	85(52)	O(10B)-S(4B)-C(48A)-F(12A)	-4(2)
O(10B)-F(12A)-C(48A)-S(4B)	5(3)	O(12)-S(4B)-C(48A)-F(12A)	114.5(18)
C(48B)-F(12A)-C(48A)-S(4B)	162(29)	C(48B)-S(4B)-C(48A)-F(12A)	-178(4)
O(10B)-F(12A)-C(48A)-S(4A)	10(3)	S(4A)-S(4B)-C(48A)-F(11)	-103(3)
C(48B)-F(12A)-C(48A)-S(4A)	167(29)	O(11)-S(4B)-C(48A)-F(11)	-38(3)
S(4B)-F(12A)-C(48A)-S(4A)	5.1(11)	O(10B)-S(4B)-C(48A)-F(11)	82(3)
C(48B)-F(11)-C(48A)-F(10)	-75(4)	O(12)-S(4B)-C(48A)-F(11)	-160(2)
C(48B)-F(11)-C(48A)-F(12A)	-175(4)	F(12A)-S(4B)-C(48A)-F(11)	86(3)
C(48B)-F(11)-C(48A)-F(12B)	4(3)	C(48B)-S(4B)-C(48A)-F(11)	-92(4)
C(48B)-F(11)-C(48A)-S(4B)	111(4)	S(4A)-S(4B)-C(48A)-F(12B)	-5.7(18)
C(48B)-F(11)-C(48A)-S(4A)	73(4)	O(11)-S(4B)-C(48A)-F(12B)	59(2)
C(48B)-F(12B)-C(48A)-F(10)	90(20)	O(10B)-S(4B)-C(48A)-F(12B)	179.2(19)
O(10A)-F(12B)-C(48A)-F(10)	-128(2)	O(12)-S(4B)-C(48A)-F(12B)	-62.4(19)
S(4A)-F(12B)-C(48A)-F(10)	-120.8(13)	F(12A)-S(4B)-C(48A)-F(12B)	-177(2)
C(48B)-F(12B)-C(48A)-F(12A)	130(53)	C(48B)-S(4B)-C(48A)-F(12B)	6(3)
O(10A)-F(12B)-C(48A)-F(12A)	-88(52)	O(11)-S(4B)-C(48A)-S(4A)	65.1(13)
S(4A)-F(12B)-C(48A)-F(12A)	-81(52)	O(10B)-S(4B)-C(48A)-S(4A)	-175.1(14)
C(48B)-F(12B)-C(48A)-F(11)	-28(20)	O(12)-S(4B)-C(48A)-S(4A)	-56.8(11)
O(10A)-F(12B)-C(48A)-F(11)	114(2)	F(12A)-S(4B)-C(48A)-S(4A)	-171.2(18)
S(4A)-F(12B)-C(48A)-F(11)	120.8(14)	C(48B)-S(4B)-C(48A)-S(4A)	11(3)
C(48B)-F(12B)-C(48A)-S(4B)	-146(20)	S(4B)-S(4A)-C(48A)-F(10)	-116(2)

O(12)-S(4A)-C(48A)-F(10)	-45(2)	C(48A)-F(12B)-C(48B)-F(12A)	-16(20)
O(10A)-S(4A)-C(48A)-F(10)	78(3)	O(10A)-F(12B)-C(48B)-F(12A)	-54(27)
O(11)-S(4A)-C(48A)-F(10)	-169(2)	S(4A)-F(12B)-C(48B)-F(12A)	-46(26)
C(48B)-S(4A)-C(48A)-F(10)	74(3)	C(48A)-F(12B)-C(48B)-S(4A)	30(20)
F(12B)-S(4A)-C(48A)-F(10)	70(2)	O(10A)-F(12B)-C(48B)-S(4A)	-8(2)
S(4B)-S(4A)-C(48A)-F(12A)	-8.9(19)	C(48A)-F(12B)-C(48B)-S(4B)	33(19)
O(12)-S(4A)-C(48A)-F(12A)	62(2)	O(10A)-F(12B)-C(48B)-S(4B)	-6(3)
O(10A)-S(4A)-C(48A)-F(12A)	-175(2)	S(4A)-F(12B)-C(48B)-S(4B)	2.3(12)
O(11)-S(4A)-C(48A)-F(12A)	-62(2)	C(48A)-F(10)-C(48B)-F(12B)	168(4)
C(48B)-S(4A)-C(48A)-F(12A)	-178(4)	C(48A)-F(10)-C(48B)-F(11)	-76(4)
F(12B)-S(4A)-C(48A)-F(12A)	177(3)	C(48A)-F(10)-C(48B)-F(12A)	-6(3)
S(4B)-S(4A)-C(48A)-F(11)	95(2)	C(48A)-F(10)-C(48B)-S(4A)	85(3)
O(12)-S(4A)-C(48A)-F(11)	166(2)	C(48A)-F(10)-C(48B)-S(4B)	49(3)
O(10A)-S(4A)-C(48A)-F(11)	-71(3)	C(48A)-F(11)-C(48B)-F(12B)	-174(5)
O(11)-S(4A)-C(48A)-F(11)	42(3)	C(48A)-F(11)-C(48B)-F(10)	77(4)
C(48B)-S(4A)-C(48A)-F(11)	-74(3)	C(48A)-F(11)-C(48B)-F(12A)	4(3)
F(12B)-S(4A)-C(48A)-F(11)	-79(3)	C(48A)-F(11)-C(48B)-S(4A)	-84(3)
S(4B)-S(4A)-C(48A)-F(12B)	174.2(18)	C(48A)-F(11)-C(48B)-S(4B)	-52(3)
O(12)-S(4A)-C(48A)-F(12B)	-114.8(17)	C(48A)-F(12A)-C(48B)-F(12B)	33(40)
O(10A)-S(4A)-C(48A)-F(12B)	8(2)	O(10B)-F(12A)-C(48B)-F(12B)	56(27)
O(11)-S(4A)-C(48A)-F(12B)	121.2(18)	S(4B)-F(12A)-C(48B)-F(12B)	51(26)
C(48B)-S(4A)-C(48A)-F(12B)	5(3)	C(48A)-F(12A)-C(48B)-F(10)	105(29)
O(12)-S(4A)-C(48A)-S(4B)	71.0(10)	O(10B)-F(12A)-C(48B)-F(10)	128(3)
O(10A)-S(4A)-C(48A)-S(4B)	-166.2(15)	S(4B)-F(12A)-C(48B)-F(10)	122.6(14)
O(11)-S(4A)-C(48A)-S(4B)	-53.0(10)	C(48A)-F(12A)-C(48B)-F(11)	-133(29)
C(48B)-S(4A)-C(48A)-S(4B)	-169(3)	O(10B)-F(12A)-C(48B)-F(11)	-110(3)
F(12B)-S(4A)-C(48A)-S(4B)	-174.2(18)	S(4B)-F(12A)-C(48B)-F(11)	-115.7(14)
C(48A)-F(12B)-C(48B)-F(10)	-87(20)	C(48A)-F(12A)-C(48B)-S(4A)	-12(28)
O(10A)-F(12B)-C(48B)-F(10)	-125(3)	O(10B)-F(12A)-C(48B)-S(4A)	11(3)
S(4A)-F(12B)-C(48B)-F(10)	-117.1(16)	S(4B)-F(12A)-C(48B)-S(4A)	5.2(9)
C(48A)-F(12B)-C(48B)-F(11)	150(21)	C(48A)-F(12A)-C(48B)-S(4B)	-17(28)
O(10A)-F(12B)-C(48B)-F(11)	112(3)	O(10B)-F(12A)-C(48B)-S(4B)	6(2)
S(4A)-F(12B)-C(48B)-F(11)	119.9(19)	S(4B)-S(4A)-C(48B)-F(12B)	176(2)

O(12)-S(4A)-C(48B)-F(12B)	-111(2)	O(11)-S(4B)-C(48B)-F(12B)	58(3)
O(10A)-S(4A)-C(48B)-F(12B)	9(2)	O(10B)-S(4B)-C(48B)-F(12B)	-179(2)
O(11)-S(4A)-C(48B)-F(12B)	120(2)	O(12)-S(4B)-C(48B)-F(12B)	-59(2)
C(48A)-S(4A)-C(48B)-F(12B)	-174(4)	C(48A)-S(4B)-C(48B)-F(12B)	-172(4)
S(4B)-S(4A)-C(48B)-F(10)	-91(2)	F(12A)-S(4B)-C(48B)-F(12B)	-175(3)
O(12)-S(4A)-C(48B)-F(10)	-18(2)	S(4A)-S(4B)-C(48B)-F(10)	105.1(19)
O(10A)-S(4A)-C(48B)-F(10)	102(2)	O(11)-S(4B)-C(48B)-F(10)	167.4(19)
O(11)-S(4A)-C(48B)-F(10)	-147(2)	O(10B)-S(4B)-C(48B)-F(10)	-70(2)
C(48A)-S(4A)-C(48B)-F(10)	-81(3)	O(12)-S(4B)-C(48B)-F(10)	51(2)
F(12B)-S(4A)-C(48B)-F(10)	93(3)	C(48A)-S(4B)-C(48B)-F(10)	-63(3)
S(4B)-S(4A)-C(48B)-F(11)	70(2)	F(12A)-S(4B)-C(48B)-F(10)	-65(2)
O(12)-S(4A)-C(48B)-F(11)	143(2)	S(4A)-S(4B)-C(48B)-F(11)	-123.3(19)
O(10A)-S(4A)-C(48B)-F(11)	-97(2)	O(11)-S(4B)-C(48B)-F(11)	-61(2)
O(11)-S(4A)-C(48B)-F(11)	14(3)	O(10B)-S(4B)-C(48B)-F(11)	62(2)
C(48A)-S(4A)-C(48B)-F(11)	80(3)	O(12)-S(4B)-C(48B)-F(11)	-177.6(17)
F(12B)-S(4A)-C(48B)-F(11)	-106(3)	C(48A)-S(4B)-C(48B)-F(11)	68(3)
S(4B)-S(4A)-C(48B)-F(12A)	-8.6(15)	F(12A)-S(4B)-C(48B)-F(11)	66(2)
O(12)-S(4A)-C(48B)-F(12A)	64.5(16)	S(4A)-S(4B)-C(48B)-F(12A)	170.4(17)
O(10A)-S(4A)-C(48B)-F(12A)	-175.5(18)	O(11)-S(4B)-C(48B)-F(12A)	-127.3(19)
O(11)-S(4A)-C(48B)-F(12A)	-64.9(17)	O(10B)-S(4B)-C(48B)-F(12A)	-4.3(18)
C(48A)-S(4A)-C(48B)-F(12A)	1(3)	O(12)-S(4B)-C(48B)-F(12A)	116.0(16)
F(12B)-S(4A)-C(48B)-F(12A)	175(2)	C(48A)-S(4B)-C(48B)-F(12A)	2(3)
O(12)-S(4A)-C(48B)-S(4B)	73.1(10)	O(11)-S(4B)-C(48B)-S(4A)	62.3(11)
O(10A)-S(4A)-C(48B)-S(4B)	-167.0(14)	O(10B)-S(4B)-C(48B)-S(4A)	-174.7(14)
O(11)-S(4A)-C(48B)-S(4B)	-56.4(10)	O(12)-S(4B)-C(48B)-S(4A)	-54.4(11)
C(48A)-S(4A)-C(48B)-S(4B)	10(3)	C(48A)-S(4B)-C(48B)-S(4A)	-168(3)
F(12B)-S(4A)-C(48B)-S(4B)	-176(2)	F(12A)-S(4B)-C(48B)-S(4A)	-170.4(17)
S(4A)-S(4B)-C(48B)-F(12B)	-4(2)		

Symmetry transformations used to generate equivalent atoms

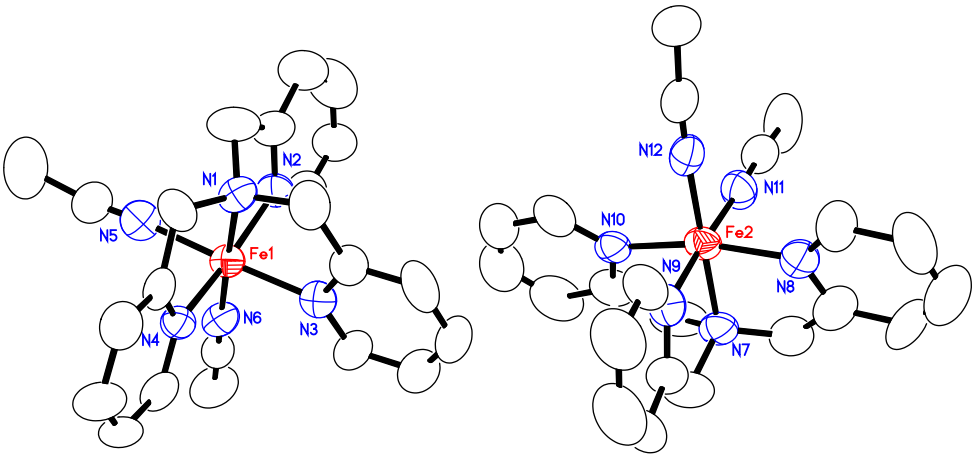

Appendix Figure 1. Molecular structure of the two independent $[Fe(TPA)(MeCN)_2](OTf)_2$ complexes. Displacement ellipsoids for non-H atoms are shown at the 50 % probability level and H atoms are omitted for clarity.)